SYNTHESIS AND CHARACTERIZATION OF POLYIMIDE DERIVATIVE ADHESIVES

A Thesis Submitted to
the Graduate School of Engineering and Sciences of
İzmir Institute of Technology
in Partial Fulfillment of the Requirements for the Degree of

DOCTOR OF PHILOSOPHY

in Materials Science and Engineering

by
Oktay ACAR

November 2018
İZMİR

We approve the thesis of **Oktay ACAR**

Examining Committee Members:

Prof. Dr. Mustafa M. DEMİR
Department of Materials Science and Engineering, İzmir Institute of Technology

Prof. Dr. Atilla CİHANER
Department of Chemical Engineering and Applied Chemistry, Atılım University

Assoc. Prof. Dr. Aylin ZİYLAN
Department of Metallurgical and Materials Engineering, Dokuz Eylül University

Assoc. Prof. Dr. Mustafa EMRULLAHOĞLU
Department of Chemistry, İzmir Institute of Technology

Assoc. Prof. Dr. Yaşar AKDOĞAN
Department of Materials Science and Engineering, İzmir Institute of Technology

23 November 2018

Prof. Dr. Mustafa M. DEMİR
Supervisor, Department of
Materials Science and Engineering,
İzmir Institute of Technology

Assoc. Prof. Dr. Seha TİRKEŞ
Co-Supervisor, Department of
Chemical Engineering and Applied
Chemistry
Atilim University

Prof. Dr. Mustafa M. DEMİR
Head of the Department of
Materials Science and Engineering

Prof. Dr. Aysun SOFUOĞLU
Dean of the Graduate School of
Engineering and Sciences

ACKNOWLEDGEMENTS

I would like to express my grateful thanks to my supervisor Prof. Dr. Mustafa M. DEMİR, for his instructive comments, motivations, and valued support throughout my thesis study. I am grateful for his helpful and understanding behavior.

I would like to express my deepest gratitude to my co-supervisor Assoc. Prof. Dr. Seha TİRKEŞ, for his guidance, motivations, and valued support throughout my thesis study.

I am sincerely grateful to my thesis committee members Prof. Dr. Atilla CİHANER, Assoc. Prof. Dr. Mustafa EMRULLAHOĞLU, Assoc. Prof. Dr. Aylin ZİYLAN, and Assoc. Prof. Dr. Yaşar AKDOĞAN for their helps, guidance, feedbacks and valuable discussions for this thesis.

I would like to thank Tuğba IŞIK for her help in SEM analysis, article preparation and thesis documentation processes.

I would like to extend my gratitude to my group coordinator Mr. Hakan DER for his support and efforts in the development and commercialization of the high temperature resistant structural adhesive that has emerged as a result of this thesis.

Special thanks to my division supervisor Dr. Serhat VARIŞ for his encouragement throughout the study. I would like to thank him for his help in NMR analysis.

I am also grateful to all my colleagues and friends for their endless support, encouragements and help throughout the entire duration of the study.

This thesis study was conducted under the cooperation between İzmir Institute of Technology and Scientific and Technological Research Council of Turkey- Defense Industries Research and Development Institute (TÜBİTAK-SAGE). I would like to thank TÜBİTAK-SAGE for their permission and support to complete my PhD thesis.

I am highly indebted to my parents and sister for their support, encouragement and patience throughout my entire life.

The words are incapable of expressing my gratitude to my precious wife and my two little lovely daughters for their patience, devotion and self-sacrifice throughout my PhD thesis study.

ABSTRACT

SYNTHESIS AND CHARACTERIZATION OF POLYIMIDE DERIVATIVE ADHESIVES

While the rapid advancement of technology is pushing the limits, today need for special advanced materials has been increased in order to obtain high-tech products with desired performance. Lightweight materials that can operate at high temperatures have critical importance in aerospace field. Between those materials, polyimides come front with their unique mechanical properties and high thermo-oxidative stabilities. They are commonly used in defense and aerospace industries as adhesives, coatings and resins in composites operating at high temperatures.

PMR-15 (Polymerization of Monomeric Reactants) is considered as a state-of-the-art high temperature resistant structural adhesive, due to its low cost, exceptional thermo-mechanical strength and thermo-oxidative resistance, up to 300 °C. However, PMR-15 has both limited processing and flexibility properties. LARC-RP46 (Langley Research Center) was developed as an alternative to PMR-15 resin. It has a higher melt flow rate to some extent.

In this thesis, MDA-BTDA-ODA copolyimide adhesives with nadic end caps were synthesized. The chemical structures of the synthesized resins were verified by FTIR and ^{1}H NMR analysis. The copolymers have thermal stabilities as high as 500 °C and T_g at around 400 °C. They showed superior adhesion performance up to 16.3 MPa. Compared to both commercial PMR-15 and LARC RP-46 polyimides, copolyimide resins showed significant processability.

Kinetics of curing process of the resins was investigated by using the autocatalytic kinetic model of Kamal – Sourour. The experimental data are well-fitted with the model. The activation energies were calculated by kinetic constants derived from the model.

ÖZET

POLİİMİD TÜREVİ YAPIŞTIRICILARIN SENTEZİ VE KARAKTERİZASYONU

Teknolojinin hızla ilerlemesi ile birlikte limitlerin daha da zorlandığı günümüzde, ulaşılan teknolojik ürünlerin istenen performansı sağlamasına yönelik özel ileri malzemelere duyulan gereksinimler giderek artmaktadır. Yüksek sıcaklıkta çalışabilen hafif malzemeler uzay ve havacılık alanında kritik öneme sahiptirler. Bu malzemeler arasından poliimidler sahip oldukları üstün mekanik özellikleri, yüksek ısıl oksidasyon dayanımları ile birlikte öne çıkmaktadırlar. Poliimid malzemeler savunma, uzay ve havacılık endüstrilerinde yüksek sıcaklıkta çalışan yapıştırıcılar, kaplamalar ve kompozitlerde yaygın olarak kullanılmaktadırlar.

PMR-15, düşük maliyeti, 300 °C'lere kadar gösterdiği mükemmel termo-mekanik mukavemeti ve termo-oksidatif direnci nedeniyle yüksek sıcaklığa dayanıklı son teknolojik yapısal yapıştırıcı olarak kabul edilmektedir. Fakat, PMR-15 sınırlı işleme ve esneklik özelliği göstermektedir. PMR-15 reçinesine alternatif olarak LARC-RP46 geliştirilmiştir. Bu malzeme de belirli ölçüde erime akış hızına sahiptir.

Bu tez çalışmasında nadik sonlu MDA-BTDA-ODA kopoliimid yapıştırıcılar sentezlenmiştir. Sentezlenen reçinelerin kimyasal yapıları FTIR ve ^{1}H NMR analizleri ile teyit edilmiştir. Bu kopolimerler 500 °C'lere kadar ısıl dayanım göstermekle T_g değerleri birlikte 400 °C'lerdedir. 16.3 MPa değerine kadar üstün yapışma performansı göstermişlerdir. Ticari PMR-15 ve LARC RP-46 poliimidlere kıyasla, kopoliimidler önemli işlenme özelliği göstermişlerdir.

Kamal-Sorour'un otokatalitik kinetik modeli kullanılarak reçinelerin kürleşme kinetikleri incelenmiştir. Deneysel veriler modelle mükemmel örtüşme göstermiştir. Modelden çıkarılan kinetik sabit değerleri kullanılarak aktivasyon enerjileri hesaplanmıştır.

Dedicated to Turkey…

TABLE OF CONTENTS

LIST OF FIGURES

LIST OF TABLES

LIST OF SYMBOLS AND/OR ABBREVIATIONS

$\partial c/\partial x$	Concentration Gradient
ρ	Density
δ	Solubility Parameters
™	Trade Mark
β	Mechanical Conversion
η	Viscosity
η^*	Complex viscosity
6FDA	Hexafluoroisopropylidene diphthalic anhydride
ASTM	American Society for Testing and Materials
ATR	Attenuated Total Reflection
BAPP	2,2’-Bis [4-(4-aminophenoxy) phenyl] propane
BMI	Bismaleimide
BPDA	3, 3’, 4, 4’- Biphenyl tetracarboxylic dianhydride
BTDA	3,3’,4,4’ -Benzophenonetetracarboxylic acid dianhydride
°C	Degree Celsius
CHP	1-cyclohexyl-2-pyrrolidinone
CED	Cohesive Energy Density
DABA	Diallylbisphenol A
DCC	N,N- dicyclohexylcarbodiimide
D_d	Mobility Constant of Macromolecules
D_f	Diffusion Coefficient
DMA	Dynamic Mechanical Analyzer/Analysis
DMAc	Dimethylacetamide
DMF	Dimethylformamide
DMSO	Dimethyl sulfoxide
DSC	Differential Scanning Calorimeter
E	Energy
E'	Tensile Storage Modulus
E''	Tensile Loss Modulus
E_a	Activation Energy

E_{coh}	The Energy Required to Separate the Macromolecules to an Infinite Distance
EMC	Electromagnetic Conduction
EMI	Electromagnetic Induction
FT-IR	Fourier Transform Infrared Spectrometer/Spectrometry
g	Gram
G	Peel Energy
G'	Shear Storage Modulus
G''	Shear Loss Modulus
h	Hour
Hz	Hertz
l_p	The Depth of Penetration of Diffusing Macromolecules
K	Constant of The Polymer in Contact
k	Rate Constant
kN	kilo Newton
LARC	Langley Research Centre
LCT	Liquid Crystal Thermosets
m	The Amount of Diffusing Material in x Direction Per Unit Area
m	Meter
m	Reaction Order
min	Minutes
mm	Millimeter
M	Molecular Weight of the Polymer
MDA	4,4’-Diaminodiphenylmethane
MPa	Mega Pascal
MeOH	Methanol
N	Avogadro’s number
n	Reaction Order
NA	Nadic Anhydride
NASA	National Aeronautics and Space Administration
NMP	N-Methyl-2-pyrrolidone
NMR	Nuclear Magnetic Resonance
ODA	Oxydianiline
ODPA	4, 4’-oxydiphthalic anhydride

PAA	Polyamic acid
PAE	Polyamic ester
PDMDA	3,3'-bis(3,4-dicarboxyphenoxy) diphenylmethane dianhydride
PMDA	Pyromellitic dianhydride
PI	Polyimide
PMR	Polymerization of Monomeric Reactants
ppm	Parts Per Million
psi	Pounds Per Square Inch
RTV	Room Temperature Vulcanizing
SEM	Scanning Electron Microscope
SIDA	Bis(phenyl carboxylic dianhydride) dimethylsilane
t	Time
$\tan \delta$	Loss factor
t_c	Time of Contact
TFMB	2,2’-bis(trifluoromethyl) benzidine
T_g	Glass transition temperature
TGA	Thermogravimetric analysis
T_{gel}	Gelation temperature
t_{gel}	Gelation time
V	Molar Volume

CHAPTER 1

INTRODUCTION

Polymers having extraordinary mechanical, thermal, and environmental durability are called as high-performance polymers. Besides the various definitions of high-performance polymers, Hergenrother defines them according to their thermal stabilities. The author states that “the polymer which can retain the useable properties at a temperature greater than 177 °C” is a high-performance polymer. Glass transitions of this type of polymers are greater than 200 °C. They keep their thermal stabilities up to 450 °C (Hergenrother 2003). High performance polymers mainly contain aromatic structures on their polymer backbones. Therefore, the rigidity of their structures is considerably higher than aliphatic structure-based polymers.

Polyimide is a significant type of high-performance polymers. In fact, repeating imide groups as well as rigid aromatic structures on their backbone give polyimides considerable thermal durability, mechanical strength and solvent resistance (King and King 1985; Mittal 2001). Aromatic polyimide polymers have a typical semi-ladder structure. They have been firstly produced by Marston Bogert in 1908 (Bogert and Renshaw 1908). Commercialization of polyimide polymers has been realized in 1960s with the release of DuPont’s Kapton H film, Vespel molded parts and Pyre-ML wire varnish. Actually, this development acted as a driving force for coming out of novel fabrications and new applications of polyimides. Some of commercial polyimides are listed in Table 1.1.

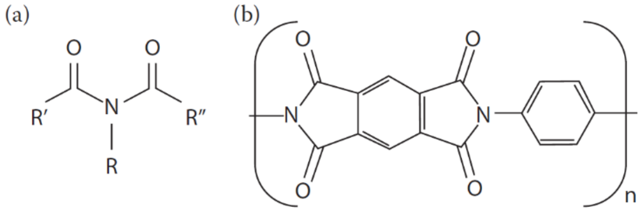

Figure 1.1. Structures of a) imide group, and b) an example of polyimides.

Table 1.1. Commodity polyimide thermoplastic resins and powders (Source: Bryant 2000)

Manufacturer	**Trade Name(s)**	**Polyimide Structure**	**Glass Transition Temperature (T_g), °C**
DuPont (USA)	Kapton Vespel Pyre-ML	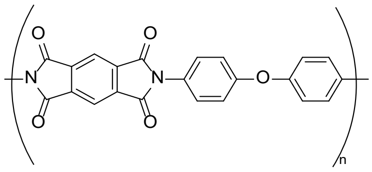	360
Ube Industries (Japan)	Upilex-R	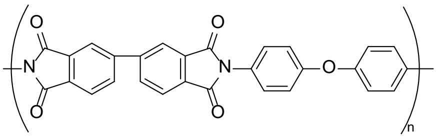	285
Mitsui Chemicals (Japan)	Aurum	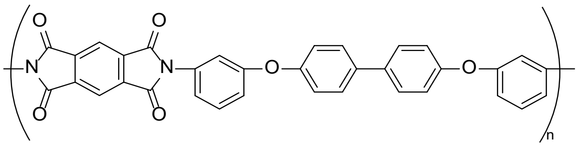	250
Shanghai Research Institute of Synthetic Resins	YS-20	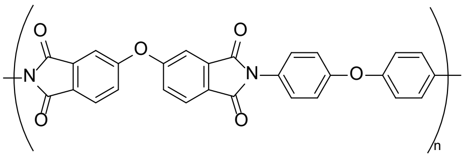	239
Saudi Basic Industries Corp. (SABIC) (Saudi Arabia)	Ultem	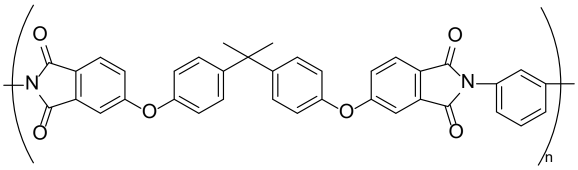	210
	Extem	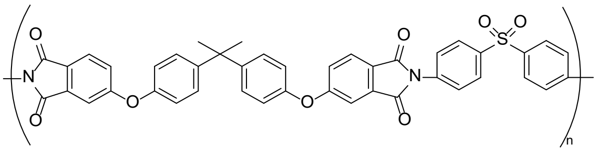	247

Table 1.2. Industrial applications of polyimides (Source: Scola 2001).

INDUSTRY	APPLICATIONS
Electronics	Flexible circuits Flexible connectors Chip carriers Tape automated bonding High-density interconnect applications Photosensitive polyimides
Aircraft	Wire insulation Motor windings Electrical switches Structural adhesives Structural composites Foam insulation Bushings Baffles Flanged bearings Thrust washers Thrust discs Seal rings
Automobile	Electrical switches
Medical	Pacemakers Eye lens implants
Machining	Abrasive cutting wheels
Gas purification	Membranes
Aerospace	Rockets Spacecraft (composite, adhesives, coatings)
Military applications	Composites, adhesives, coatings

Polyimides have broad application areas due to their modifiable molecular structures according to specific purposes. Their thermal performances and solubilities depend on the presence of ether, methylene, isopropylidene, hexafluoroisopropylidene and carbonyl units in their backbones. In other words, those units provide flexibility to the backbone. Highly aromatic polyimides bearing flexible units display high thermal and thermo-oxidative stabilities up to 400 °C (Liaw et al. 2012). Besides their non-flammability, they exhibit high mechanical stabilities and excellent adhesive properties at room temperature and high temperature conditions. Fluoride-containing polyimides exhibit the same properties as described above, but also have low dielectric constants. (Scola 1993; Scola and Wai 1994; Hu et al. 1999). Polyimide polymers are used in various ranges of applications such as flexible circuits and liquid crystalline displays in electrical industry; coatings, wire insulation, adhesives and composites in aerospace as well as defense; membranes for gas purification and polymer electrolyte fuel cells, etc. General application areas are shown in Table 1.2. Moreover, polyimides containing high temperature composites are used in some parts of both military and commercial engines (Scola 2001).

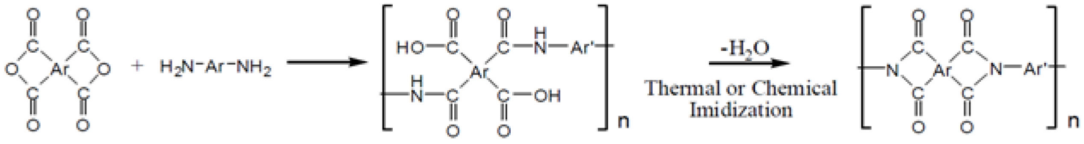

Figure 1.2. Two-step route for synthesis of polyimides.

Aromatic polyimides with high molecular weights were produced in 1955 (Abadie 2012). The synthesis of the polymer was realized by two-stage polycondensation of diamines with pyromellitic dianhydride (see Figure 1.2). The presence of aromatic units in the backbone causes strong interchain interactions and rigidity. Actually, fully aromatic polyimides have poor solubility in common solvents. They start to soften at very high temperatures. In other words, the situation makes processing of the polymer more difficult (Hrdlovič 2004; Hasegawa and Horie 2001). Going to the final product with the use of a soluble poly(amic acid) precursor is the most common synthetic method to solve the problem. For this, poly(amic acid) is first casted, and then dehydrated to obtain cyclic imide structure. However, problems such as inefficient cyclisation, difficulty in removal of water and microvoids formation are observed during the process.

Thermal and mechanical performance of polyimides can be tailored by modifying the chemistry, processing, reaction conditions and controlling molecular weight of the polymer (Cheng et al. 1991; Eashoo et al. 1993). In literature, there are many studies about changing molecular interactions of polyimides (Ghosh and Mittal 1996; Liaw 2004). Three major modification approaches (Liaw et al. 2012) are:

- Introduction of flexible unsymmetrical units (i.e. -O-, $-CH_2-$, $-SO_2-$ and hexafluofoisopropylidene) in the backbone,
- Incorporation of bulky pendant substituents to the polymer chain,
- Disordering the regularity by copolymerization.

Flexible groups act as swiveling unit that causes to decrease the rigidity of the polymer backbone and inhibition of close packaging of the chains. The solubility of the polymer increases as a result. Ultem®, a product of General Electric Co., can be given as a good example of such a polymer. Besides its good processability, Ultem® has high thermal and mechanical properties. Both T_g and thermo-oxidative stability of a polyimide considerably increase with the introduction of bulky substituent to the backbone. In addition, the solubility of polyimides is also enhanced by flexible units in the backbone. Bulky and asymmetrical substituents decrease the crystallinity as well as inter-chain interactions of the polymer. In this case, solubility of polyimides can be increased at the expense of thermal properties. Therefore, keeping the balance between those properties is essential.

Polyimides with special functionalities can be produced by using different kinds of amine and anhydride components containing certain specialized groups or species. PMR-15, a type of PMR (Polymerization of Monomeric Reactants) polyimides, is considered as a state-of-the-art high temperature resistant structural adhesive, due to its low cost, exceptional thermo-mechanical strength and thermo-oxidative resistance, up to 300°C (Xiao et al. 2001; Ruggles-Wrenn and Noomen 2018). However, PMR-15 has both limited processing and flexibility problems because of its rigid backbone and low melt flow. LARC-RP46 which contains flexible ether groups in its backbone was developed as an alternative to PMR-15 resin. It has a higher melt flow rate to some extent. The main subject of this thesis is to synthesize and characterize a series of random copolyimide adhesives having improved processability and adhesion performance compared to the both commercial PMR-15 and LARC RP-46 polyimide resins. For this purpose, it was attempted to reduce the rigidity and regularity of the polymer backbone by changing 4,4'-diaminodiphenylmethane (MDA) with 3,4’-oxydianiline (ODA) in different increments. In addition, the thermal stability and low raw material cost was also tried to be maintained. Therefore, the processability and toughness of the polymer were aimed to be improved while maintaining the thermal stability and low cost. The literature with respect to the goals of the conducted research is reviewed in Chapters 2 and 3. Information focused on the polyimide chemistry, thermal and mechanical performances of polyimides is provided in Chapter 2. In the next chapter, adhesives, high temperature adhesives, and polyimides as adhesives are mentioned. And then, in Chapter 4, conducted research for the fabrication of polyimide adhesives is presented. Chemical, mechanical, and thermal characteristics, as well as adhesion properties of the novel adhesive are discussed. Rheokinetics of PMR-

15 polyimide resin and nadic end capped MDA-BTDA-ODA copolyimide polymer are investigated in Chapters 6 and 7, respectively. As a result, it has been concluded that the processability of the adhesive has been increased with the deterioration of the chemical symmetry and the involvement flexible structures into the polymer backbone. The kinetic parameters and behavior of conversion rate confirm that the curing process occurs at autocatalytic level. Kinetic constants obtained from Kamal-Sourour model can be used for calculation of activation energy.

CHAPTER 2

POLYIMIDES

Polyimide polymers can be categorized by their chemical structures and thermal behaviors. For long-term use, the polyimides are divided into two groups: those capable of serving up to 230 °C and serviceable up to 315 °C. Short term applications are also possible up to 480 °C (Liaw et al. 2012). Bismaleimides, phenylethynyl terminated polyimides and some condensation type polyimides are some examples for the long-term heat resistant materials. PMR-15, LARC-TPI, Avimid-N and BPDA/TFMB are belonging in the latter type of polyimides (Scola 2001).

From the chemical aspect, polyimides can be grouped as thermoplastic (condensation type) polyimides and cross-linked (addition type) polyimides. Thermoplastic polyimides are produced by condensation reaction of anhydrides with diamines. On the other hand, cross-linked polyimides are synthesized by addition reaction occurred between unsaturated groups of imide monomers or oligomer precursors. Addition type polyimides contain end-caps with different kinds of unsaturated molecular structures such as vinyl, nadic, acetylene and phenylethynyl functional groups. General structures of addition-type polyimides are shown in Figure 2.1. From those polymers, phenylethynyl end capped polyimides exhibit excellent thermal stability, mechanical strength and adhesion (Hergenrother, Connell, and Smith 2000; Smith, Connell, and Hergenrother 2000; Hergenrother and Smith 1994).

Both of condensation and addition type polyimides have some advantages and disadvantages. In fact, condensation type polyimides show thermoplastic property. Because of their linear long chains, they have high melt viscosities that can lead to difficulty in processing. Additionally, volatiles can also be released during the processing. These types of polyimides have high thermo-oxidative stabilities, good toughness and mild glass transition temperatures (T_g) because of their highly aromatic structures within the backbones (Scola 2001). On the other hand, addition type polyimides are thermoset polymers that are produced by thermal cross-linking or chain extension of oligomer precursors. The processability, T_g, and cross-linking level or chain extension of these types of polymers can be tailored by adjusting molecular weight of the preformed oligomers. On contrary to the condensation types, no volatiles are released during the processing of addition type polyimides. Polymerization reaction occurs at melting or softening temperature of the preformed oligomers. By the way, processing of addition type polyimides is easier than the condensation types. While addition type polyimides have high glass transition temperatures, they are brittle and have poor thermal stabilities as well as thermo-oxidative stabilities.

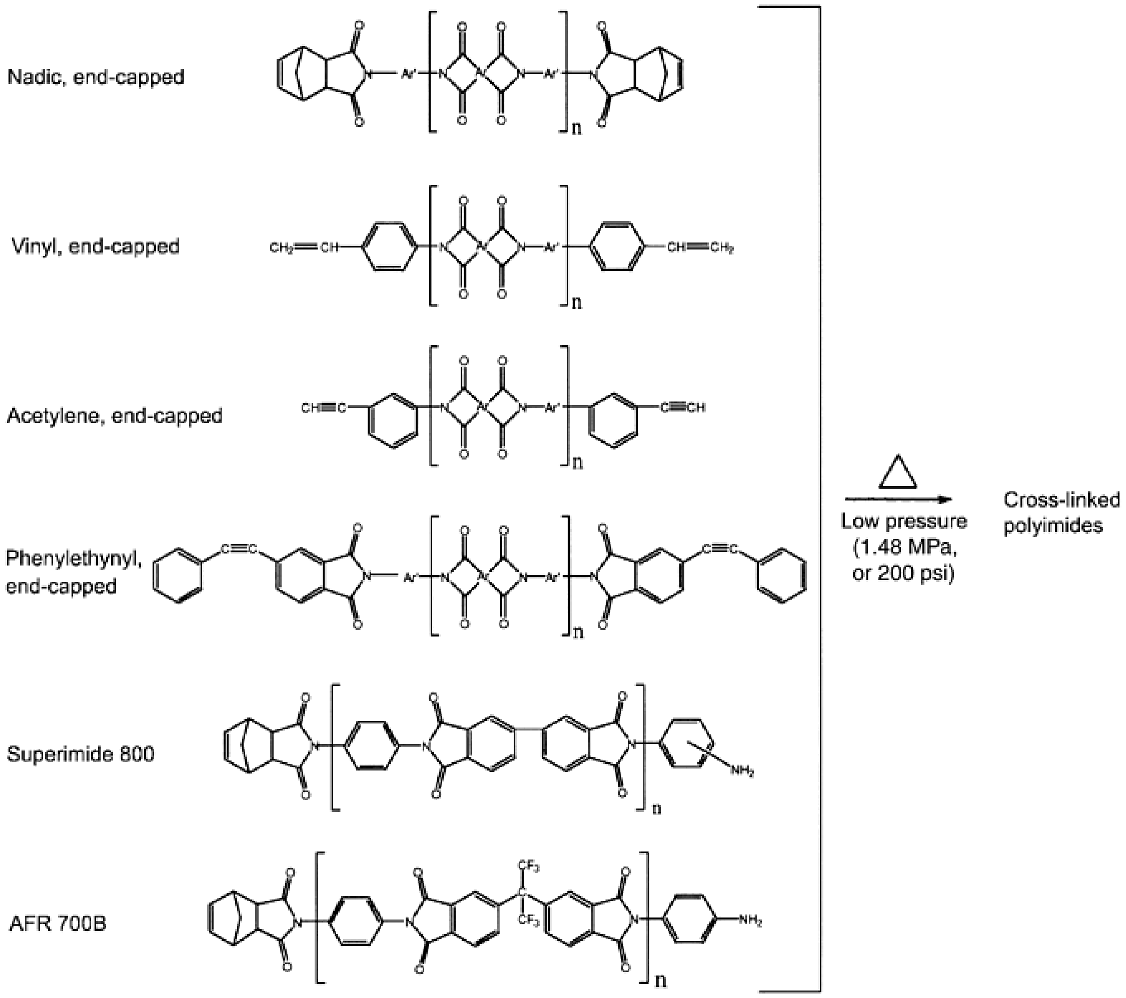

Figure 2.1. General structures of addition-type polyimides (Source: Scola 2001).

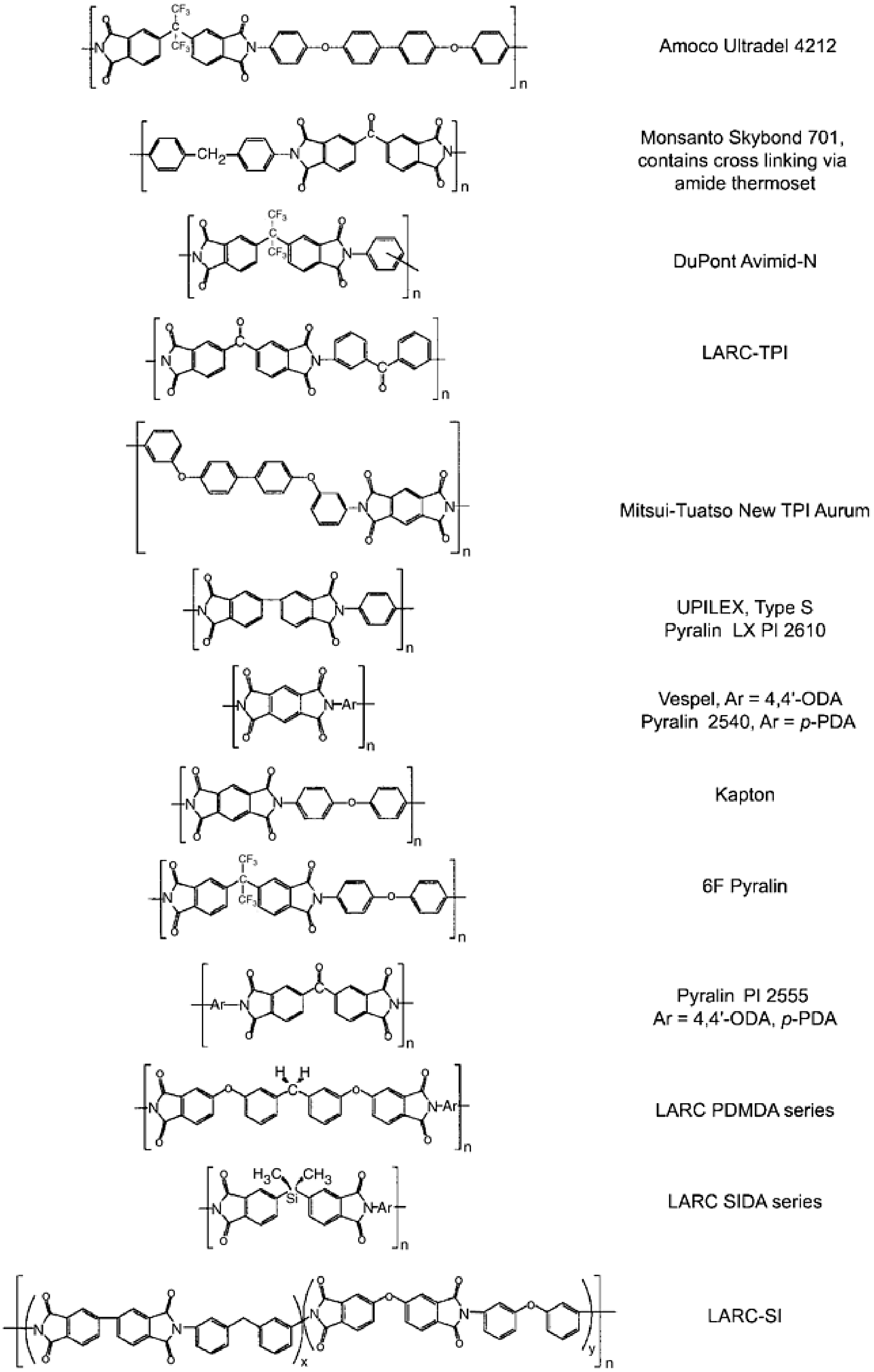

Figure 2.2. Molecular structures of some of commercially available condensation-type polyimides (Source: Scola 2001).

2.1. Synthesis of Polyimides

The research and development activities for the synthesis of polyimides have been considerably increased since the first commercial polyimide, Kapton, has emerged (Sroog 1976; Mittal 2013; Bessonov et al. 1987; Doug Wilson, Stenzenberger, and Hergenrother 1990; Ghosh and Mittal 1996). In particular, the difficulties in processing of these polymers have triggered the investigation for new types of polyimides (Ghosh and Mittal 1996). In this section, the routes for synthesis of polyimides are mentioned.

2.1.1. Two-Step Method for Polyimides via Poly(amic acid)s

Two-step method is the most common and widely used technique for the synthesis of polyimides. The method enhances the processing of insoluble and infusible polyimides. Two-step method comprises, firstly, preparing the soluble polymer precursor, poly(amic acid), and subsequently, imidizing the precursor to the polyimide (Sroog et al. 1965). The synthesis of Kapton can be given as an example for the process (See Figure 2.3).

2.1.1.1. Thermal Imidization of Poly(amic acid)

Poly(amic acid)s can be converted to polyimides by the application of thermal process. Amic acid groups in the polymer chain are transformed into imide rings at around 250 – 350 °C. This process is useful for the fabrication of films, powders, and coatings due to prevention of voids in the final product. When the curing cycle is considered, heating at slow rate is crucial in avoiding the formation of bubbles in the last stage (Ghosh and Mittal 1996). During the thermal imidization process, the molecular weight decreases initially due to depolymerization. However, as the temperature increases, it is recovered (Ayesha 2011). The ring closure mechanism of amic acids is shown in Figure 2.4. In fact, the thermal imidization process consists of interconnected interactions and varying physicochemical properties. Due to this complexity, it is difficult to incorporate the process into simple kinetic approaches (Ghosh and Mittal 1996).

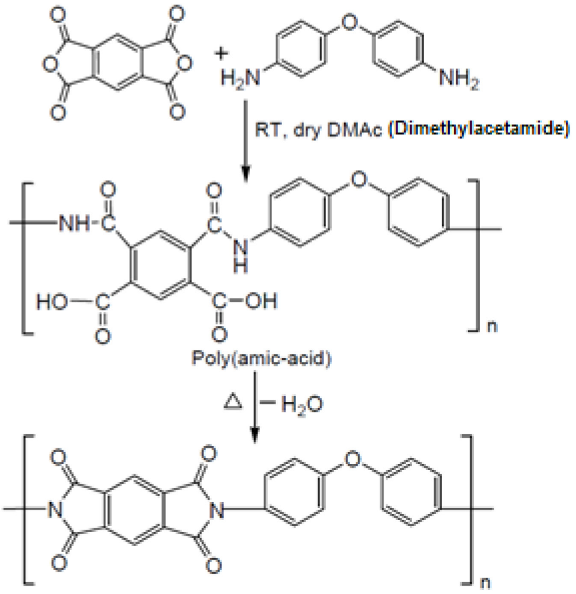

Figure 2.3. Synthesis route for Kapton.

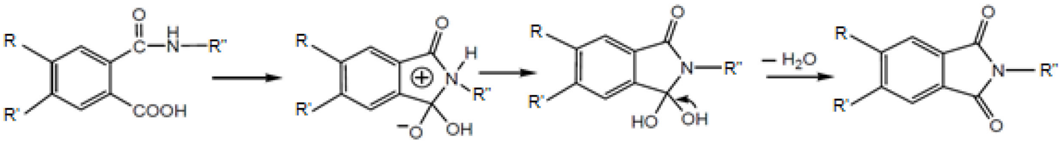

Figure 2.4. Reaction mechanism of thermal imidization.

2.1.1.2. Chemical imidization

In chemical imidization process, ring closure reaction occurs at moderate temperatures by means of a dehydrating agent in the presence of catalysts (Frost and Kesse 1964). Trialkylamines, pyridine, methylpyridines, lutidine and Nmethylmorpholine are commonly used as catalysts. Dehydrating agents include acetic anhydride, n-butyric anhydride, and propionic anhydride. Actually, depolymerization problem causing to the reduction of molecular weight does not occur in chemical imidization (Wallach and Manassen 1969). The imidization process starts with the formation of intermediate dehydrating agent through the reaction occurred between acid anhydride and amine (Figure 2.5). The imide or isoimide ring closure occurs as a result of the interaction between amic acid and intermediate dehydrating agent. Then, isoimide moieties are rearranged to imide rings which are more stable (Figure 2.6).

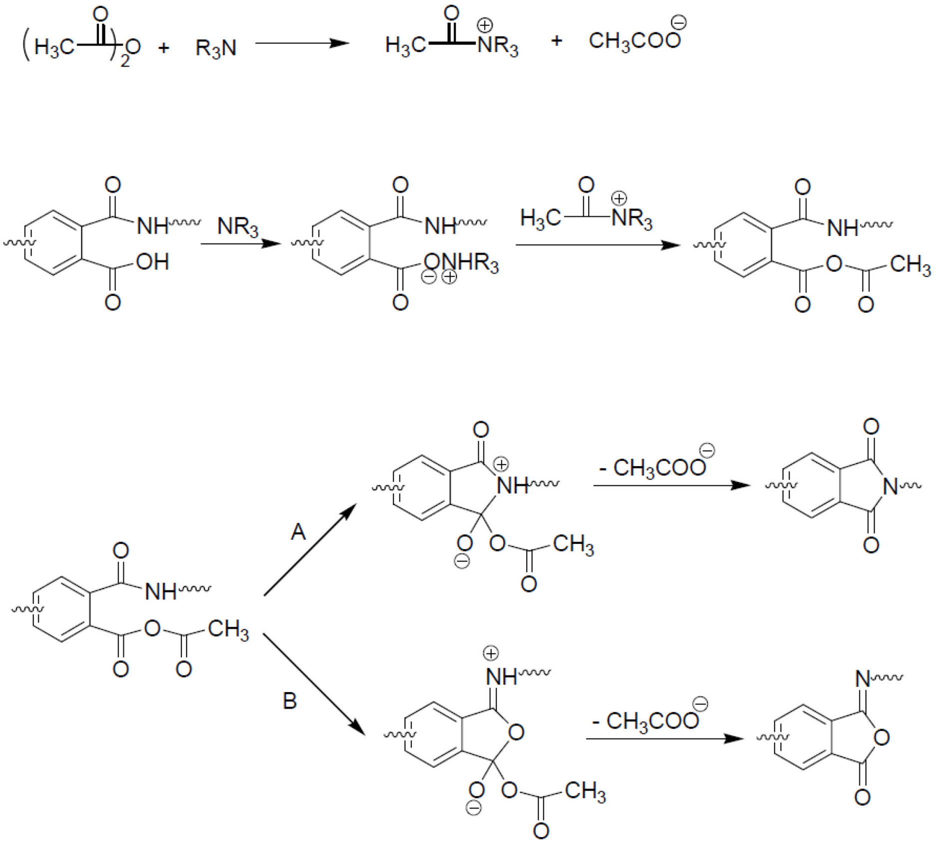

Figure 2.5. The reaction mechanism of chemical imidization.

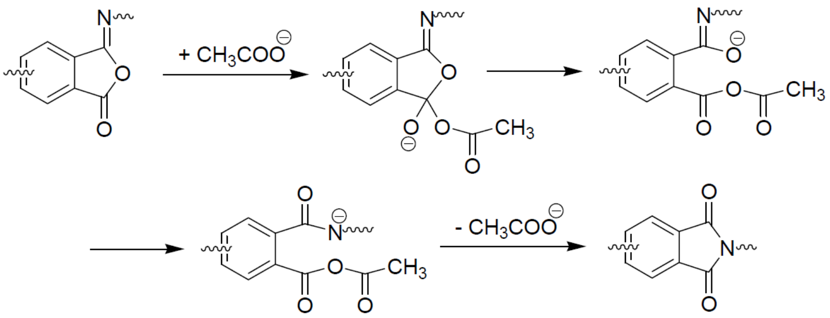

Figure 2.6. Rearrangement mechanism of isoimide rings to imides.

2.1.1.3. Solution Imidization

Solution imidization is another method for the synthesis of polyimides. Polyimides are synthesized at 160 – 200 °C by using high boiling solvents. Compared to thermal imidization, polymers with higher molecular weight are achieved by the method of solution imidization of poly(amic acid)s (Kreuz et al. 1966; Ayesha 2011).

2.1.2. Polyimides via Diesters of Tetracarboxylic Acids with Diamines

Tetracarboxylic acid esters are formed as a result of the reaction between aromatic dianhydrides and alcohols (Ghosh and Mittal 1996). The chemistry of PMR-15 polyimide which is developed by Lewis Research Center in NASA depends on amic ester (Serafini, Delvigs, and Lightsey 1972). As indicated in the Figure 2.7, anhydrides are converted to carboxylic acid ester by means of reaction with methanol. Dianhydrides are converted into esters to prevent further reaction below room temperature. (Ghosh and Mittal 1996). After the conversion, diamine is added into carboxylic ester / methanol solution. Poly(amic ester) is formed as a result of reaction between carboxylic acid ester and diamine. Subsequently, poly(amic ester) is thermally imidized at around 150 – 250 °C. The fact that methanol can be removed more easily than dipolar amide solvents gives an extra advantage for preparation of polyimides. The opportunity of isolating poly(amic ester) polymers by precipitation makes these polymers storable for a long time at ambient temperature. Further, PMR-15 polyimide can be cross-linked by further post curing process.

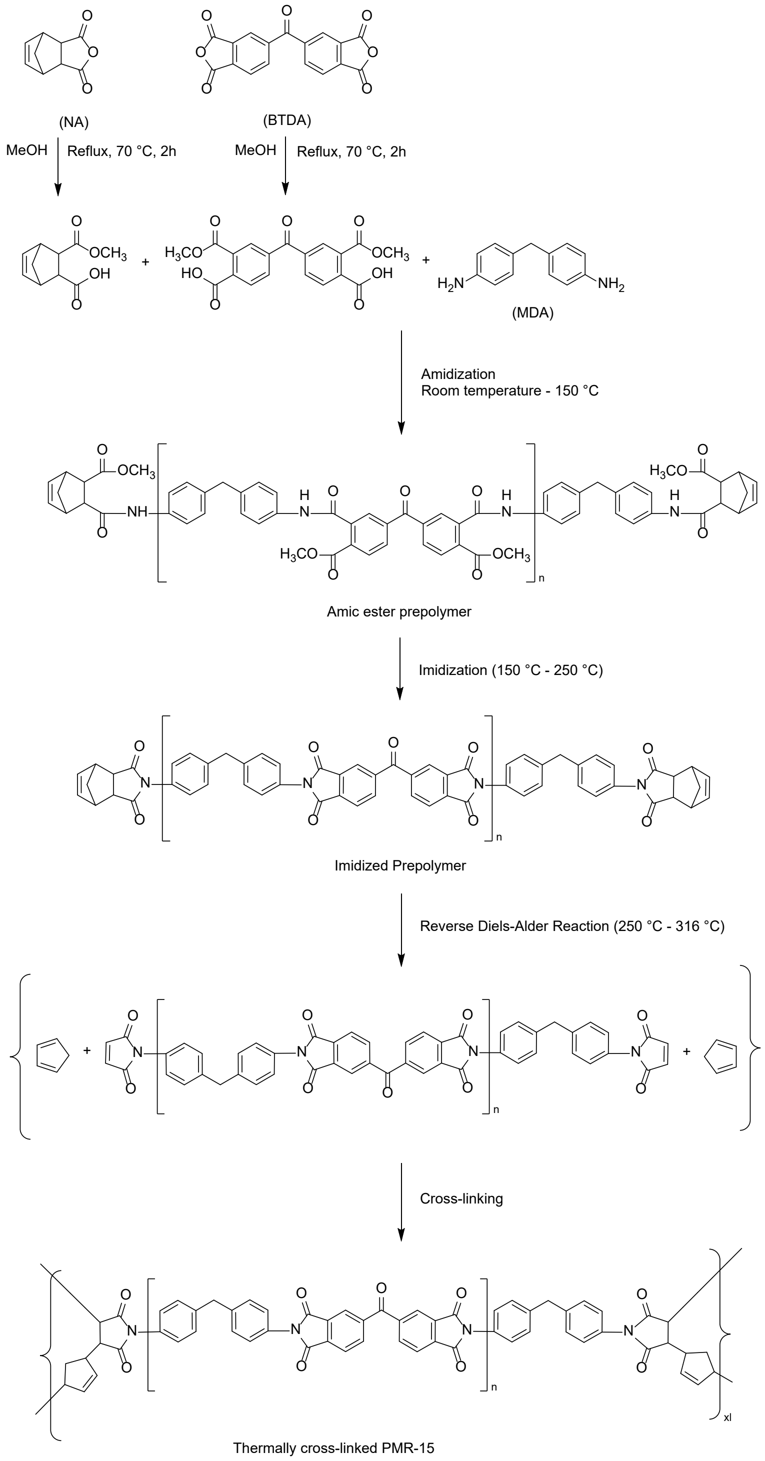

Figure 2.7. Synthesis route of PMR-15

2.1.3. Polyimides via Polyisoimides

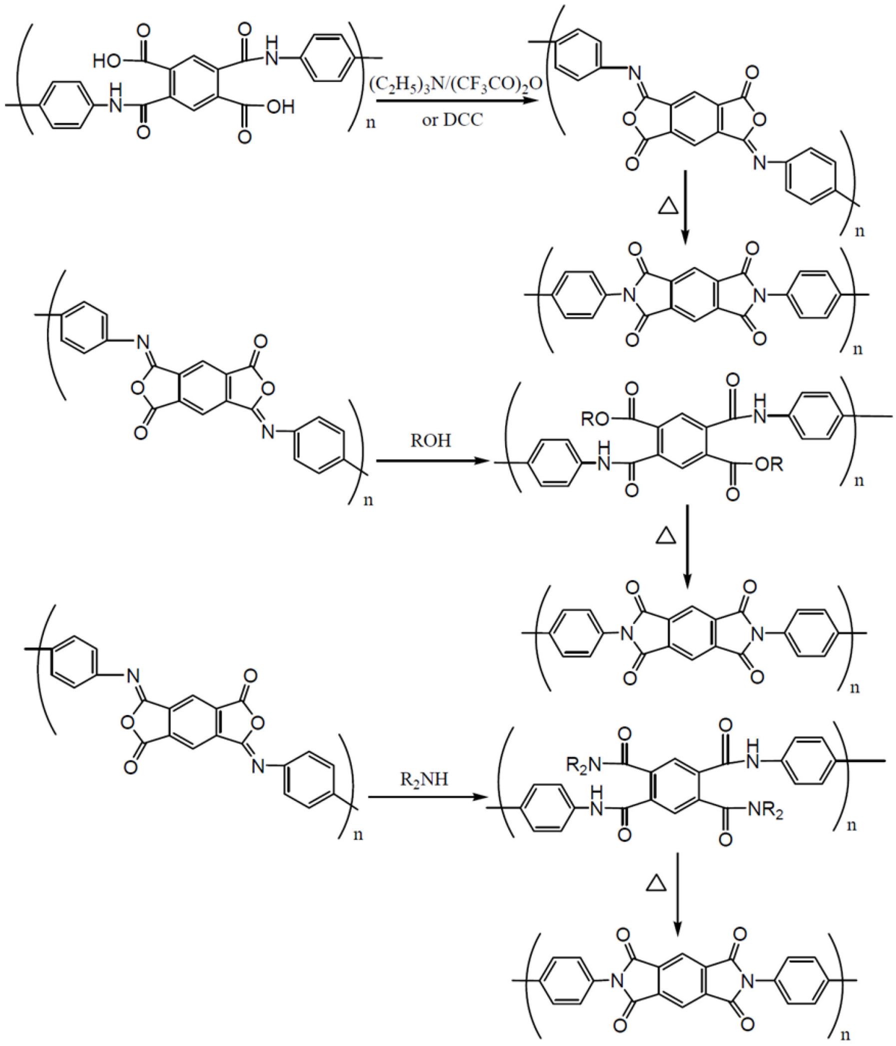

Figure 2.8. Synthesis of polyimides from polyisoimides.

Isoimides are derivatives of cyclic imides. Polyisoimides are synthesized from a reaction of a poly(amic acid) with a dehydrating agent, such as trifluoroacetic anhydride, in the presence of trimethylamine or N,N- dicyclohexylcarbodiimide (DCC) (Pilyugin and Gutsulyak 1963). On the other hand, polyimides are also synthesized by thermal treatment of pol(amic acid)s which are produced as a result of reaction of polyisoimides with amines (Delvigs, Hsu, and Serafini 1970). Polyisoimides, on reaction with alcohols, yield poly(amic ester)s. Then, poly(amic ester)s are similarly switched to polyimides by heating (Ghosh and Mittal 1996). Reaction scheme for the synthesis of polyimides from polyisoimides is indicated in Figure 2.8.

Due to their higher structural asymmetry and irregularity, polyisoimides usually have higher melt flow indices, higher solubilities and lower T_g than counterpart polyimides (Ghosh and Mittal 1996). These factors provide advantage in processing of the polymer. After shaping the material, polyisoimides can be thermally converted to corresponding polyimides above 250 °C (Ghosh and Mittal 1996).

2.1.4. One-Step Solution Polymerization Method

This technique is applicable to polyimide polymers that are soluble in organic solvents (Ghosh and Mittal 1996). Actually, there are a variety of single-step solution polymerization approaches for imidization. In high temperature solution imidization technique, the mixture of dianhydride and diamine monomers in a high boiling point solvent or solvent mixture is heated up to 140 – 250 °C. Then, imidization reaction takes place suddenly. Nitrobenzene, benzonitrile, α-chloronaphthalene, trichlorobenzenes and meta-cresol are widely used as high boiling point solvents in this technique. Additionally, toluene, o-dichlorobenzene, and 1-cyclohexyl-2-pyrrolidinone (CHP) are used as a co-solvent to remove the water coming from condensation reaction.

In fact, poly(amic acid) acts as an unstable intermediate in the process. It imidizes or returns to the starting monomers rapidly at high temperature (Ghosh and Mittal 1996). In an approach developed by Jin et al., polyphosphoric acid is used as a catalyst for the synthesis of aromatic polyimides at 220 °C (Jin et al. 2009). Behniafar and Ghorbani developed another technique for one-step solution polyimidization (Behniafar and Ghorbani 2008). They produced high molecular weight polyimides by reacting diamines with dianhydrides in the presence of glacial acetic acid at a high temperature. On the other hand, some of polyimides can also be synthesized by one-step method at room temperature. Kim and Moore synthesized a polyimide by reacting bis(dicyanomethylidene) derivative of PMDA (pyromellitic dianhydride) and ODA (oxydianiline) in NMP (N-methyl-2-pyrrolidone) (Kim and Moore 1993). The intermediate poly(amic acid) resulting from the reaction undergoes partial imidization at room temperature. After 24 hours, 75% of the reaction is completed. In fact, tetracarboxylic acids can also be used instead of dianhydrides in one-step method. While the use of tetracarboxylic acids does not affect the results, they are more stable and easily purified in comparison to anhydrides. In conclusion, one-step polyimide synthesis method has the advantage of higher imidization ratios and yielding high molecular weight polymers.

2.1.5. Polyimides via Dianhydrides and Diisocyanates

Reacting aromatic diisocyanates with dianhydrides is another technique for the polyimide synthesis (Moy, DePorter, and McGrath 1993; Johnston, Meador, and Alston 1987; Hurd and Prapas 1959; Alvino and Edelman 1978; Ghatge and Dandge 1976; Shinde, Ghatge, and Patil 1985). In this method, monomers react at nearly ambient temperatures in the presence of dipolar aprotic solvents, alcohols, water or tertiary amines (Carleton, Farrissey, and Rose 1972; Alvino and Edelman 1975; S. H. Han et al. 2004). The reaction scheme of the approach is shown in Figure 2.9 (Avadhani, Wadgaonkar, and Vernekar 1990). High molecular weight polyimides are formed on the removal of carbon dioxide from heterocyclic intermediate resulting from the reaction of dianhydride and isocyanate (Subramani et al. 2000).

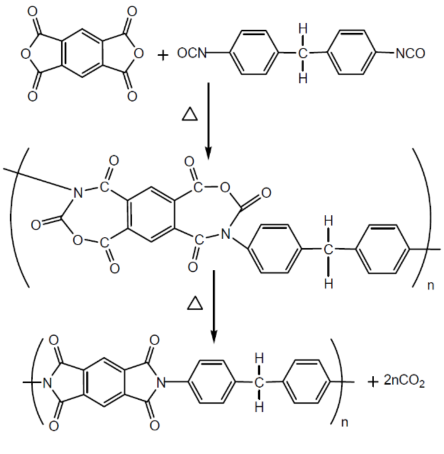

Figure 2.9. Polyimides via a dianhydride and a diisocyanate.

2.1.6. Polyimides via C-C Coupling

In addition to the methods mentioned above, polyimides can also be synthesized by Michael addition and Diels-Alder reactions (Kuramoto, Hayashi, and Nagai 1994; Laurienzo et al. 1994). The research dealing with carbon-carbon coupling imidization reactions catalyzed by palladium or nickel are also mentioned in literature (See Figure 2.10) (Perry, Tunney, and Wilson 1996; C. Gao et al. 2004; Schmitz, Rehahn, and Ballauff 1993).

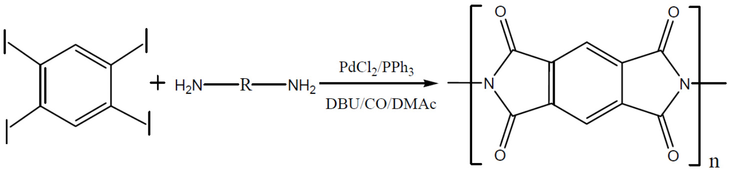

Figure 2.10. Polyimides via metal catalyzed C-C coupling (Source: Perry, Tunney, and Wilson 1996).

2.2. The Effect of Structure on Properties of Aromatic Polyimides

Physical and mechanical characteristics of polyimides can be modified by changing chemical structure and chain size of the polymer. Molecular symmetry, regularity, steric hindrance and chemical compositions of the backbone and side groups on polymer chains are factors that determine the chemical structure of the polymer. There is a lot of information in the literature describing the effect of modifications in structure of polyimides on its physical and mechanical properties (Maya et al. 2004; Ghosh and Mittal 1996).

CHAPTER 3

ADHESION

Throughout history, different kinds of joining techniques have been used during the assembling of different parts. Some of the techniques are mechanical fastening, welding, breezing and adhesive bonding. Selection of the technique changes according to desired functions of the joints. In this thesis, adhesive bonding is one of the topics that is to be focused on. Actually, comprehensive and definite description of adhesion is difficult. According to ASTM D907, adhesion is defined as "the state in which two surfaces to be held together by interphase forces" (ASTM 2005). Adherends are parts which are wanted to be held together by adhesive bonding process (ASTM 2005). An adhesive is an interphase material which is used for adhesion of adherends (International 2010).

Adhesives have been used since ancient times. The first known adhesive material is bitumen (Akram 2015). Today, adhesives can be seen everywhere, for example consumer goods, electronics, packages, buildings, vehicles, etc. Adhesives can be classified according to their origin or function in the whole structure. In the aspect of their origin, adhesives can be grouped as natural or synthetic types. Natural adhesives are made from animal or herbal sources. Synthetic adhesives are mostly based on polymer materials. On the other hand, adhesives can be divided into two categories in terms of their structural, and nonstructural functions. Although there is no clear distinction between the two types, structural adhesives can be identified as bonding agents which have shear stress higher than 7 MPa and provide the structural durability in within the structural design values (Ebnesajjad and Landrock 2014; Mittal 2012b). Additionally, this type of adhesives has also resistance to environmental conditions. Nonstructural adhesives are, generally, used for bearing very low stress. Pressure-sensitive tapes can be given as examples for nonstructural adhesives.

3.1. Functions of Adhesives

Ebnesajjad mentions that the strength of mechanical fasteners is just limited to the structures in touching area (Ebnesajjad and Landrock 2014). Therefore, the stress can be intense in some regions. Adhesives act as a junction between parts. In contrary to mechanical fasteners, the stress between the adherends is distributed more homogenously throughout the joint with the help of adhesion (Ebnesajjad and Landrock 2014). Actually, mechanical strength of adhesive bonds is not greater than the strength of structural parts, generally. However, mechanical performance of adhesive joining can sometimes be the same as or even higher than the mechanical fasteners. Furthermore, adhesive bonding has not only cost effective but also weight effective performance in comparison to conventional assembling techniques.

In conventional fastening, destructions such as holes, grooves, etc. are used. Therefore, the stress is concentrated in small regions. However, the stress distribution between adhered parts can be spread in large areas with the help of adhesive bonding. On the other hand, smooth surfaces which are important requirements in aerospace industry can be obtained by adhesives (Ebnesajjad and Landrock 2014). By the way, thermal management and minimization of drag force can be achieved.

Many types of adhesives are used to join different types of materials. Dissimilar or the same combinations of materials such as metals, ceramics, polymers, composites can be joined by adhesives. In fact, the use of adhesives provides a great deal of convenience when considering the stress caused by thermal expansion of different surfaces at different temperatures. Therefore, flexible adhesives are widely used to prevent damages caused by thermal expansion (Ebnesajjad and Landrock 2014). Electrical conductivity of adhesives can be changed by using different kinds of additives in the ingredients of the base product. Conductor or insulator types of adhesives are used especially in EMI or EMC applications in order to provide electrical integrity. Besides the functions mentioned above, adhesives are also used for many purposes such as sealing, shock absorbing, cyclic strain absorbing, etc.

3.2. Advantages of Joining Using Adhesives

Some advantages of adhesive bonding technique are summarized below (L H Sharpe 1966; Harper 2002; DeLollis 1970):

- Homogeneous distribution of stress and spreading the stress to large areas
- Bond materials having any shape and any thickness
- Bond adherends being similar or dissimilar
- Reduce or inhibit electrochemical corrosion between dissimilar metals
- Withstand cyclic stress and fatigue
- Offer joints with minimized roughness forms
- Act as a sealant against environmental conditions
- Conduct/insulate heat and electricity
- Joint fixation temperature is usually too low for occurrence of deformation on metal parts
- Absorb vibration and shock
- Offer a considerable strength/weight ratio
- Faster and/or lower cost than mechanical fastening.

3.3. Disadvantages of Joining Using Adhesives

Some disadvantages of adhesive bonding are listed below (L H Sharpe 1966; Harper 2002; DeLollis 1970):

- Visual inspection of joints is impossible in case of use of opaque adherends.
- Surface preparation is critical to achieve strong bonds.
- Corrosive chemicals are used for surface treatment, generally.
- Long cure process may be required.
- Autoclaves, ovens, presses, and fixtures may be needed.
- Most of the adhesives have low service temperature up to approx. 177 °C. High temperature adhesives which can be used up to 371 °C are available

whereas they are usually more expensive

- Life of the joint depends on the environmental conditions.
- Can be affected by biological environment.
- Health and safety precautions are critical.
- Difficulty in disassembling.

3.4. Requirements for Successful Adhesive Joining

Some requirements for adhesive joints with high quality are mentioned below (Harper 2002):

- Proper selection of the right adhesive
- Proper joint design
- Cleanliness of adherend surfaces
- Wetting of adherends
- Proper curing and solidification processes

There are many adhesive options to perform the bonding process. The situations of surfaces to be joined, shear strength which is required for end use, and the curing process are important factors that should be evaluated to address the right adhesive.

Proper joint design is another factor that can affect the mechanical strength of joint (Troughton 2008). Therefore, stronger joints can be produced by the combination of the right joint design with the right adhesive type.

Cleanliness of surfaces to be joined is essential for strong adhesive bonding. Dust, oil, moisture, and oxide layers are some of impurities that must be carefully cleaned before the joining process. Actually, if these elements are not removed properly, the applied adhesive can be easily peeled off. Surfaces of substrates can be cleaned by using different chemical and physical surface treatments (Ebnesajjad 2014).

Another factor for good adhesion is wetting. Wetting is continuous molecular contact between an adhesive and surfaces of adherends. The efficiency of adhesion increases with successful wetting (Tracton 2005).

The process of adhesive bonding is a critical issue for good adhesion. Determination of correct temperature, pressure as well as the time periods for the application are important parameters of the process. Petrie reports that there are three ways for conversion of liquid adhesives to solid (Harper 2002). The method of solidification can be changed according to the type of adhesive. The author lists the following methods:

- “Chemical reaction by any combination of heat, pressure, and curing agents”
- “Cooling from molten liquid”
- “Drying by solvent evaporation”

3.5. Theories of Adhesion

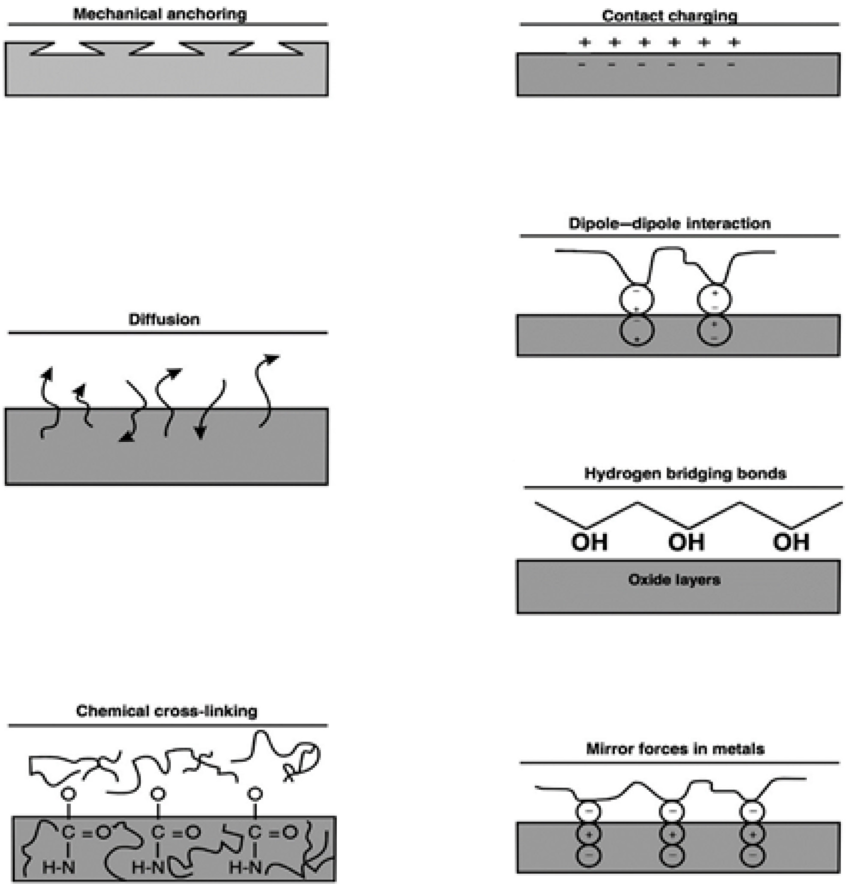

Figure 3.1. Physical and chemical factors causing for adhesion (Source: Goldschmidt and Streitberger 2003).

Although the formation of adhesion is not clear, there are some approaches trying to explain the subject. Generally accepted theories about the mechanism of adhesion are mechanical locking, electrostatic interaction, diffusion, and adsorption/surface reaction (Ebnesajjad and Landrock 2014). Wettability, chemical bonding, acid-base interaction, and weak boundary layer are some expanded theories of the last. Physical and chemical factors causing for adhesion are shown in Figure 3.1. In fact, it is not true to rely the mechanism of adhesive joining just only on one theory. Different combinations of all the theories can play a role for adhesion.

It is obvious that all the interactions between an adhesive and an adherend are mainly realized at atomic and molecular level. Perhaps, interactions at microscopic and macroscopic scales should be evaluated in order to understand different types of adhesion theories. Scales of adhesions are indicated in Table 3.1. For instance, surface roughness of adherends noticeably affects the mechanical interlocking between adhesives and adherends. The total surface area, being the microscopic parameter for the process, increases with increasing surface roughness. Therefore, the adhesive-adherend interaction increases. Surface roughness can be analyzed by electron or optical microscopy. Electrostatic interactions between adhesives and adherends involves the macroscopic parameter of surface charge. Lastly, diffusion is formed as a result of interactions at atomic and molecular scales.

Table 3.1. Scales of adhesion (Source: Ebnesajjad and Landrock 2014).

Traditional Theories	**Recent Theories**	**Scale of Action**
Mechanical interlocking	Mechanical interlocking	Microscopic
Electrostatic interaction	Electrostatic interaction	Macroscopic
Diffusion	Diffusion	Molecular
Adsorption/surface reaction	Wettability	Molecular
	Chemical bonding	Atomic
	Acid-base	Molecular
	Weak boundary layer	Molecular

3.5.1. Mechanical Interlocking Theory

Mechanical interlocking theory describes the adhesion as interlocking of an adhesive into rough surfaces of adherends. According to the theory, an adhesive penetrates into voids in the rough surface by flowing. After solidification of the adhesive, adhesion occurs by interlocking. In addition to interaction at atomic level, mechanical interlocking provides extra strength to the bond. Therefore, adhesion strength on rough surfaces is higher than on smooth surfaces.

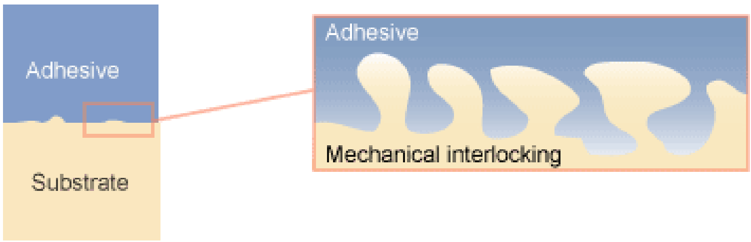

Figure 3.2. Mechanical interlocking theory (Source: Akram 2015).

Surface treatment processes have been categorized according to properties of roughness (Venables 1984). These are:

Group I: Macro -roughness (pore size > 0.1 mm) or no micro-roughness (pore size < 0.1 mm) producing surface processes

Group II: Large degree of macro-roughness producing surface processes

Group III: Surface processes producing a high percentage of micro-roughness from the porous oxide layer (no/low degree macro-roughness)

Ebnesajjad et al. reports that enhancement in bonding performance with the application of abrasion may be originated form formation of (i) a clean surface, (ii) a reactive surface (iii) an increase in surface area, and (iv) mechanical interlocking (Ebnesajjad and Landrock 2014). Petrie propose that the strength of adhesion increases by adjusting physical and chemical properties of adherend surfaces (Petrie 2004). For example, wetting capability of the surface area can be improved by increasing the surface area. Therefore, adhesion performance of adhesives can be improved. Besides the supportive information in the literature about advantages of increased surface roughness, there are also conflicting remarks reporting disadvantages of increased roughness (Allen 1993).

3.5.2. Diffusion Theory

Diffusion theory proposes that adhesion occurs due to interdiffusion of macromolecules between the adhesive and the substrate (Voyutskii and Vakula 1963). The detailed mechanism of the theory studied by Voyutskii. The author states that diffusion theory is mostly applicable for adhesives and substrates which have sufficiently mobile and soluble macromolecular chains (Voyutskii and Vakula 1963). The direction of the formation of diffusion depends on joining conditions as well as structure of materials. Diffusion typically happens in the rage of 1-100 nm sized interfacial thickness. This theory is generally valid for polymer-based adhesives and substrates. Welding of thermoplastics by heat takes place by diffusion of macromolecules (Petrie 2004).

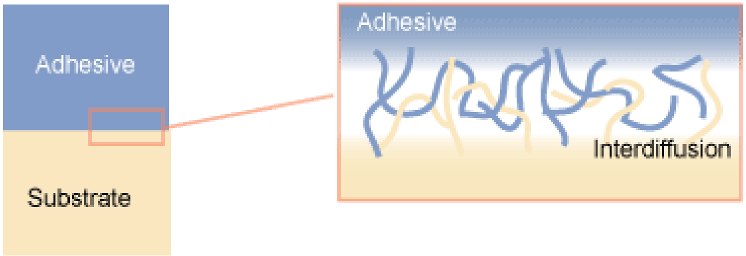

Figure 3.3. Diffusion theory (Source: Akram 2015).

In fact, diffusion occurs as a result of thermodynamic potential difference between an adhesive and an adherend. According to Vasenin's diffusion model, the amount of diffusing material (m) in x direction per unit area is related to concentration gradient ($\partial c/\partial x$), diffusion coefficient (D_f), and the time, t (Vasenin R.M. 1960).

$$\partial m = -D_f \partial t \frac{\partial c}{\partial x} \tag{3.1}$$

Vasenin proposes that the depth of penetration of diffusing macromolecules (l_p) can be predicted by using mobility constant of macromolecules (D_d), time of contact (t_c):

$$l_p \sim -\, k(\pi D_d t_c^{0.5})^{0.5} \tag{3.2}$$

k: constant

Therefore, Vasenin calculates the peel energy (G) by using the depth of penetration of macromolecules and the number of polymer chains at the interface. Therefore, G can be estimated by using the following equation:

$$G \sim K \left(\frac{2N\rho}{M}\right)^{2/3} (\pi D_d t_c^{0.5})^{0.5} \tag{3.3}$$

K: Constant of the polymer in contact
N: Avogadro’s number
ρ: Density
M: Molecular weight of the polymer

Ebnesajjad and Arthur reports that stress concentration does not exist in the interface due to continuity of physical properties (Ebnesajjad and Landrock 2014). According to the authors, bonding formation due to diffusion can be explained by cohesive energy density (*CED*). They imply that joining strength increases while solubility parameters (δ) of the adhesive and the substrate are getting closer. This situation can be indicated by the following equations:

$$CED = \frac{E_{coh}}{V} \tag{3.4}$$

$$\delta = \sqrt{\frac{E_{coh}}{V}} \tag{3.5}$$

E_{coh} is the energy required to separate the macromolecules to an infinite distance, and V is the molar volume.

3.5.3. Electrostatic Theory

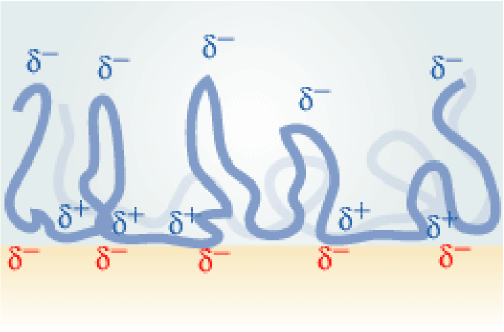

Figure 3.4. Electrostatic theory (Source: Akram 2015).

According to electrostatic theory which is introduced by Deryaguin and co-workers, adhesion happens due to electrostatic interaction between materials (See Figure 3.4) (Derjagin and Krotova 1948; Derjaguin and Smilga 1967; Derjaguin and Toporov 1983; Mittal 2012a). The authors state that both an adhesive and a substrate must have dissimilar electronic band arrangements for occurrence of adhesion. They also say that electrostatic forces in the form of electrical double layer will be formed due to electron transfer between an adhesive and a substrate in case of contact. Therefore, the forces contribute to the adhesion strength between the materials by providing extra resistance to separation.

Adhesively bonded joints formed by polymer-metal interface can be explained by this theory. However, Roberts reports that the effect of electrostatic interaction on adhesion is smaller than chemical bonding theory (Roberts 1977b, 1977a).

3.5.4. Wetting Theory

Wetting theory suggests that adhesion takes place by interfacial forces between materials as a result of their contact (Ebnesajjad and Landrock 2014). The theory is applicable to solid-liquid materials. The efficiency of adhesion is related to wetting of adherend surface. Wetting can be described as formation of continuous contact between an adhesive and a substrate. The wetting capability of adhesives increases with decreasing surface tension.

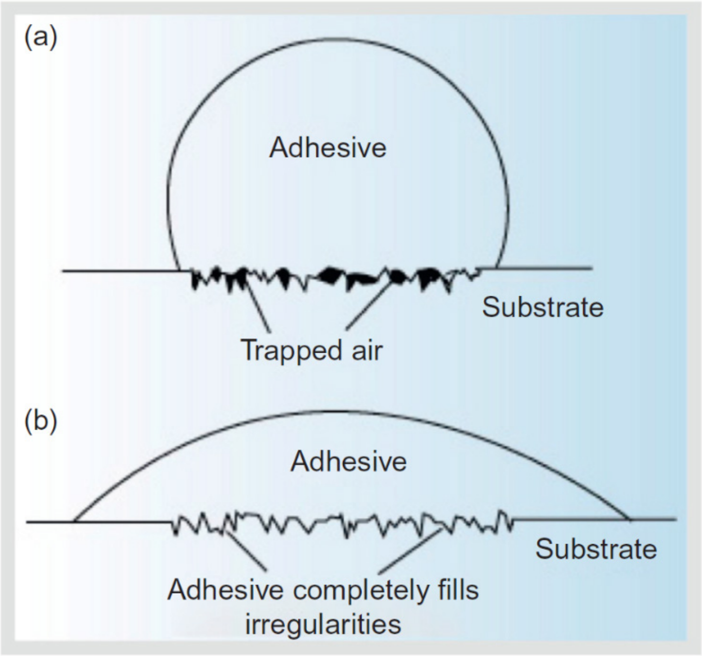

Figure 3.5. Examples of (a) poor and (b) good wetting adhesives spreading on a surface (Source: Petrie 2004).

The illustration of good and poor wetting adhesives spreading on a surface is indicated in Figure 3.5. Complete wetting results when the adhesive penetrates into all of the irregularities on the adherend surface. On the other hand, incomplete wetting is caused by the reduced contact area between an adhesive and adherend surface (Petrie 2004). Poor wetting lowers adhesion due to the formation of interfacial weaknesses in the adhesive bond. The highest adhesion strength occurs as a result of good wetting.

For complete wetting, the surface tension of the adhesive should be lower than those of the adherend (Petrie 2004). Besides the most adhesives which easily wet metal substrates, Petrie states that surface tensions of many adherends are lower than those of various adhesives. For example, adhesively bonded metal-epoxy joints are stronger than untreated polymer-epoxy joints. Therefore, different types of surface treatment processes are used in order to increase the surface energy of plastic adherends.

3.5.5. Chemical Bonding Theory

Chemical bonding theory relates the formation of adhesion to chemical interactions. Covalent bonds, hydrogen bonds, Lifshitz – van der Waals forces, and acid – base interactions are involved in chemical bonding. The formation of the type of interactions depends on the chemical structure of the adhesive and the adherend. The magnitudes of some interactions are listed in Table 3.2. As it is seen in the table, covalent, ionic, and hydrogen bonds are stronger than the dispersion types.

Table 3.2. Energies of Lifshitz – van der Waals Interactions and Chemical Bonds (Source: Ebnesajjad and Landrock 2014).

Type	Example	*E* (kJ/mol)
Covalent	C – C	350
Ion – Ion	Na^+ …. Cl^-	450
Ion – Dipole	Na^+ …. CF_3H	33
Dipole – Dipole	CF_3H …. CF_3H	2
London Dispersion	CF_4 …. CF_4	2
Hydrogen Bonding	H_2O …. H_2O	24

Covalent and ionic bonds which are the types of chemical bonding are much stronger than the secondary bonds. Therefore, they have higher adhesion strength. On the other hand, secondary bonds, such as hydrogen bonds, are physical forces having weaker adhesion strength. Secondary bonds are usually found in materials containing polar functional groups. Other adhesion mechanisms such as mechanical interlocking, diffusion, and electrostatic interaction may also strengthen such interactions (Ebnesajjad and Landrock 2014).

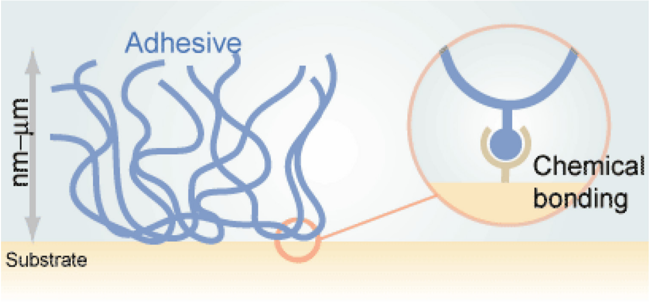

Figure 3.6. Adhesion by chemical bonding (Source: Petrie 2004).

The descriptions of intermolecular forces are mentioned below:

Dipole (polar molecule) is a molecule whose allocations of negative and positive charges are centered in different poles.

Dipole–dipole forces arises when positive end of a polar molecule is aligned near the negative end of another.

Hydrogen bonding occurs by the interaction between a hydrogen atom and the lone pairs of electrons of a hydrogen bonded F, O, and N atoms.

London dispersion forces (dispersion forces) are forces arising from instantaneous dipoles occurring during the changes in the positions of electrons around the nuclei.

Covalent bonds generally occur at cross-linked adhesives and thermosets (Ebnesajjad and Landrock 2014). In comparison to the other bonds, the strength and durability of covalent bonds are generally the highest. However, surfaces of adherends should contain reactive functional groups in order to produce bonds. The surfaces of some materials such as polymers, and composites already consist of different reactive groups. On the other hand, some surfaces which have no reactive groups should be treated with special techniques, such as corona, to develop functional groups.

Organosilanes are commonly used for making glass fibers compatible with the resins in fiberglass-reinforced composites. Therefore, the adhesion between the glass and the resin is stimulated. In addition, organosilanes are used as primers to promote adhesion of adhesives to various type of materials. Organosilanes are converted to silanol groups during the process. These silanol groups react with silanol groups on surfaces of substrates such as glasses or metal oxides. Therefore, strong ether bridges are produced. In addition, adhesives consisting of carboxyl or hydroxyl groups can form strong chemical bonds with materials having the similar functional groups. Adherends containing hydroxyl groups may also form chemical bonds with isocyanate group containing adhesives such as polyurethanes. Additionally, resins containing epoxy groups tend to adhere strongly to substrates containing hydroxyl groups (Ebnesajjad and Landrock 2014).

3.5.5.1. Acid – Base Theory

Acid-base theory is one of the recent theories that has been put forward to describe adhesive joining. The mechanism of the theory depends on Lewis acid and base concepts which are suggested by J. N. Bronsted and G. N. Lewis. In 1938, Lewis defined an acid as an electron acceptor (i.e. electron poor) substance; a base as an electron pair donor (i.e. electron rich) substance (S.P. 1992). According to this definition, every cation and chemical substances, such as BF_3 and SiO_2, are acids (Ebnesajjad and Landrock 2014). On the other hand, every anion and substances, such as NH_3, PH_3 and $C_6H_5CH_2NH_2$, are bases. Acid-base theory states that adhesion occurs by the attraction between Lewis acids and bases. Fowkes and co-workers, Gutmann, and Bolger and Michaels have some researches regarding with the effect of acid – base interactions on adhesion (F. M. Fowkes 1981; Frederick M. Fowkes 1964; F M Fowkes and Mostafa 1978; Frederick M Fowkes and Mostafa 1977; Staemmler 1979; Bolger and Michaels 1968).

BF_3 and NH_3 can be taken as an example for the explanation of acid – base theory. Fluorine which is an electronegative atom attracts the shared electrons on itself. Therefore, the positive charge is centered in boron and negative charge is centered in fluorine. On the contrary, nitrogen which is the electron rich atom on NH_3 acts as negative charge center. Therefore, polar attraction between the positive boron side of BH_3 and negative nitrogen side occurs (Ebnesajjad and Landrock 2014).

3.5.6. Adsorption Theory

Adsorption theory was introduced by Sharpe and Schonhorn (Louis H. Sharpe and Schonhorn 1964). According to the theory, materials stick to each other due to the interatomic forces resulting from interaction between the adhesive and the adherend. Secondary forces, especially van der Waals forces, are factors that are effective in the mechanism resulting from the adsorption. Chemical bonds, as well as the corresponding forces, impart more strength to adhesion (Kinloch 1980).

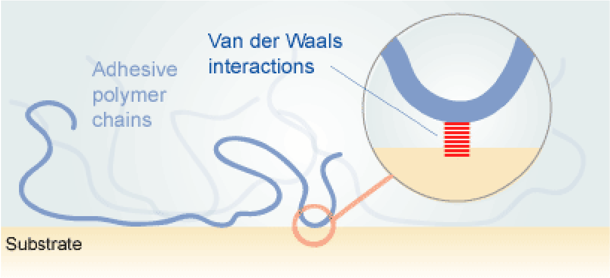

Figure 3.7. Van der Waals interactions between the adhesive and the substrate (Source: Akram 2015).

3.5.7. Weak Boundary Layer Theory

Weak Boundary Layer Theory, being proposed by Bikerman, explains the failure of bonds results from a weak layer on the adherend, in the adhesive or at the interface between them (Bikerman 1967). Generally, cohesive failures occur as a result of the presence of weak boundary layers. In fact, elements coming from the adhesive, the substrate, or the environment may cause weak boundary layers (Ebnesajjad and Landrock 2014). Formation of the layers occur before or during the application of the adhesive. If the adhesive is considered, impurities, releasing agents, or insufficiently preparation of the adhesive are some factors that cause weak boundary layers. Oils, dust, oxides, air, moisture, or foreign objects are weak boundary layers on adherend surfaces. On the other hand, corrosion or rust layers are some weak layers resulting from the environment.

3.6. High Temperature Adhesives

Most of the adhesives are polymer based and start to decompose above 200 °C. The mechanical properties of metal-based structures begin to change slowly at high temperatures. However, degradation in adhesives occurs because of the polymer-based nature of these materials. Therefore, the chemical and mechanical strength of adhesives at high temperatures are among the most important limiting criteria for these materials (Marques et al. 2015). Consequently, in applications requiring thermal stability, the appropriate adhesive should be chosen.

Table 3.3. Typical glass transition temperatures of adhesives.

Adhesives	**T_g (°C)**
Epoxies	
Hardened Epoxy	50–150
Epoxy Phenolic	200
Epoxy Nylon	50
Epoxy Polysulfide	50
Phenolics	
Nitrile Phenolic	120
Vinyl Phenolic	70
Neoprene Phenolic	70
High Temperature Adhesives	
Bismaleimides	210–280
Polyimides	340–430
Hard Polyurethanes	20–50
Anaerobics	120
Cyanoacrylates	80
Modified Acrylics	60–120

One of the important indicators of the suitability of the adhesive for high temperature applications is T_g (glass transition temperature). At temperatures below T_g, the adhesives exhibit high modulus and mechanical strength properties, while the ductility of these materials is reduced. Therefore, the T_g of the adhesive must be high in order to exhibit effective adhesion performance at high temperatures. Polyimide, bismaleimide, acrylic, epoxy, phenolic, and ceramic adhesives as well as room temperature vulcanized silicone adhesives are among the widely used adhesives. The T_g values of the adhesives are given in Table 3.3.

3.6.1. Polyimide Adhesives

Polyimides from high temperature adhesives attract attention due to their outstanding performance over 200 °C. They are usually used with supports such as nylon, polyester or glass fiber reinforced films. While many researches on polyimides have been carried out by NASA, intensive studies have been made especially on high performance LARC type polyimides (Stenzenberger 1986). These adhesives are mostly used for bonding metals, such as aluminum, titanium, stainless steel, copper and bronze. The polyimide adhesives are cured by undergoing imidization at low pressure and at temperatures close to 350 °C. Progar and Clair did lap shear tests on LARC-TPI type polyimide adhesives (Progar and ST. Clair 1994). They found that such adhesives exhibit lap shear strengths in the range of 20.7 to 41.4 MPa at room conditions. On the other hand, they found that the polyimides exhibit adhesion strength ranging from 13.8 to 20.7 MPa at high temperatures. Tests carried out by Hergenrother et al. on different polyimide adhesives in amorphous form showed that these materials reached maximum strength up to 54.1 MPa at room conditions and this value decreased to 28.3 MPa at 121 °C (Harris, Beltz, and Hergenrother 1987).

3.6.2. Bismaleimide Adhesives

Bismaleimide (BMI) resins are a type of thermosetting polymers that are non-flammable. These polymers exhibit very good mechanical strength performance at high temperatures and high humidity levels (Stenzenberger 1986). Their working temperatures can reach up to the range of 230 – 290 °C. In terms of operating temperature, these temperature values are close to the high-performance polyimide resins. On the other hand, BMI resins are very brittle due to high density of crosslinks in their chemical structures. As a result of the investigations, this problem was solved by adding diallylbisphenol A (DABA) to the BMI structure, but it was understood that the toughness of the formed copolymer is close to the high performance epoxy resins (Stenzenberger 1986). Another noteworthy property of BMI is that these resins do not release volatile substances during the curing process. For this reason, the formation of small voids can be avoided by applying less contact pressure than the pressure applied to the polyimides during the bonding process.

3.6.3. Acrylic Adhesives

While acrylic adhesives are generally presented to the market as pressure sensitive adhesive products, some types of acrylics can be used at high temperatures (Creton 2017). Though cyanoacrylate adhesives are more brittle than acrylic adhesives, acrylics can provide the mechanical strength required in many applications. Adhesives such as poly(methyl methacrylate)s can work up to temperatures of around 105 °C. In addition, some acrylic adhesives which are developed with epoxy chemistry can also be used at temperatures higher than 149 °C (Schneberger 1983). Lu et al. have developed a similar type of pressure sensitive acrylic adhesive that can be used up to a temperature of 150°C (X. Lu et al. 2014). They obtained the product by using specific crosslinking compounds.

3.6.4. Phenolic Adhesives

Phenolic adhesives with phenol formaldehyde content are among the first known synthetic resins. These adhesives have high adhesion strength on polar surfaces. They exhibit notable mechanical strength and combustion resistance as well as good performance at high temperatures (Schneberger 1983). Phenolic resins have flame retardant and low smoke emission properties. Therefore, they are used in the production of carbon fiber reinforced composites which can exhibit superior combustion resistance performance up to 500 °C. On the other hand, phenolic resins, known as materials with low toughness, are very hard due to the high amount of crosslinks in the structures (Ritter 2008). Therefore, phenolic adhesives containing the mixture of phenolics and nitrile rubbers are used in order to solve the problem of rigidity in space and aviation applications. Thus, the chemical and thermal resistance of the phenolic resins are combined with the toughness and fuel compatibility of the nitrile rubbers to achieve the desired properties (Schneberger 1983). The adhesives obtained by the way are used as metal binders which have the capability of operating between -55 and +300 °C. In addition, phenolic adhesives can gain better thermophysical properties by conversion to carbon-coal at nearly 1000 °C (Hendricks and Hale 1985; Lefebvre et al. 2005; Jiang et al. 2007; J. Wang, Jiang, and Jiang 2009b, 2009a). With additives such as nanosilica, fused silica and boron carbide, the mechanical and thermal strength of these adhesives can be further increased from 4 MPa to 17 MPa (Haddadi, Mahdavian-Ahadi, and Abbasi 2014; Bhowmik et al. 2006).

3.6.5. Ceramic Adhesives

Ceramic adhesives are another adhesive that can be used at high temperatures above 300 °C. The working temperature of some ceramic adhesives varies from -185 °C to +1290 °C (Bhowmik et al. 2006). Such adhesives generally consist of two components, binder and filler. The curing temperatures of ceramic adhesives are between 260 °C and 1000 °C. For this reason, when these materials are used, the parts to be bonded must be resistant in this temperature range. Although they do not show good mechanical strength compared to high performance ceramics, it was pointed out that they performed satisfactorily in some studies (Abuhaimed, Nawareg, and Baier 2014; Goldstein, Leiser, and Katvala 1978). Therefore, the application areas of ceramic adhesives are limited to places that do not require high mechanical strength such as halogen lamps, high temperature sensors, heaters and igniters. It has been found that adhesion strength performances up to 40 MPa at 800 °C and up to about 30 MPa at 1000 °C can be achieved with recently developed BC_4 and glass powder admixed pre-ceramic polymer adhesives (X. Z. Wang, Wang, and Wang 2012; X. Wang, Wang, and Wang 2013). With the further development of ceramic adhesives, relevant work is ongoing.

3.6.6. Room Temperature Vulcanizing Silicone Adhesives

Most space and aeronautical applications require materials that can operate under harsh conditions. In these applications it is possible to use adhesives with a thermal resistance between -60 °C and 200 °C. While materials such as polysulfides, flexible epoxies, silicones, polyurethanes, and toughened acrylics exhibit flexibility up to -30 °C, they show poor mechanical strength compared to other structural adhesives (Marques et al. 2015). RTV (Room Temperature Vulcanizing) silicones have been used in high and low temperature conditions since 1957(Banea and da Silva 2010) .

3.6.7. Other Adhesives

Liquid crystal thermosets (LCTs) are among the potential adhesive candidates for high temperature applications. These materials are mostly used at temperatures above 100 °C. Among the resulting LCT materials, it has been noted that Vectra ™, a fully aromatic polyester, can operate at a temperature range of 100 – 150 °C (J Economy and Andreopoulos 1993; James Economy, Gogeva, and Habbu 1992). As a result of their research, Iqbal et al. obtained a different type of LCT adhesive with glass transition temperature above 150 °C, low moisture absorption, better chemical and mechanical strength (M. Iqbal et al. 2010). This adhesive maintains 11 MPa lap shear strength up to 150 °C whereas the value drops to 4 MPa above the temperature.

Another type of adhesive that is in the development stage is the polytriazole resins. In a study, it was reported that crosslinkable polytriazole resins have 13 MPa adhesion strength on iron samples at room temperature (Yanpeng et al. 2013). The crosslinkable polytriazole resin shows superior adhesive strength (9 MPa) at 180 °C compared to epoxy adhesives. On the other hand, Tang et. al noted that the polytriazole adhesives, being hyperlinked with the click polymerization technique, exhibit 100 times higher adhesion strengths at room temperature than the other commercial adhesives (Tang et al. 2010). And also, they reported that the polymer demonstrates 5 times higher adhesion strength (e.g. 21 MPa at 250 °C) at high temperatures.

In recent years, polybenzimidazoles (PBI) are among the most sought-after materials due to their superior performance at high temperatures. These polymers have 425 °C glass transition temperature with 160 MPa mechanical strength and begin to decompose at 500 – 600 °C. Therefore, these materials take place among the materials that have the potential to be used as high temperature adhesives. Due to the difficulty of processing the polybenzimidazoles, special processing techniques need to be developed for adhesive applications of these materials (H. M. S. Iqbal, Bhowmik, and Benedictus 2014).

CHAPTER 4

SYNTHESIS AND CHARACTERIZATION OF NOVEL HIGH TEMPERATURE STRUCTURAL ADHESIVES BASED ON NADIC END CAPPED MDA-BTDA-ODA COPOLYIMIDE

4.1. Abstract

A series of random copolyimide adhesives was synthesized using 4,4’-diaminodiphenylmethane (MDA), 3,4’-oxydianiline (ODA) and 3,3’,4,4’-benzophenonetetracarboxylic acid dianhydride (BTDA) as co-monomers, and nadic anhydride as an end cap reagent. The adhesives with different MDA and ODA content were examined in terms of their structures, thermal stability, mechanical properties, and adhesive performance. They have thermal stabilities up to 500 °C and glass transition temperature (T_g) at around 400 °C. The effect of diamine monomer compositions on adhesion performance and processability of the copolyimides were studied. The copolyimides exhibit adhesion strength up to 16.3 MPa at room temperature. Nadic end capped MDA-BTDA-ODA copolyimide resin gained adjustable and controllable processability with the addition of ether bridged aromatic segments. The copolyimide adhesive with equimolar composition of MDA:ODA is distinguished form the both commercial PMR-15 and LARC RP-46 polyimides in terms of its better processability and mechanical performance.

4.2. Introduction

Lightweight materials provide considerable advances by improving the fuel efficiency and performance of various vehicles. Aluminum and titanium alloys, and fiber reinforced polymer composites have been extensively used as structural materials due to their superior mechanical properties along with their lightweight features (Matsuzaki, Shibata, and Todoroki 2008; Naito, Onta, and Kogo 2012; Cole and Sherman 1995; Immarigeon et al. 1995). Different kinds of assembling techniques such as adhesive bonding, fastening and welding are used in order to join structural materials together. Adhesive bonding has been preferred to integrate the polymeric and metallic nature of materials because of their superior fatigue resistances, low weight, low costs, and large tolerances to damage (Adams and Wake 1984; Da Silva, Öchsner, and Adams 2011; Marques et al. 2015).

Indeed, most adhesives are polymer based, such as epoxies, phenolics, bismaleimides and acrylics (Hornung and Hajj 2009). Therefore, they have poor heat-resistant properties, which often lead to oxidation and failure at high-temperatures (Marques et al. 2015; Song, Muliana, and Palazotto 2016). The requirements of having thermal stability, good mechanical property and retention capability at elevated temperatures render the initiation of production of aromatic polymers, which are composed of aromatic rings linked to various functional groups (Saeed and Zhan 2007a). Aromatic polyimides (PI) exhibit amazing thermo-oxidative stabilities, low dielectric constants, high electrical resistivities, high glass transition and melting temperatures, and chemical stabilities (Scola 2001). However, the processing of polyimides is challenging due to their rigid polymer backbones and strong chain interactions that bring along insolubility and infusibility (Yi, Huang, and Yan 2016; Huo et al. 2011).

PI adhesives are promptly concerned in automobile, railway transport, aerospace and microelectronic industries (Ding 2007). The fabrication of PIs starts with the production of prepolymers consisting of polyamic acid solutions in polar solvents such as *N*-methylpyrrolidone, *N,N*- dimethylformamide or dimethylacetamide. Polyamic acids are produced by the reaction of diamines with dicarboxylic acid diesters as comonomers, and they are subsequently converted to polyimides by thermal or chemical treatments (Volksen, Miller, and Dubois 2009). The first commercial polyimide, Kapton™ was developed by DuPont in 1955 (Ghosh and Mittal 1996). Then, NASA Langley Research Centre developed the high performance thermoset polyimide PMR-15 in 1970's (Serafini, Delvigs, and Lightsey 1972). Because of its low cost for manufacturing and excellent performance at high temperatures, PMR-15 has shown to be promising candidate for high-temperature structural adhesives (Castelli, Sutter, and Benson 1998; Y. C. Lu et al. 2010; Ratta et al. 1999; Rozhanskii, Okuyama, and Goto 2000; Saeed and Zhan 2007b;

Douglas Wilson 1988) However, PMR-15 has both limited processing capability and flexibility problems because of its rigid backbone structure (Serafini, Delvigs, and Lightsey 1972). LARC RP-46, an alternative polymide homopolymer to PMR-15, was developed by NASA Langley Research Centre (R. P. Pater 1991). LARC RP-46 resin incorporates flexible 3,4'-oxydianiline (3,4'-ODA) monomers instead of methylenedianiline moieties in PMR-15. Pater's group reported that introduction of 3,4'-ODA into PMR structure offers improved processability due to the increase in resin flow (R. P. Pater 1991; Soucek and Pater 1993). Hou *et. al.* proposed that replacing the methylenedianiline moieties in PMR-15 with 3,4'-oxydianiline improves the structural durability, higher composite mechanical properties at high temperatures (Hou et al. 1996).

The challenge of enhancing PI's processability can be eliminated by some approaches such as the introduction of flexible ether linkages, fluorinated groups, bulky substituents and copolymerization (R. Pater and Morgan 1988; Chao et al. 2012; Chen, Qin, and Huang 2008; Chun 1994; J. P. Gao and Wang 1995; Y. Han, Fang, and Zuo 2010; Tamai, Yamaguchi, and Ohta 1996; Yi, Huang, and Yan 2016). PIs could exhibit low thermo-mechanical properties when they were synthesized from flexible monomers. While 3,3',4,4'-benzophenonetetracarboxylic acid dianhydride (BTDA), 4,4'-hexafluoroisopropylidene diphthalic anhydride (6FDA) and 4, 4'-oxydiphthalic anhydride (ODPA) are preferred as semi-rigid dianhydride monomers, 4,4'-diaminodiphenylmethane (MDA), 2,2'-bis [4-(4-aminophenoxy) phenyl] propane (BAPP) and 3,4'-oxydianiline (3,4'-ODA) are used as semi-flexible diamine monomers. Many researches have been performed to adjust the molecular structures of polyimides to enhance processing, while keeping the thermo-oxidative stability of the material. Copolymerization is one of the most efficient ways to improve the processability of the polymer (Chao et al. 2012). When a second dianhydride or diamine is introduced into the reaction, the symmetry and repetition of molecular structure is destroyed. Ultimately, the interaction between the rigid chains and crystallinity of the copolymer is reduced (Li et al. 2015). In literature, PMR-15 and LARC RP-46 polyimide homopolymers have been worked; however the effect of both MDA and 3,4'-ODA co-monomers on the processability of the copolyimide consisting these co-monomers has not been studied in detail (Liaw et al. 2012).

In the present study, novel nadic end capped high temperature copolyimide adhesives, MDA-BTDA-ODA, were synthesized at various MDA and ODA compositions. The effect of diamine composition on thermal, mechanical and adhesion properties of the resulting copolymers was investigated. Changing the composition of PMR-15 by replacing 4,4'-MDA with 3,4'-ODA in increments, 25%, 50%, and 75% was expected to reduce the rigidity or regularity of the backbone. Therefore, the processability and toughness of the polymer were aimed to be improved while maintaining the thermal stability.

4.3. Experimental

4.3.1. Materials

3,3’,4,4’-benzophenonetetracarboxylic dianhydride (BTDA) (98%), 3,4’-oxydianiline (3,4’-ODA) (98%) and nadic anhydride (NA) (98%) were purchased from Ivy Fine Chemicals. 4,4’-methylene dianiline (MDA) (≥ 97.0%) was delivered from Fluka. N,N-dimethyl formamide (≥ 99.98%) was received from Aldrich. Methanol (≥99.98%) was supplied by Merck. All chemicals were used as received without further purification. AVSIL 7PS pre-shrunk silica fabric was purchased from AVS Industries, LLC. 304 grade stainless steel alloy was used as the adherents. All the surfaces to be bonded were sanded using an automatic sanding pad with abrasive paper of grit size P80.

4.3.2. Synthesis of Polyimide Polymers

The synthesis of polyimides and copolyimides were carried out via a two-step method, which includes the preparation of polyamic ester (PAE) as a precursor along with thermal imidization process. The route for the synthesis of the copolyimide was explained in Figure 4.1 (Simone et al. 2005).

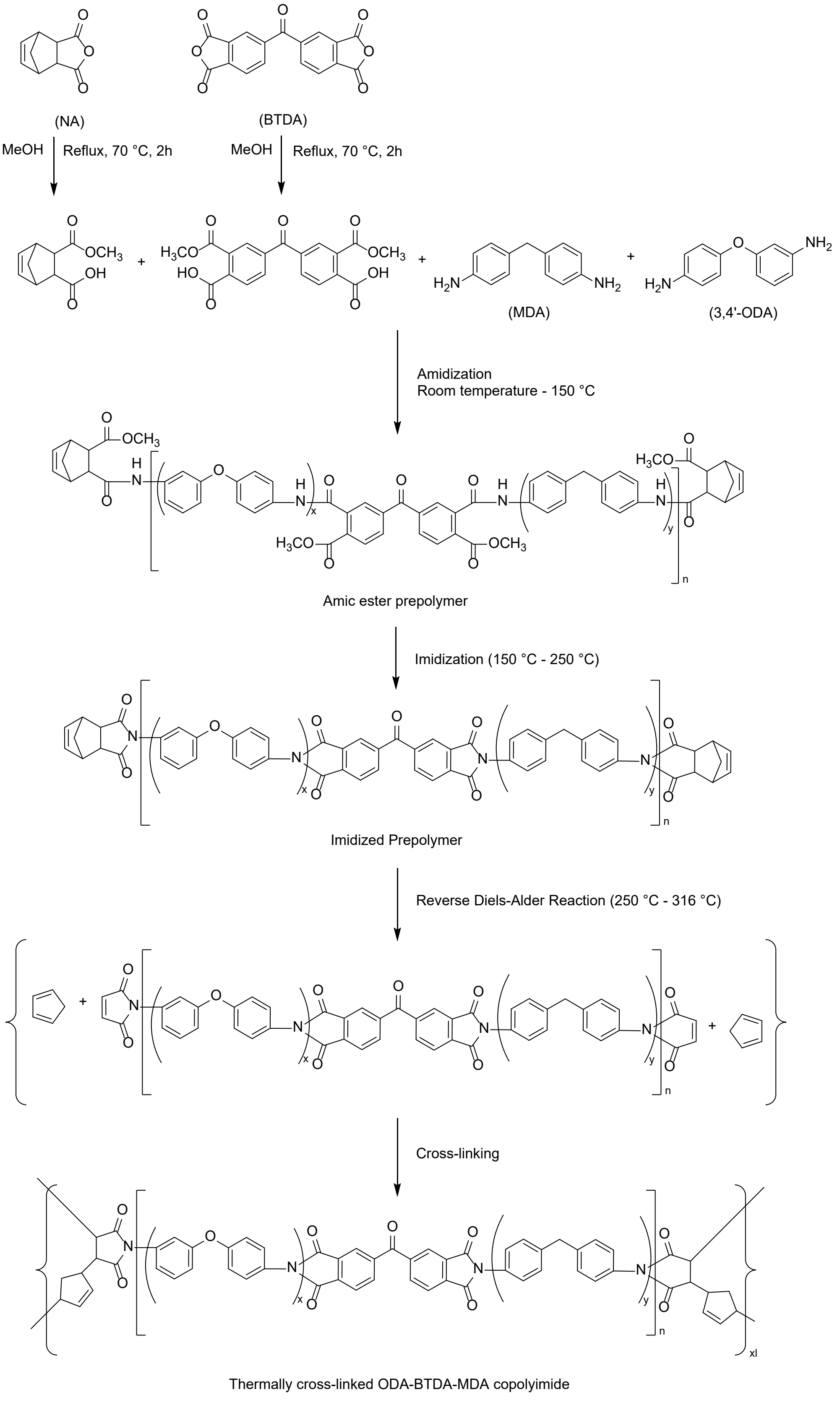

Figure 4.1. Reaction scheme for the synthesis of nadic end capped MDA-BTDA-ODA copolyimide polymers.

Four types of PAE samples with different MDA:ODA molar ratios (100:0, 75:25, 50:50, 25:75 and 0:100) were synthesized, namely PMR-15 prepolymer, PAE MDA:ODA [75:25], PAE MDA:ODA [50:50], PAE MDA:ODA [25:75] and LARC RP-46 prepolymer, respectively. PMR-15 prepolymer was prepared according to the procedure of Meador et al.(Meador, Johnston, and Cavano 1997) LARC RP-46 prepolymer was synthesized according to the procedure of Soucek et al.(Soucek and Pater 1993) Then, PAE samples were converted into the corresponding polyimides through thermal imidization. The mole ratio of NA:BTDA:(MDA+ODA) for the target molecular weight (1500 g/mol) was calculated as 2:n:(n+1) by using the Carothers equation (n = 2.087). In the synthesis of PAE MDA:ODA [50:50] for example: NA (3.28 g, 20 mmol) and BTDA (6.72 g, 20.9 mmol) were refluxed in 18.14 g of methanol for 2 h at 70 °C. At the reflux process, the solid chemicals dissolved forming a clear solution. After reflux, the solution was cooled to room temperature. Then, MDA (3.06 g, 15.4 mmol) and ODA (3.09 g, 15.4 mmol) were added into the solution. After that, the solution was stirred at room temperature until MDA and ODA were dissolved. At the end of the process, PAE resin solution is obtained.

Some of the resin solution were used as adhesive. PAE powder was also obtained from the resin solution by removing methanol through rotary evaporation at 35 °C under vacuum. After removing the solvent, the resulting PAA foam was gently crushed to fine solids.

4.3.3. Preparation of Lap Shear Strength Test Specimens

The lap shear strength test specimens were prepared in accordance with ASTM D1002 (International 2010). The size of the adherend was 101.6 x 25.4 x 1.6 mm. Two pieces of steel adherends were prepared and the surfaces of the adherends were sanded Figure 4.2). The sanded adherends were cleaned by acetone and dried at room temperature before bonding.

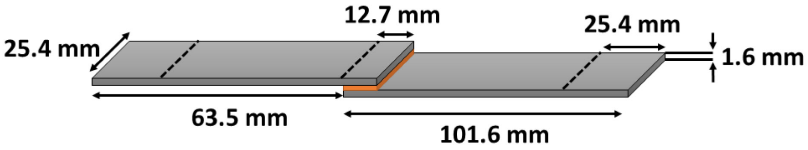

Figure 4.2. Dimensions of the single lap-joint specimen.

The adherends were degassed at 35 °C for 30 min. in a vacuum oven to remove bubbles after polyimide precursor solution had been spread. Two pieces of steel sheet adherends, which were gummed with prepolymer coating, were stuck together in such a manner to get an overlap of 12.7 mm. The single lap-joint samples were anchored with a fixture, and they were placed into air circulation oven to undergo a stepwise imidization process. The adhesive was cured through thermal imidization by raising the temperature to 150, 200, 250, 275 and 316 °C, and the sample was held for 1 h at each of these temperatures.

4.3.4. Characterization

Infrared spectra (FT-IR) of the synthesized polyimide and copolyimide samples were recorded on a Perkin Elmer Spectrum One Spectrometer by using attenuated total reflection (ATR) probe with spectral resolution of 4 cm^{-1} in the frequency range of 650−4000 cm^{-1}. ^{1}H NMR spectra of the prepolymer samples were recorded on Bruker AVANCE III 400 MHz Liquid NMR Spectrometer using DMSO-d_6 as solvent.

The thermal gravimetric analyses (TGA) of polyimides were performed using Perkin Elmer Pyris 1 Thermal Gravimetric Analyzer. TGA curves were obtained at a heating rate of 10 °C/min under N_2 atmosphere. The viscosity data of the prepolymer resins were obtained with a heating rate of 5 °C/min from room temperature to 375 °C using shear for liquid holder of Metravib +450 model Dynamic Mechanical Analyzer under 1 Hz frequency and 5 x 10^{-6} m displacement. Dynamic thermo-mechanic analysis (DMA) of silica fabric/resin tape samples was performed by using Metravib +450 Dynamic Mechanical Analyzer with a heating rate of 10 °C/min from room temperature to 430 °C at 1 Hz frequency. The storage modulus (*E'*) and tangent of loss angle (*tan δ*) were obtained as a function of scanning temperature using tension mode. Silica fabric/resin samples were prepared by thermal imidization of [PAE powder:DMF] solution (50 weight %) impregnated silica fabrics.

Lap shear strength tests of bonded samples were carried out in accordance with ASTM standard D1002 by using Zwick tensile tester with a load cell of 5 kN at a constant crosshead speed of 1.0 mm/min. All tests were conducted under the laboratory environment at room temperature (23±3 °C and 30±5 % relative humidity). Three specimens were tested to obtain an average value of the lap shear strength. The fracture morphology of these adhesive joints was examined using a stereo microscope (Zeiss, Stemi 2000) and an optic microscope (Zeiss, Axioskop 2 Mat).

4.4. Results and Discussion

4.4.1. Spectroscopic Analysis

The synthesized polyimides (PIs) were characterized by vibrational spectroscopy (Figure 4.3). The formation of polyimide is confirmed by the characteristic absorption bands of the imide ring observed at 1778 cm^{-1}, 1707 cm^{-1}, 718 cm^{-1} and 1370 cm^{-1}. Strong absorption bands at 1707 cm^{-1} and weak ones at 1778 cm^{-1} are due to the symmetric and asymmetric carbonyl stretching vibrations of the imide rings. The signals at 1370 cm^{-1} correspond to the stretching vibrations of -C-N-C- groups. The shoulders at 1600 cm^{-1} together with the broad band at 1707 cm^{-1} are owing to the stretching vibrations of the >C=O groups in the benzophenone rings. Peaks at around 1240 cm^{-1} are due to aromatic ether groups. The weak absorption bands at 1590 cm^{-1} and medium absorption signals at 1510 cm^{-1} are due to -C=C- stretching vibrations of para-disubstituted aromatic rings. The bands at 718 cm^{-1} are due to flexural vibrations of -C=O groups.

PIs are infusible and cannot be melted because of their rigid backbone. Therefore, structural identification of PIs was attempted by ^{1}H NMR analysis of polyamic ester precursors (Supporting Information Figure S1-5). The absence of any carboxylic acid signal in the ^{1}H NMR spectra proves the formation of methyl ester of polyamic ester (PAE) instead of polyamic acid itself. Since PAE consists of polymeric groups (MDA and ODA), the ^{1}H NMR spectra are quite complex. The signals are broad due to the presence of repeating polymeric units. The signal integrals are not as sharp as expected. The general interpretation of spectra can be as follows:

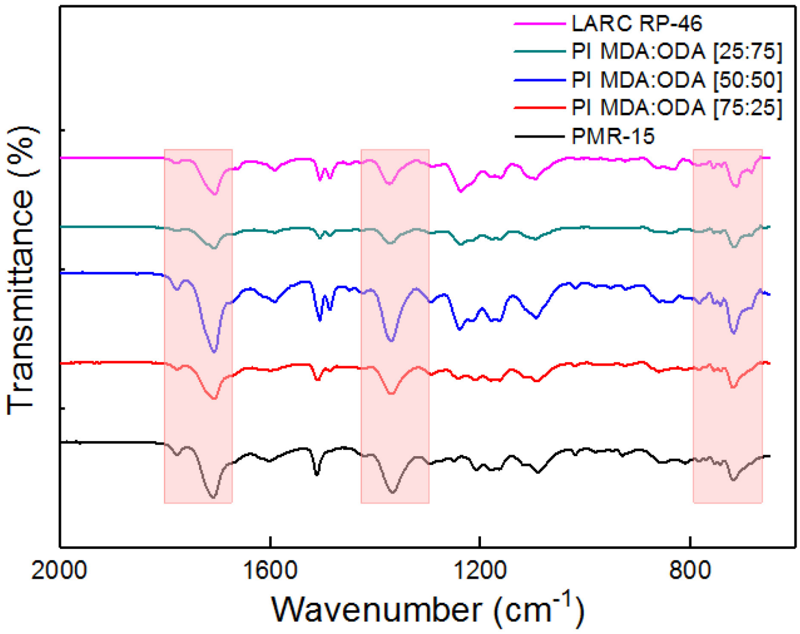

Figure 4.3. FTIR spectra of PMR-15, LARC RP-46 and cured PI MDA:ODA copolyimide samples.

The signals at low field, especially the singlet signal at around 10 ppm belong to the protons of secondary amine groups. The multiplet signal between 6-8 ppm is due to the phenyl moieties on the main chain backbone. The doublets at around 6 ppm belong to double bond of the bicyclic moiety at the ends. The signal between 3-4 ppm stands for methine (CH) groups of the bicyclic moiety. In all copolymers having MDA as the repeating unit, the characteristic singlet signal at around 3.6 ppm may stand for the methylene group of the MDA repeating unit. The other singlet signals at around 4.0 ppm are due to the methyl protons of ester groups. The interpretation of these singlet signals are in accordance with the spectrum of PMR-15 in article prepared by Hammadi et al. (Milhourat-Hammadi et al. 1994). The relation of the area under characteristic methylene singlet of MDA and the percentage of MDA has been questioned; however, satisfactory results have not been obtained due to the complexity of the NMR spectra. A decrease in the intensity of methylene signal has been observed from 100 % MDA to 0 % MDA homopolymer. The high field signal at around 1.6 ppm belongs mainly to the bridgehead protons of the bicyclic end group.

PAE MDA:ODA [100:0] (PMR-15 Prepolymer): ^{1}H NMR (400 MHz, DMSO-*d*$_6$) δ 10.51 and 9.60 (s, amine), 8.22 – 6,56 (m, phenyl), 6.20 (d, double bond of bicyclic), 3.81 – 2.95 (m, bicyclic CH), 3.98 (s, methoxy), 3.62 (s, MDA CH$_2$), 1.58 (s, bridge head CH$_2$). (Supporting Information Figure S1).

PAE MDA:ODA [75:25]: ^{1}H NMR (400 MHz, DMSO-*d*$_6$) δ 10.43 and 9.82 (s, amine), 8.16 – 6.59 (m, phenyl), 6.17 (double bond of bicyclic), 3.77 – 3.06 (m, bicyclic CH), 3.98 (s, methoxy), 3.48 (s, MDA CH$_2$), 1.58 (s, bridge head CH$_2$). (Supporting Information Figure S2).

PAE MDA:ODA [50:50]: ^{1}H NMR (400 MHz, DMSO-*d*$_6$) δ 10.46 and 9.82 (s, amine), 8.15 – 6,6 (m, phenyl), 6.17 (d, double bond of bicyclic), 3.85 – 3.04 (m, bicyclic CH), 3.98 (s, methoxy), 3.61 (s, MDA CH$_2$), 1.58 (s, bridge head CH$_2$). (Supporting Information Figure S3).

PAE MDA:ODA [25:75]: ^{1}H NMR (400 MHz, DMSO-*d*$_6$) δ 10.26 and 9.83 (s, amine), 8.14 – 6.57 (m, phenyl), 6.13 (double bond of bicyclic), 3.75 – 3.01 (m, bicyclic CH), 3.98 (s, methoxy CH$_2$), 3.62 (s, MDA CH$_2$), 1.58 (s, bridge head CH$_2$). (Supporting Information Figure S4).

PAE MDA:ODA [0:100] (LARC RP-46 Prepolymer): 1H NMR (400 MHz, DMSO-*d*$_6$) δ 10.52 and 9.78 (s, amine), 8.31 – 6.41 (m, phenyl), 6.19 (d, double bond of bicyclic), 3.84 – 3.00 (m, bicyclic CH), 1.59 (s, bridge head CH2). (Supporting Information Figure S5).

4.4.2. Thermal Stability

PIs have high temperature resistance because of their heterocyclic and rigid structures. The thermal stabilities of most PIs was assessed by thermo-gravimetric analysis (Lee et al. 1999; Turk et al. 1999). The TGA thermograms of the synthesized polyimide and copolyimide adhesives are illustrated in Figure 4.4. There is almost no weight loss up to 400 °C. The onset temperatures for the decomposition of copolyimides with [75:25], [50:50], and [25:75] MDA:ODA compositions are 461°C, 458°C and 463°C, respectively. Therefore, the imidization process is reasonably complete. The 5% and 10% mass loss temperatures of the polyimide samples are in range of 442.0 – 463.0 °C and 490.6 – 500.6 °C, respectively. The results show that the thermal stability of the copolyimide samples remains generally stable due to the presence of reactive benzylic hydrogens in the structure (Alston 1992). These hydrogens lead to formation of free radicals upon cleavage of C–H bonds. Therefore, additional crosslinking may occur before degradation (W. Xie, Pan, and Chuang 2001).

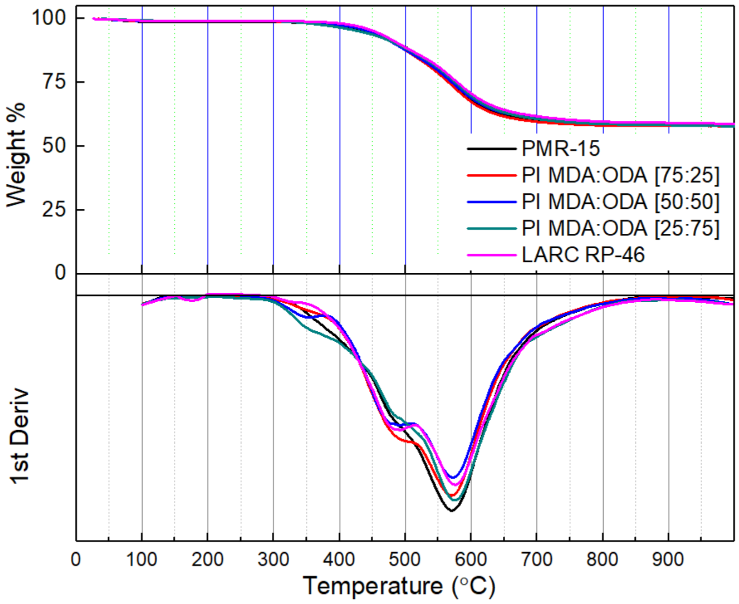

Figure 4.4. TGA thermograms of the copolyimides, LARC RP-46 and PMR-15.

4.4.3. Dynamic Mechanical Properties

Viscoelasticity of polyimide samples was analyzed by running loss tangent (*tan δ*) measurements via Dynamic Mechanic Analyzer. *tan δ* is the ratio of the loss modulus (*E''*) to storage modulus (*E'*) for materials.

$$tan\,\delta \; = \frac{E''}{E'} \qquad (4.1)$$

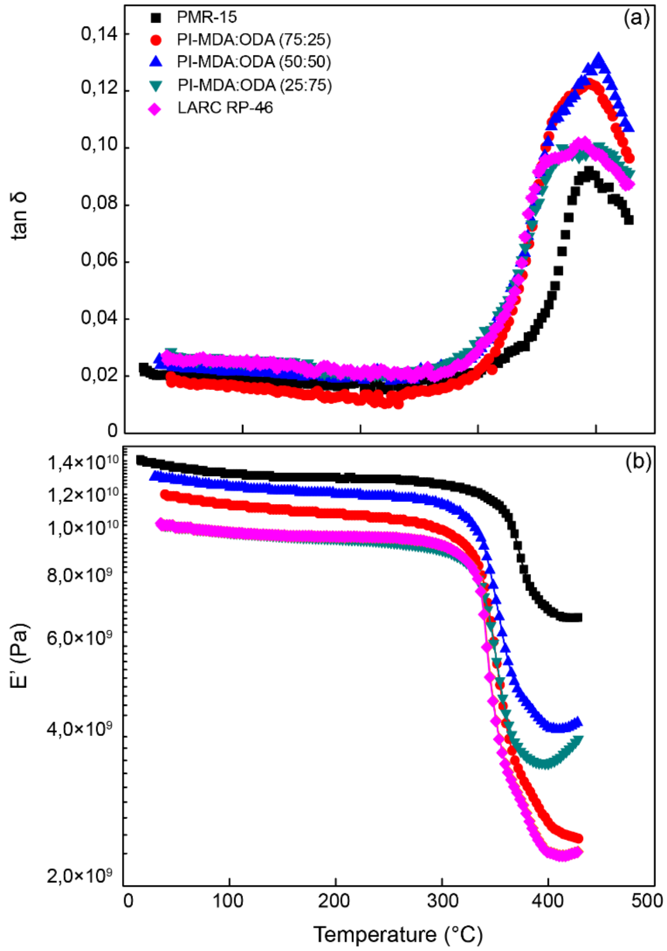

Figure 4.5. Temperature dependent a) loss factor (tan δ) and b) storage modulus (E') curves of PMR-15, LARC RP-46 and the synthesized copolyimides.

Materials display viscoelastic liquid-like behavior when *tan δ* >1. On the other hand, they behave like viscoelastic solids when *tan δ* < 1. Polymer adhesives having *tan δ* values > 1 offer enhanced wetting in composite materials even under low pressures (< 2 MPa). However, high pressures are required for those adhesives having *tan δ* < 1 in order to achieve wetting (W. J. Gao 1994). The same argumentation is also valid for wetting of adherend surfaces (Saeed and Zhan 2007a). Glass transition temperature (T_g) changes from the glassy into the rubber-elastic state at the maximum *tan δ* value. According to the DMA results illustrated in Table 4.1, T_g values of the samples remain nearly stable. The reason of this situation may originate from the steric hindrance of the methylene group of MDA. In comparison to ODA ether group, MDA comonomer leads to the formation of more steric hindrance around methylene group. Moreover, the interaction between hydrogen atoms of methylene and phenyl blocks the movement of the benzene structures (Yu-wei et al. 2012). Therefore, the movement of the segments gets harder. And finally, T_g remains nearly unchanged.

Table 4.1. T_g values of PMR-15, LARC RP-46 and synthesized copolyimides with different MDA:ODA ratios.

Polyimides	**T_g (°C) by *tan δ***	**T_g (°C) by *E'***
PMR-15	395	357
PI MDA:ODA [75:25]	394	330
PI MDA:ODA [50:50]	402	330
PI MDA:ODA [25:75]	401	331
LARC RP-46	388	332

The peak value of *tan δ* indicates the damping property of materials. As can be seen in Figure 4.5 the maximum *tan δ* value of LARC RP-46 is higher than that of PMR-15 because of the presence of flexible ether units in the structure of LARC RP-46. On the other hand, damping properties of [MDA:ODA] polyimide copolymers are higher than those of both PMR-15 and LARC RP-46 homopolymers. The situation can be related to the decrease in the rigidity of the polymers due to the disruption of the molecular symmetry.

4.4.4. Processability

Ether groups in polymer backbone act as a swivel that enhances the flexibility of the polymer chain. The ratio of ether group (ODA%) in the backbone affects the processability of the polyimide resins. As illustrated in Figure 4.6, dynamic viscosity modulus of the polyimides decreases with the increasing ODA% content up to 75% ODA mol ratio. However, it increases suddenly at 100% ODA content (LARC RP-46) because of the increase in molecular symmetry and regularity of the polymer structure (Yi, Huang, and Yan 2016; Chao et al. 2012; Chen, Qin, and Huang 2008; Chun 1994; J. P. Gao and Wang 1995; Y. Han, Fang, and Zuo 2010; Tamai, Yamaguchi, and Ohta 1996). As it is indicated in the figure, copolyimides having 50% and 75% ODA are more processable than PMR-15 and LARC RP-46. Therefore, more processable PI resins can be obtained by decreasing the regularity of the polymer's molecular structure and incorporation of flexible ether-bridged aromatic segments into polyimide backbone. On the other hand, the increase in dynamic viscosity with increasing temperature originates from the formation of cross-linking (Simone et al. 2005).

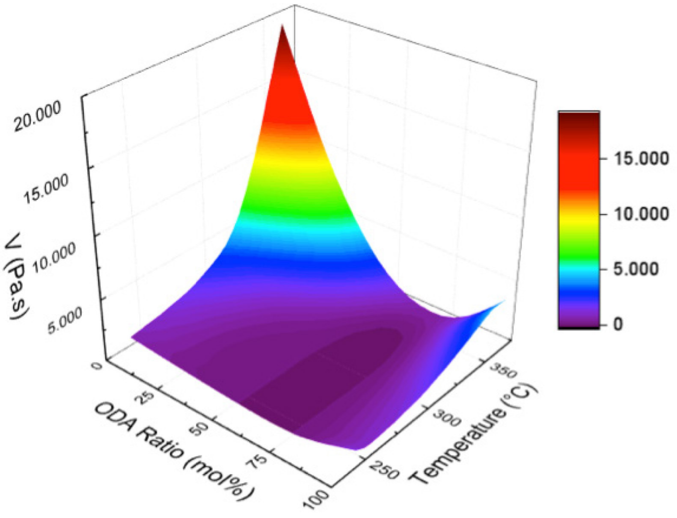

Figure 4.6. Dynamic viscosity modulus curves of PMR-15, LARC RP-46 and copolyimide samples with different ODA ratio.

4.4.5. Adhesion Performance

Depending on different application requirements and fracture modes, several mechanical measurement techniques for assessment of the adhesion performance can be used, such as double cantilever beam (DCB) tests and single-lap shear tests. Of these, double cantilever beam tests are one of the frequently preferred fracture tests in Mode-I because they are easy to be implemented and require simple samples. However, besides the difficulty of measuring crack propagation in DCB tests, the determined toughness of an adhesive can vary considerably depending on the elastic moduli and approaches (Khayer Dastjerdi, Tan, and Barthelat 2013). On the other hand, despite its tendency to exhibit high variability, the single-lap joint configuration is widely used in industry to determine shear strength in Mode-II fracture due to economical and practical advantages of the method. However, it is to be noted that the shear strength is 'apparent' due to non-uniform stress field that occurs along the bond line in a lap shear joint according to the shear lag concept suggested by Volkersen in 1938 (Volkersen 1938). The concept discloses the transfer of the load between two elements joined together by separate connections, such as mechanical fasteners, or a continuous layer such as an adhesive.

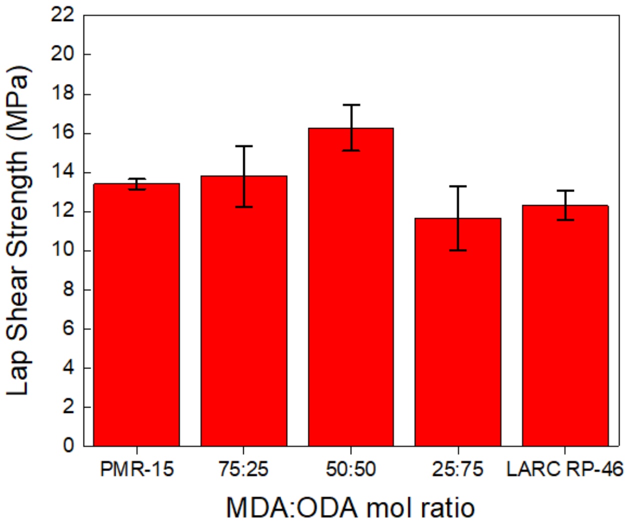

Figure 4.7. Adhesion strengths of polyimide adhesives with different molar ratios of MDA:ODA diamines.

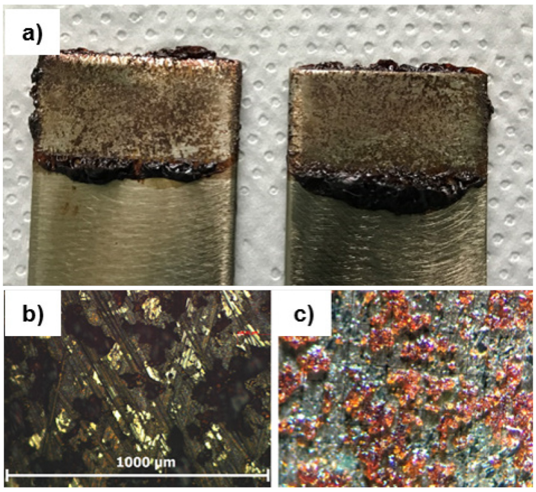

Figure 4.8. (a) Failure mode of the copolyimide samples, (b) stereo microscope image of the interfacial fractured surface of single lap joint, and (c) microscope image of the interfacial fractured surface of single lap joint.

Nevertheless, Volkersen also proposes that uniform stress field could be a reasonable assumption if the adherends are sufficiently stiffer and thicker than the adhesive. In this study, the adhesion performances of the PIs were determined by single-lap shear test (International 2010). In order to achieve optimum bonding performance, the factor of molar ratio of the diamine monomers was studied. The results of single lap shear stress tests of the PI resins are shown in Figure 4.7. The maximum shear strength is achieved by equimolar mixture of MDA:ODA molar ratio that can be explained by reaching optimum mechanical strength and wetting capability of the copolymer, and this result is consistent with the literature (Li et al. 2015). The increase in ODA content in the PI copolymers leads to the increase in fluidity that causes the enhancement of polymer-adherend interaction. On the other hand, mechanical strength of the cured resin decreases with the incorporation of ether groups into the polymer backbone (R. Pater and Morgan 1988; Furukawa, Yamada, and Kimura 1997; Kadiyala, Sharma, and Bijwe 2016). Therefore, the effect of wettability and mechanical strength on the adhesive performance are balanced at 50:50 (MDA:ODA) molar ratio. The adhesion strength values of the copolyimides are nearly in the same range with MDA-BAPP-BTDA co-polyimide synthesized by Li et al.(Li et al. 2015). The authors modify the adhesion strength of the copolyimide by changing the viscosity of the polymer with different monomer ratios. The strong adhesion formed between the polyimide-metal interface can be explained by the electrostatic interaction between metal atoms and heterocyclic polyimide rings when these chemical groups are accessible on the surface (Ramos, Stoneham, and Sutton 1993). Metal-polymer complexes are formed by transferring the delocalized charge from the metal to the polymer (Ho 1989). In addition to interaction at atomic level, mechanical interlocking provides extra strength to the bond.

If the effect of temperature is taken into consideration, it is expected that the relative performance of the adhesives will change significantly at an operating temperature higher than the glass transition temperature. Xu and Wu's group reported that the rigidity of adhesives decline due to the gradual increase in macromolecular motion with the increase of the temperature around T_g (Wu et al. 2012; Xu and McKenna 2011). Therefore, the shear strengths of the adhesives are supposed to decrease.

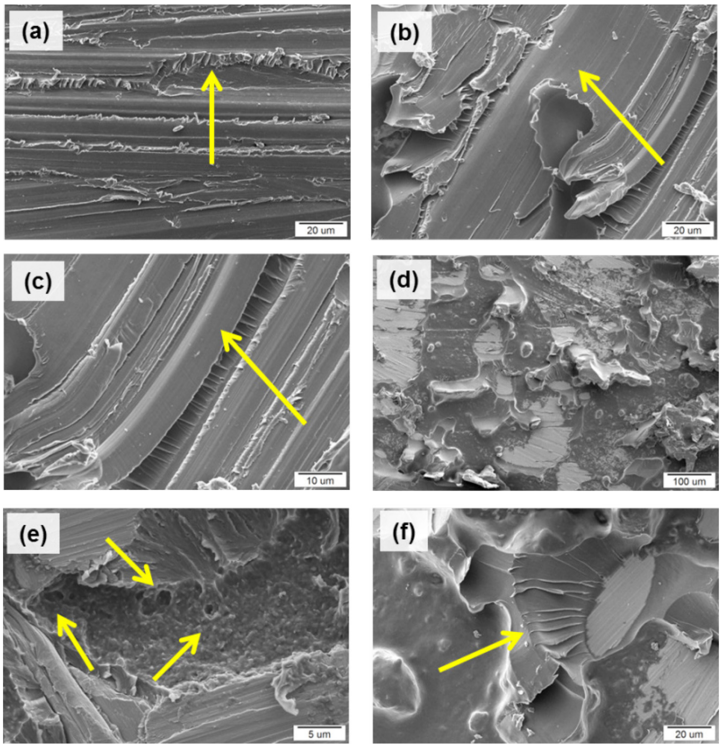

Figure 4.9. SEM micrographs of fractured joints of PI MDA:ODA [50:50] (a-c) shear directions, (d) shear cup, (e) microvoids, and (f) shear delamination.

The image showing the failure mode of the copolyimide adhesives is given in Figure 4.8a. Micrographs of interfacial fractured surfaces at the middle of single lap joints are shown in Figure 4.8 (b-c). The failures for single lap joints were started at the interface between the adherend surface and the adhesive. In fact, both of cohesive and interfacial failures are observed as a result of propagation of cracks through the adhesive.

The morphology of fractured joints of PI MDA:ODA [50:50] adhesive lap joint was investigated via SEM. Figure 4.9 (a-c) shows the river-like pattern, which was emanated perpendicular to the shear direction and crack formation. The cup and cone type morphology of surfaces between the cracks reveals the cohesive and ductile nature of the fracture (Li et al. 2015; Kadiyala, Sharma, and Bijwe 2016).

The plastic deformation mechanism could be observed from the micrographs such that cup and cone formation with microvoids are the signs of ductile fracture (Li et al. 2015). While Figure 4.9d demonstrates the formation of shear cups, Figure 4.9e shows the microvoids throughout the cracks. Microvoids coming from the evaporation of solvent may be the reason for the failure formation. Cohesive type fracture is a desirable condition in adhesive applications, because of the stronger interaction between adherend surface and adhesive. So, greater effort is required to separate them (Kadiyala, Sharma, and Bijwe 2016). Lastly, Figure 4.9f indicates the cohesive fracture coming from shear delamination with cup and cone formation. Considering these fractographic investigations, as-synthesized PI adhesives are preferable due to their cohesive and ductile fracture behavior.

4.5. Conclusions

MDA-BTDA-ODA copolyimide adhesives with nadic end cap were successfully synthesized by a two-step method, including the preparation of polyamic ester prepolymer and thermal imidization. They were structurally characterized by FTIR and ^{1}H NMR. Thermal stabilities, dynamic mechanical properties and adhesion performances of the polyimides were investigated. The copolymers have considerable thermal endurance. The DMA results demonstrate that the synthesized copolyimides exhibit higher processing capability than the commercial PMR-15. They lose only %10 weight when heated to 500 °C. The glass transition temperatures of all copolymers have been found at around 400 °C. The thermoset copolyimides exhibit promising adhesion performance. The highest adhesion strength at room temperature was 16.3 MPa. The processing capability of the polymer increases with the increasing ODA comonomer content up to 75% ODA mol ratio. Thus, the polyimide resins possess a significant processability with the introduction of flexible ether bridged ODA monomer into the backbone and reducing the regularity of polymer structure. MDA:ODA [50:50] polyimide has been found to have optimum processability and maximum adhesion performance. And also, it is more processable than both PMR-15 and LARC RP-46 polyimides.

CHAPTER 5

AN INVESTIGATION ON RHEOKINETICS OF PMR-15 POLYIMIDE RESIN BY DYNAMIC MECHANICAL ANALYSIS

5.1. Abstract

The curing behavior of PMR-15 thermoset polyimide was investigated using dynamic mechanical analysis experiments in the shear mode. Effects of temperature, curing time, and oscillation frequency on rheological properties of PMR-15 were examined. An increase in storage modulus (*G'*), loss modulus (*G''*) and complex viscosity (η^*) was observed with start of curing. The gel point, T_{gel}, was determined by interception of *G'* and *G''*. Rate of gelation process was found to be increased with increasing temperature. Kinetics of isothermal network formation in terms of mechanical cure state was followed by Kamal-Sourour model at different isothermal curing temperatures. The model was well fitted with experimental data. Therefore, mechanical conversion at different temperatures can be well predicted by the kinetic data.

5.2. Introduction

Developed by NASA, PMR-15 is a high-performance polymer which is widely used as a matrix in high temperature composites and an adhesive in the aviation industry. Because of its durability to extreme thermo-mechanical loads up to 300 °C, it is also used as a matrix resin in composite structures used in military aero-engines, helicopter gear cases and missile fins (Kumar et al. 2018; Rupnowski, Gentz, and Kumosa 2006). The outstanding property of PMR-15 comes from the imide groups it contains together with the heterocyclic and stiff nature of the polymer backbone (Hou et al. 1996). These features provide superior thermal, mechanical and chemical stability to the polymer.

The kinetics of network formation phenomena during the curing process have considerable effects on the final situation of thermosetting materials in terms of their mechanical properties. Therefore, the last stage of materials can be optimized by controlling the curing process with the help of using the information about curing kinetics. In recent decades, a lot of research has been done on the curing process of thermosetting polymers. However, the topics of cross-linking mechanism and morphology of cured resins is still tried to be solved due to the insolubility of the cured thermoset polymers and complexity of the curing reactions (Matsumoto et al. 2010). Curing kinetics of thermoset resins can be investigated chemically by various analytical methods, such as DSC (differential scanning calorimetry) (Montserrat and Martín 2002; Ivanković et al. 2002; Leroy, Dupuy, and Maazouz 2001), FTIR (Fourier transform infrared spectroscopy) (Ton-That et al. 2000; Hopewell, George, and Hill 2000; Brill and Palmese 2000), ^{13}C-NMR (nuclear magnetic resonance) (Scariah et al. 2003; Krishnan, He, and Shang 2004; Hwang and Lee 2000; Wright, Schorzman, and Pence 2000) and SEC (size exclusion chromatography) (Mititelu et al. 2000; Urbaczewski et al. 2018). However, these techniques are not capable of providing information about final stage of curing process. Because their sensitivity significantly decreases due to the reduction in reactive moieties. On the other hand, it is possible to determine temperature dependent mechanical and viscoelastic properties of cured thermoset resins and prepregs. However, this type of characterization techniques is performed by the means of subsequent mechanical measurements of thermoset materials cured at different isothermal temperatures. Then, they do not give sufficient information for optimum curing process, as well as curing kinetics (Madbouly, Xia, and Kessler 2012). In view of that, kinetic behavior of the material can be learned by monitoring the change in viscoelastic property during the curing, which is a more challenging issue (Abouhamzeh et al. 2015; van't Hof et al. 2007; Mulle et al. 2009; Boehme et al. 2009; Sadeghinia, Jansen, and Ernst 2012b, 2012a).

Kinetics of curing process can be investigated alternatively to the chemical methods by dynamic mechanical analysis. This analytical technique is widely used to evaluate the cross-linking process according to the change in viscoelastic behavior of thermosetting resins. Most commonly, DMA includes all measurement methods that apply a certain oscillating force to the sample at some frequency range and measure the viscoelastic properties by processing the response of the sample (Frey, Große-Brinkhaus, and Röckrath 1996). Compared to other rheological techniques (Halley and Mackay

1996; Vilas et al. 2001; Malkin et al. 1997), the behavior of the viscosities of the resins can be examined by the DMA prior to the network formation process. Viscoelastic properties at the final stage of curing can be measured by the method since it has a higher sensitivity than the previously mentioned chemical measurement techniques (M. Xie et al. 2009). Although DMA is commonly used for measurement of viscoelastic properties of resins, there are limited studies for evaluating the rheokinetics of curing process by using DMA.

The objective of this research is to investigate the curing kinetics of PMR-15 polyimide resin by using dynamic mechanical analysis. The rheokinetics were examined by monitoring the time, temperature and frequency dependent behavior of viscoelastic properties such as viscosity, loss factor, storage and loss moduli during the curing process. The effect of imidization and crosslink formation processes rheological behavior PMR-15 prepolymer were examined. Time dependent isothermal viscoelastic behavior of the resin in close proximity to the gelation temperature was studied. The autocatalytic approach of Kamal and Sourour was applied to the viscoelastic degree of curing data in order to evaluate mechanical curing kinetics of the prepolymer. Glass transition teperature of cured resin was measured by DMA.

5.3. Experimental

5.3.1. Materials

3,3’,4,4’-benzophenonetetracarboxylic dianhydride (BTDA) (98%), and nadic anhydride (NA) (98%) were obtained from Ivy Fine Chemicals. 4,4’-methylene dianiline (MDA) (≥ 97.0%) was supplied from Fluka. N,N-dimethyl formamide (≥ 99.98%) was purchased from Aldrich. Methanol (≥ 99.98%) was received from Merck. All substances were used as received. PMR-15 prepolymer was prepared according to the procedure of Meador et al.(Meador, Johnston, and Cavano 1997). The 50% (w/w) solution of PMR-15 prepolymer in methanol was used for both rheological and DMA measurements.

5.3.2. Rheological Measurements

The rheokinetics of crosslink formation process was examined for a 50% (w/w) methanol solution of PMR-15 prepolymer using a Metravib DMA 450+ dynamic mechanical analyzer. For the measurements, holders for liquids were used (see Figure 5.1). Both isothermal and non-isothermal rheological tests were performed under controlled thermal conditions.

Figure 5.1. Holders for liquids

Two different types of rheological tests were carried out in this study:

1. A temperature ramp test with 5 °C/min rate at a multiple frequency mode and a single dynamic displacement. The test was run for the evaluation of the temperature effect on viscoelastic properties during the process and determination of the gelation point.
2. Isothermal rheological tests at different temperatures with multi-frequency mode and a constant displacement in order to examine viscoelastic and kinetic properties.

5.3.3. DMA Measurements

Dynamic mechanical analysis was performed by using a Metravib DMA 450+ dynamic mechanical analyzer. The cured thermoset resin was heated at 5 °C/min rate from 55 to 380 °C and at frequency of 10 Hz during the analysis

5.4. Results and Discussion

5.4.1. Effects of Imidization and Crosslink Formation Processes on Rheological Behavior

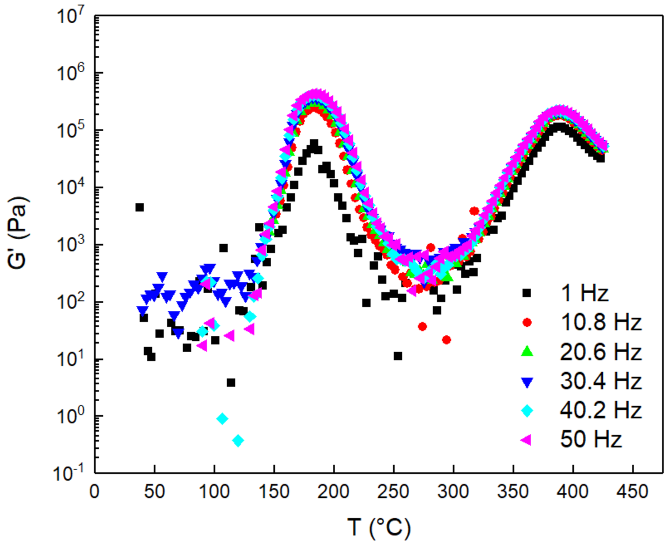

Figure 5.2. The temperature dependence of G' at a heating rate of 5 °C/min and different frequencies.

Effects of imidization and crosslink formation processes for PMR-15 prepolymer on its rheological behavior were examined. The storage modulus (*G'*), the loss modulus

(*G”*) and the viscosity were investigated in this context. *G’* shows the specimen elasticity. *G”* indicates the viscous dissipation. Complex viscosity, η^*, gives information about the resistance to flow. The temperature dependence of storage modulus, *G’*, during a temperature ramp from 37 to 440 °C at heating rate of 5 °C min^{-1} and different frequencies was represented in Figure 5.2. Firstly, the value of *G’* increases with increasing temperature up to 182 °C because of imidization reaction. After that, it starts to decrease up to the temperature of 275 °C as a result of melting. A gradual increase in the storage modulus was observed after 275 °C due to the formation of 3-dimensional thermoset network in the structure. The value of *G’* considerably increases with increasing temperature owing to the substantial increase in cross-links. In Figure 5.2. it is seen that *G’* is more or less frequency dependent in all the temperature range.

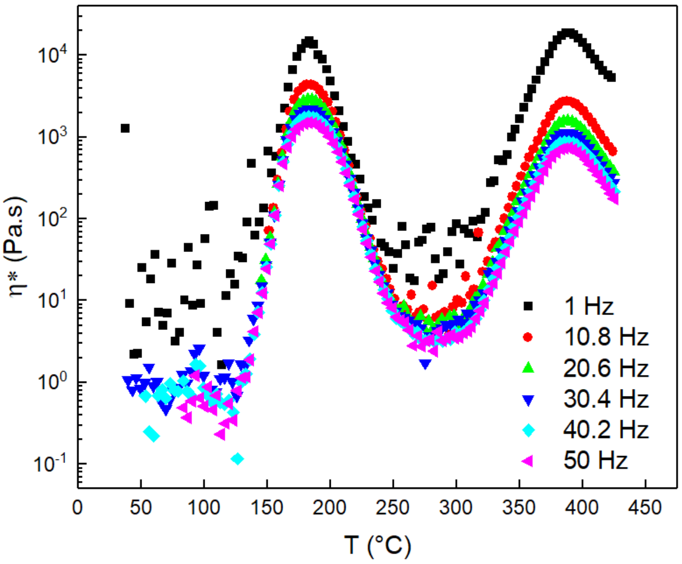

Figure 5.3. The temperature dependence of η* at heating rate of 5 °C/min and different frequencies.

The complex shear viscosity behavior of the polymer during the process reveal a slightly different situation. As shown in Figure 5.3., η^* is much more frequency dependent (non-Newtonian behavior) especially at the temperatures of 183 and 388 °C. This behavior is related to the formation of solid-like structure. Particularly, the complex shear viscosity at around 388 °C is attributed to the construction of cross-linked structure.

The kinetics and curing behavior of PMR-15 thermoset polyimide can be studied rheologically by evaluating the changes in its isothermal and non-isothermal visco-elastic properties, such as *G'*, *G"*, and η^* at different curing periods and frequencies. In fact, the determination of the gelation temperature, T_{gel}, is essential for the issue. T_{gel} is the temperature at which 3D infinite network structure of PMR-15 thermoset is formed. The temperature of gelation can be determined by non-isothermal variation of *G'* and *G"* as shown in Figure 5.4. In terms of chemorheology, materials act as a liquid-like viscoelastic behavior where the value of *G"* is higher than *G'*. On the other hand, they behave as a solid-like manner where the values are vice versa. Here, the resin shows solid-like behavior at 185 °C. It starts to soften, and then melt around the temperature of 200 °C.

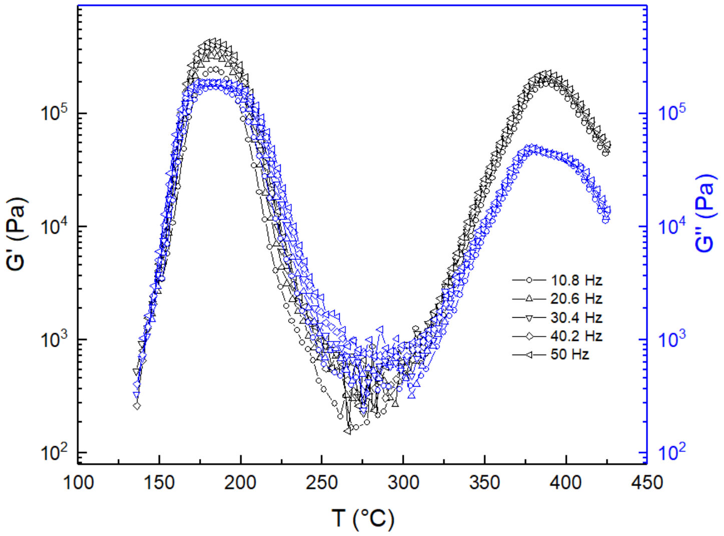

Figure 5.4. The temperature dependence of G' and G" at heating rate of 5 °C/min and different frequencies.

Above the gelation temperature, crosslinking process occurs and the rate of increase of *G'* becomes higher than the *G"*. Actually, it can be said that the value of T_{gel} is frequency dependent. T_{gel} at the frequencies of 30.4 and 50 Hz. is approximately 290 and 314 °C, respectively. As a matter of fact, in literature, the point at which *G'* and *G"* coincide is not generally considered to be the only criterion for the detection of gelation temperature because of its dependency on frequency (Madbouly and Ougizawa 2004; Zhao et al. 2003). In this study, the gelation point can vary up to 20 degrees relative to the frequency. According to the work carried out by Zhao et al., it was revealed that the intersection temperature of *G'* and *G"* depends on shear stress and frequency (Zhao et al. 2003). On the other hand, Winter et al. mentioned that if there is uncertainty in the gelation temperature from the intersection of *G'* and *G"*, T_{gel} could be associated with the critical conversion temperature of network formation. Therefore, the following conclusion can be reached. Branching of the polymer chain gets considerable level and crosslink formation is triggered at the gelation temperature (Madbouly, Xia, and Kessler 2012). At the temperatures higher than the gelation point, branching of polymer continues until the formation of 3D polymer structure (Madbouly, Xia, and Kessler 2012).

5.4.2. Isothermal Rheological Measurements During Crosslink Formation Processes

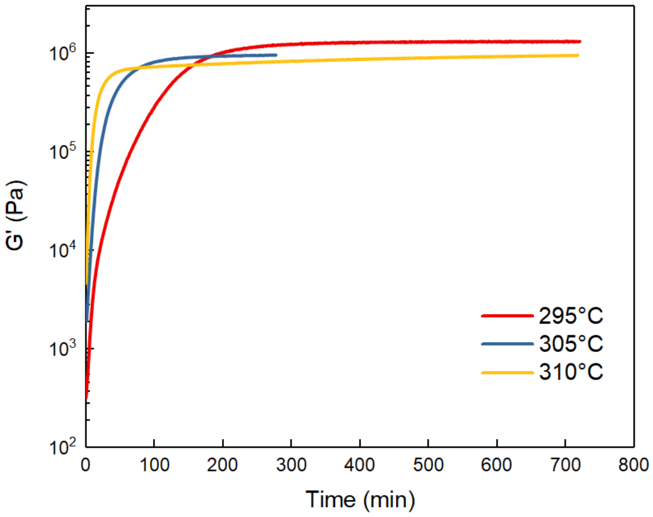

Figure 5.5. Time dependent behavior of storage modulus at 10 Hz frequency and constant temperatures of 295, 305 and 310 °C.

Time dependent viscoelastic behavior of the resin in close proximity to the gelation temperature is examined in this part. Figure 5.5 shows the effect of curing in isothermal manner on the storage modulus at a frequency of 10 Hz and at the temperatures of 295, 305 and 310 °C. As it is clearly seen in the figure that firstly, *G'* dramatically increases due to crosslinking. The values reach to the plateau as time progresses. The rate of increase of *G'* strongly depends on the temperature. Whereas the leveling off period takes a long time at low temperatures, it decreases as the temperature increases. In addition, the rate of rise of *G'* increases with rate of gelation and crosslink formation processes. Madbouly et al. reports that the value of *G'* at the plateau depends on curing temperature and equilibrium modulus (Madbouly, Xia, and Kessler 2012). Curing process at 310 °C is faster than 305 and 295 °C. Therefore, the time necessary for leveling off is shorter at 310 °C.

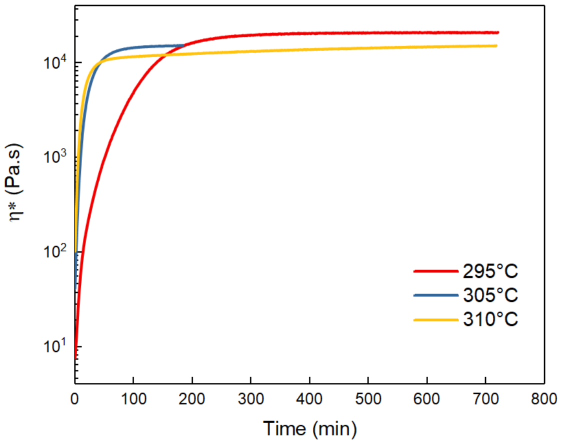

Figure 5.6. Time dependent behavior of complex viscosity at 10 Hz frequency and constant temperatures of 295, 305 and 310 °C.

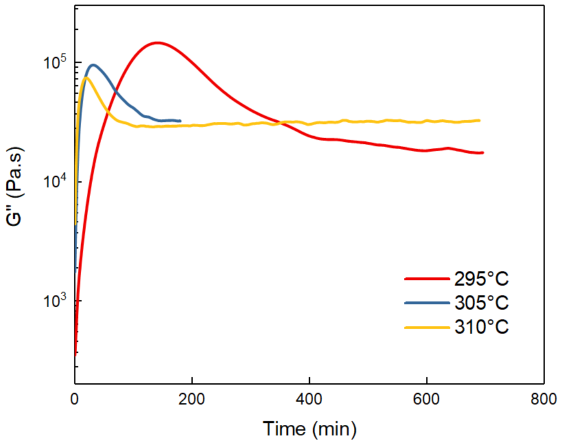

Figure 5.7. Time dependent behavior of loss modulus at 10 Hz frequency and constant temperatures of 295, 305 and 310 °C.

In terms of isothermal time dependency of complex viscosity and loss modulus, a similar situation was found for the resin as indicated in Figure 5.6 and Figure 5.7. Under the same parameters of frequency and displacement at a constant temperature, it is observed that the level of increase in *G”* 'is lower than that of *G’*. This is the result of the elastic behavior being dominant as a result of storage of the energy in the cross-links (Madbouly, Xia, and Kessler 2012).

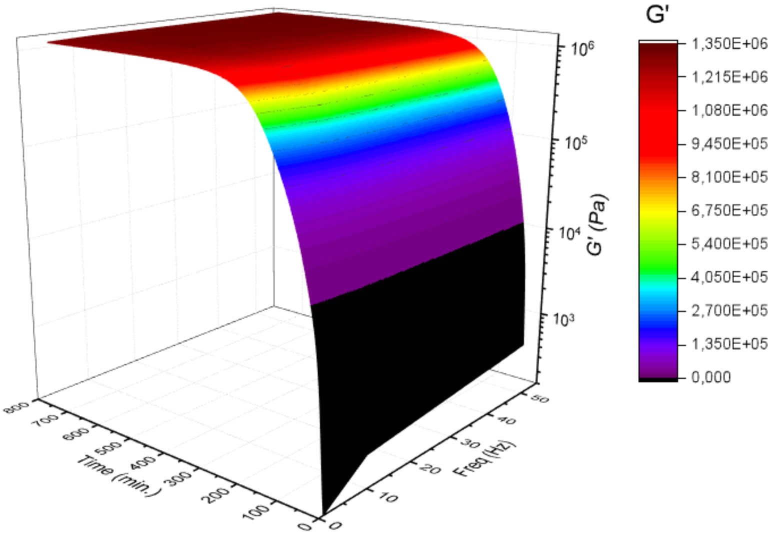

Figure 5.8. Time and frequency dependence of G′ during the curing process of PMR-15 prepolymer at 295 °C.

The curing process of PMR-15 prepolymer is also investigated as a function of different frequencies at a constant temperature. The effect of time and frequency on *G’* at the temperature of 295 °C is exhibited in Figure 5.8. As it is seen in the figure, the storage modulus of the resin follows two different stages during the curing process. While the values of *G’* increases rapidly up to 300 minutes, there is no significant increase due to the completion of the curing process after that time. Actually, the processes of crosslink and branch formation is time dependent at early stages of curing. At the end of 300 minutes, *G’* almost does not change and becomes independent of time due to the completion of the curing process. In addition to all of these mentioned above, it can be clearly seen from the figure that the change in *G’* is not dependent on the frequency in all the stages due to the formation of equilibrium modulus.

Figure 5.9 shows time and frequency dependence of η^* at 295 °C. It can be seen that the complex viscosity is nearly independent of frequency at the initial stages of curing. η^* increases with the formation of three-dimensional network and then remains almost constant. At the later stages of crosslinking process, the resin shows a non-Newtonian behavior due to the frequency dependent variation of η^*.

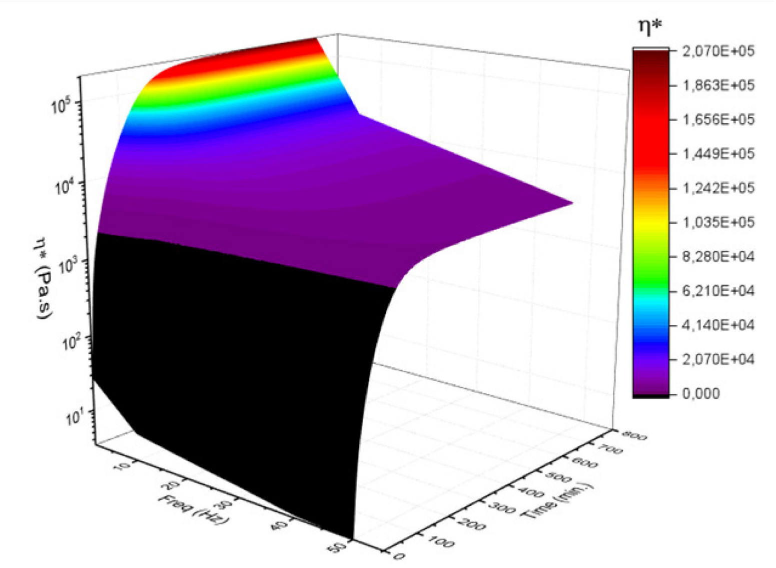

Figure 5.9. Time and frequency dependence of η* during the curing process of PMR-15 prepolymer at 295 °C.

5.4.3. Determination of Gelation Time

In literature, there are variety of methods to detect gelation time, t_{gel}, of thermosets. Winter-Chambon approach is one of the most preferred methods (Chambon and Winter 1987; Winter, Morganelli, and Chambon 1988). According to the technique, gelation time is defined as the point where both of storage and loss moduli show a linear response with a frequency and relaxation value dependent power law. This can be explained by the following equation:

$$G' \sim G'' \sim f^n \qquad (5.1)$$

Here, "*f*" is frequency. "*n*" is the relaxation value which is dependent on microstructural properties of cured thermoset polymers. If the equation (5.1) matches wide range of frequencies at gelation time, loss factor, *tan δ*, can be expressed by the following equation:

$$tan\,\delta = tan\left(\frac{n\pi}{2}\right) \tag{5.2}$$

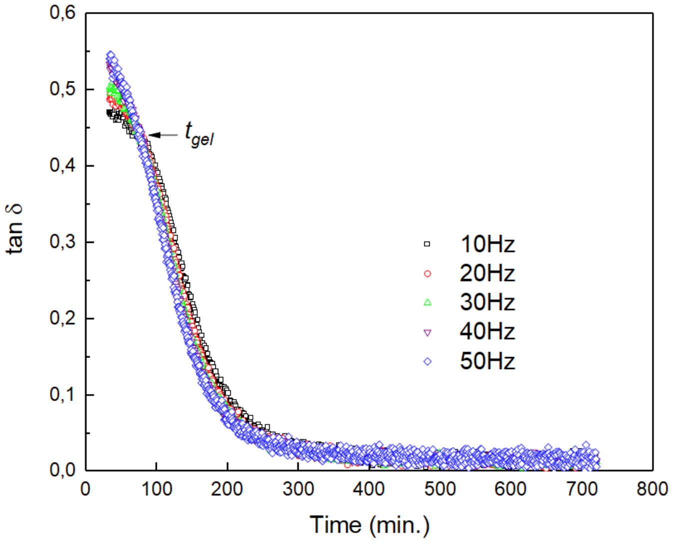

Figure 5.10. Loss factor, tan δ, as a function of time at 295 °C for the curing process of PMR-15 at different frequencies. The gelation time, t_{gel}, is the intersection point of different tan δ curves.

According to Kramers-Kronig approach, *tan δ* is dependent on relaxation exponent, *n*, at t_{gel}, while it is independent of frequency (Ferry 1980). This rule is applicable to the most of thermoset resins containing cross-linking structure. The isothermal effect of time and different frequencies on *tan δ* at 295 °C is indicated in Figure 5.10. It is obviously seen that as the resin begins to gel at the 79th minute, *tan δ* becomes independent of the frequency. Thereafter, the formation of cross-link proceeds. Therefore, the loss factor decreases with the increase of difference between the rise rates of *G'* and *G"*. In other words, the magnitude of *G'* reaches higher level than *G"* with the increase of three dimensional network in the resin structure (Madbouly, Xia, and Kessler 2012).

The order of the curves that change depending on the frequencies is reversed after this point. The behavior of the resin found to be coherent with Winter- and Chambon criterion. Therefore, it can be applied over many frequencies for the determination of critical gel formation.

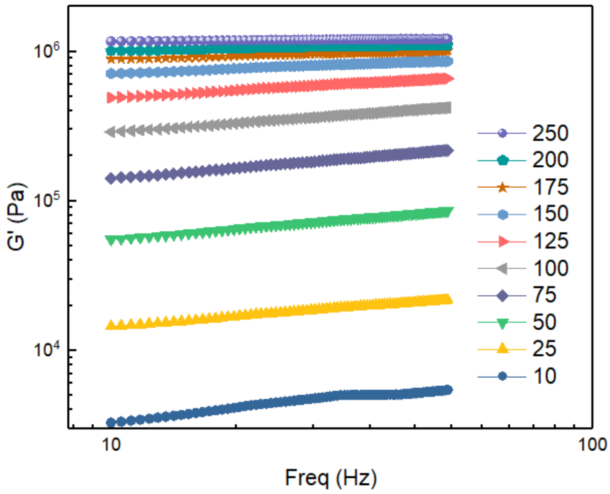

Figure 5.11. Frequency dependence of storage modulus at different curing times of PMR-15 at 295 °C.

Frequency dependence of storage modulus at different curing times of PMR-15 at 295 °C is indicated in Figure 5.11. As the duration of curing process increases, the slope of *G'* versus frequency decreases while the value of *G'* increases on the other hand. Due to the elastic and cross-linked nature of the resin, *G'* becomes nearly independent of frequency and shows stabilized behavior towards the end of curing. Figure 5.12 indicates the frequency dependence of loss modulus at different curing times of PMR-15 at 295 °C. In comparison to the variation at the storage modulus, *G"* is found to be more frequency dependent. On the other hand, it increases at lower level. The situation can be related to decrease in the energy dissipation capability of the resin caused by the formation of branched and cross-linked structure. In trying to evaluate all the mentioned investigations, it can be said that the characterization of three-dimensional network formation of PMR-15 can be successfully accomplished by the examination of its viscoelastic behavior during the curing process. Gelation time can be effectively detected by using power law depending on Winter-Chambon method.

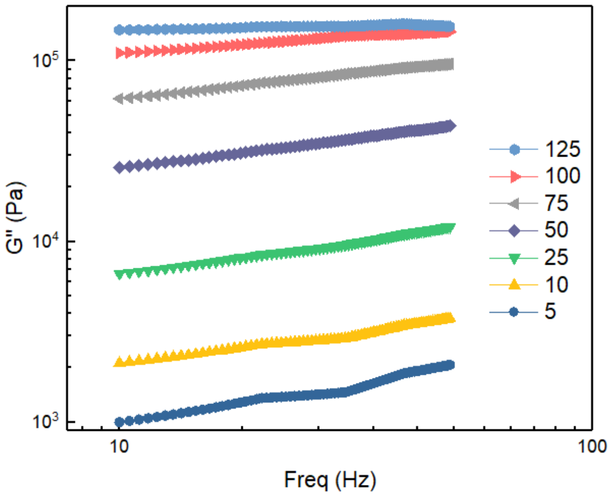

Figure 5.12. Frequency dependence of loss modulus at different curing times of PMR-15 at 295 °C

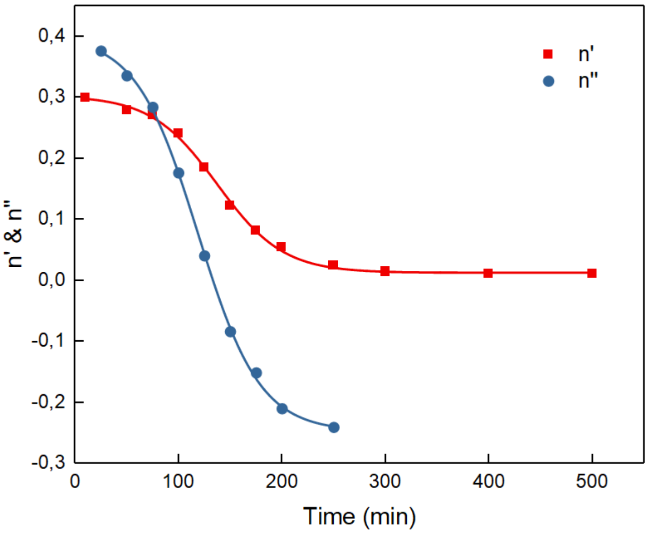

Figure 5.13. Isothermal variation of n’ and n” as a function of time at 295 °C (derived from the slopes of G’ and G” vs. frequency lines).

If the data in Figure 5.11 and Figure 5.12 are examined, it will be found that the behavior of *G’* and *G”* along the changing frequency agrees with the power law of Equation 5.1. The corresponding values of *n’* and *n”* mentioned in Equation 5.1 can be derived from the slopes of the lines in *G’* and *G”* vs. frequency graphs. Figure 5.13 shows that *n’* and *n”* vary as a function of time at 295 °C, isothermally. Both of the values of the exponents decrease over time and become identical at t_{gel}. Gelation time,79th min, obtained from this technique overlaps with the result given by isothermal *tan δ* versus time graph (Figure 5.10).

5.4.4. DMA Measurements

Dynamic mechanical analysis was performed at 5 °C/min heating rate and 10 Hz frequency for PMR-15, which is isothermally cured at 300 °C for 100 min. The glass transition temperature was deduced from the maximum peak of *tan δ*. By using DMA result indicated in Figure 5.14, T_g of PMR-15 thermoset is found as 357 °C. Storage modulus, *G'*, is constant up to 283 °C and then, it starts to decrease with the relaxation of polymer chains. After that, *G'* becomes constant due to limitation in the movements of the chains caused by crosslinks.

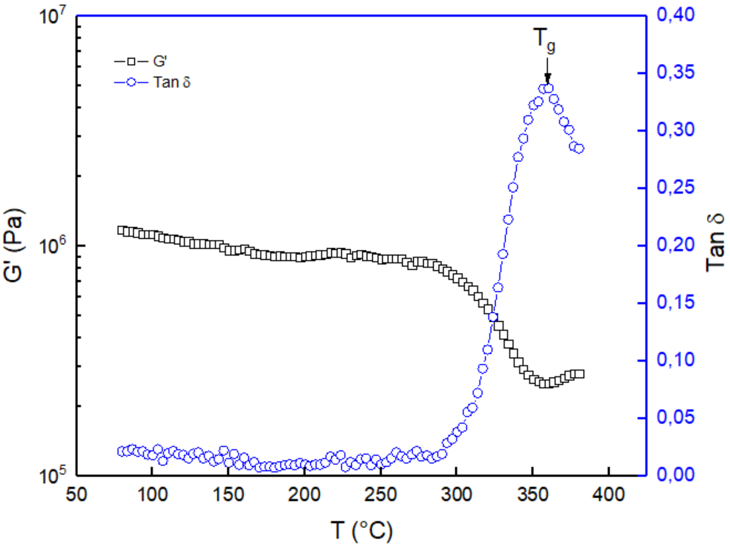

Figure 5.14. DMA results of PMR-15 thermoset at 5 °C/min heating rate and 10 Hz frequency (G': storage modulus; tan δ: loss factor)

5.4.5. Kinetic Analysis

In fact, there are two types of models, namely phenomenological models and rheological models, that define the kinetics of curing (M. Xie et al. 2009). In phenomenological or empirical models, the curing process is usually described by chemical analyses. This method is a widely used technique in which positive results are obtained. On the other hand, while research on the rheological method continues, this method can be used in rheological evaluation of the curing kinetics. Monitoring of the kinetics of the curing at higher conversions can be performed using the dynamic mechanical analysis. Because this method can give more precise results than the calorimetric and chemical methods at high degree of curing (Malkin, Gorbunova, and Kerber 2005). Therefore, the mechanism of network formation can be investigated in terms of rheokinetics by adapting DMA data to empirical cure kinetic models.

The cross-linking process occurring during the curing reaction can be evaluated according to the behavior of *G'* during the process since the value of the storage modulus varies depending on the cross-link density (Yilgör, Yilgör, and Wilkes 2015). Therefore, the use of dynamic mechanical analysis is beneficial in terms of revealing viscoelastic properties of the resin during the network formation related to chemical bonds and physical entanglements. The rheological conversion β, i.e. the degree of cure related to the viscoelastic properties of the resin can be defined as (George 2009; Malkin and Kulichikhin 2008; Malkin et al. 1997):

$$\beta = \frac{G'_t - G'_0}{G'_\infty - G'_0} \qquad (5.3)$$

where G'_t, G'_0, and G'_∞, are the storage shear moduli at time t, at the beginning, and at the end of the curing process, respectively. Time dependent rheological conversions are shown in Figure 5.15. The plots are obtained from *G'* values measured by isothermal rheological analysis based on Equation 5.3. From the figure, it can be seen that the rheological conversion value increases rapidly with the initiation of the curing process. Then it slows down and becomes stable after completion of the network formation process due to the increase in molecular mass and hindrance. The steep increase in the conversion as an "S" shape nature indicates that the curing reaction proceeds in autocatalytic manner (Malkin and Kulichikhin 1991; Santhosh Kumar, Reghunadhan Nair, and Ninan 2006).

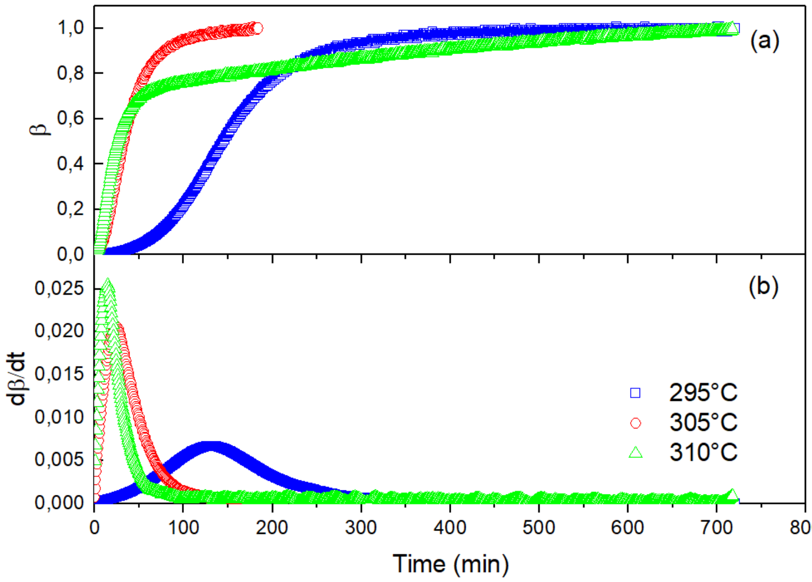

Figure 5.15. Time dependent (a) rheological conversion β and (b) conversion rate dβ/dt for the curing reaction of PMR-15 at different temperatures of 295, 305 and 310 °C.

The curing kinetics of PMR-15 prepolymer can be evaluated in terms of rheology by using Kamal – Sourour model which is the most frequently used empirical model (Kamal and Sourour 1973). This autocatalytic model describes rheokinetics of the network formation by using the following phenomenological equation:

$$\frac{d\beta}{dt} = (k_1 + k_2\beta^m)(1-\beta)^n$$

$$k_1 = A_1\, exp\left(-\frac{E_{a1}}{RT}\right) \qquad k_2 = A_2\, exp\left(-\frac{E_{a2}}{RT}\right) \tag{5.4}$$

where k_1 and k_2 are rate constants; m and n are order of autocatalytic reaction and of nth order reaction, respectively. A_1 and A_2 are pre-exponential factors. E_{a1} and E_{a2} are the apparent activation energies. R is gas constant. T is the absolute reaction temperature. The conversion dependent curing rate and fitted curves at the temperatures of 295, 305 and 310 °C are indicated in Figure 5.16. As can be seen in figure, the rate of degree of cure increases with increasing temperature. The kinetic parameters k_1, k_2, m and n are determined by using nonlinear multiple regression analysis.

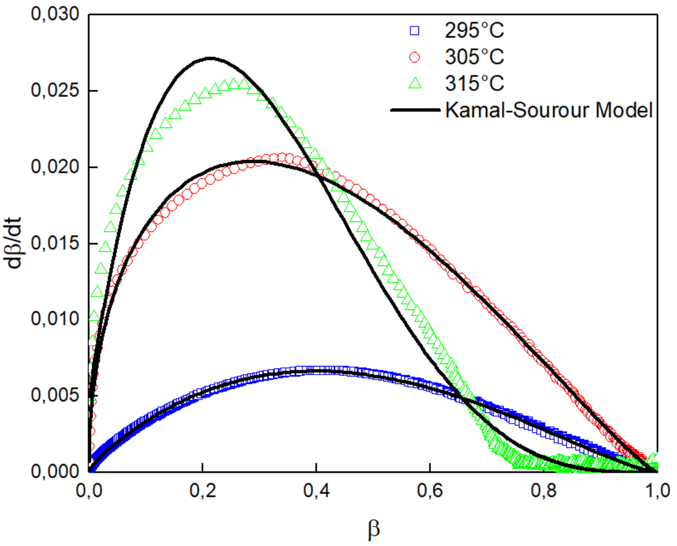

Figure 5.16. The conversion dependent curing rate of PMR-15 prepolymer at the curing temperatures of 295, 305 and 310 °C.

Table 5.1. Rheokinetic parameters at different isothermal curing temperatures of PMR-15 prepolymer.

Temperature (°C)	$k_1 \cdot 10^{-8}$ **(min^{-1})**	$k_2 \cdot 10^{-2}$ **(min^{-1})**	m	n	$m + n$	$\beta_{max} = m/(m+n)$	R^2
295	1.86	2.90	0.87	1.33	2.20	0.40	1.003
305	6.64	5.54	0.48	1.20	1.68	0.28	0.998
310	49.63	17.32	0,73	3.05	3.77	0.19	0.972

The values obtained at different isothermal curing temperatures are listed in Table 5.1. A good agreement between experimental results and model was obtained for all the temperatures obtained with an $R^2 \geq 0.97$. An accelerating rate of isothermal reaction is observed in the figure. In a typical autocatalytic model, the reaction rate initiates with a non-zero value, and then reaches a peak value towards the halfway of the conversion (M. Xie et al. 2009). Also, the value rate constant k_2 is much higher than k_1. The same situation is observed in the figure. In terms of kinetics, this is indicative of the characteristic feature of the autocatalytic reaction mechanism. Values of the rate constants increase with increasing temperature. A good agreement between calculated and experimental conversion values, β_{max}, that correspond to maximum conversion rate is observed (Table 5.1). In terms of rheokinetics, the cure development of PMR-15 prepolymer can be easily explained by using Kamal – Sourour model and derived kinetic parameters.

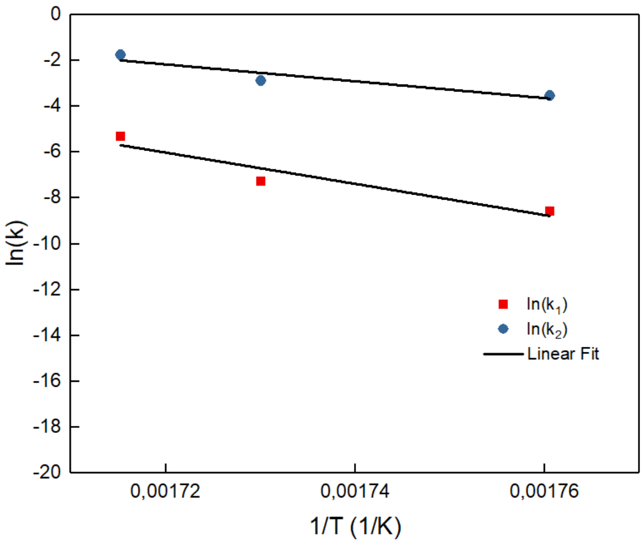

Figure 5.17. Arrhenius graphs of rate constants k_1 and k_2.

Apparent activation energy of cross-linking reaction can be calculated from Arrhenius expression which is derived from Equation 5.4. The slopes of the linear lines shown in *lnk* versus *1/T* graph (Figure 5.17) give E_{a1} and E_{a2} activation energies. The activation energy for n^{th} order reaction path (E_{a1}) is higher than for the autocatalytic path (E_{a2}). The values of E_{a1} and E_{a2} are 566.3 and 305.7 kJ/mol, respectively.

5.5. Conclusion

Rheological effects of curing time, temperature and frequency on the curing behavior and viscoelastic properties of PMR-15 polyimide were evaluated in terms of dynamic mechanical analysis measurements. In addition to the increase in viscosity, a gradual increase in the values of storage and loss moduli was observed in the temperature sweep experiments. The gelation temperature was found by the determination of the temperature at which *G'* and *G"* are identical. Isothermal rheological investigations during crosslink formation were carried out by monitoring the variations in complex viscosity, *tan δ*, storage and loss moduli at different temperatures (295, 305 and 310 °C) and frequencies. Gelation time of the resin was determined from time dependent crossover point of *tan δ* at different frequencies. It was also found that the value of *tan δ* becomes independent from frequency at t_{gel}. Gelation time was also successfully determined by using power law depending on Winter-Chambon method which is applicable to wide range of frequencies. The value of t_{gel} which was obtained from the overlapping point of *n'* and *n"* exponents are identical to the value that was found from the intersection of *tan δ* as a function of time. As a result of the DMA measurements, T_g value of the cured resin was found to be 357 °C.

The kinetics of cross-link development of PMR-15 prepolymer were modeled with a conventional autocatalytic model by using dynamic mechanical analysis data. Model fitting kinetics of Kamal – Sourour was chosen for description of rheological curing process. The kinetic parameters and behavior of conversion rate ensure that the cross-linking process occurs at autocatalytic level. Kinetic constants deduced from Kamal – Sourour model were used for calculation of activation energy.

CHAPTER 6

AN INVESTIGATION ON RHEOKINETICS OF NADIC END CAPPED MDA-BTDA-ODA COPOLYIMIDE BY DYNAMIC MECHANICAL ANALYSIS

6.1. Abstract

The curing behavior of a nadic end capped MDA-BTDA-ODA copolyimide was investigated using dynamic mechanical analysis experiments in the shear mode. The studied copolyimide consists of a combination of 50:50 molar compositions of 4,4’-diaminodiphenylmethane (MDA) and 3,4’-oxydianiline (ODA) together with 3,3’,4,4’-benzophenonetetracarboxylic acid dianhydride (BTDA). Effects of temperature, curing time, and oscillation frequency on rheological properties of the resin were examined. An increase in storage modulus (*G’*), loss modulus (*G”*) and complex viscosity (η^*) was observed with start of curing. The gel point, T_{gel}, was determined by interception of *G’* and *G”*. Rate of gelation process was found to be increased with increasing temperature. Kinetics of isothermal network formation in terms of mechanical cure state was followed by Kamal-Sourour model at different isothermal curing temperatures. The model was well fitted with experimental data. Therefore, mechanical conversion at different temperatures can be well predicted by the kinetic data.

6.2. Introduction

In chapter 4, the synthesis of a series of MDA-BTDA-ODA copolyimide resins is mentioned (Acar et al. 2018). The copolyimide with equimolar composition of MDA:ODA has superior processability and adhesion performance compared to commercial PMR-15 polyimide. The resin can be used as a high temperature adhesive, as well as a matrix for high temperature resistant composite structures. In fact, studying the curing kinetics of the MDA-BTDA-ODA copolyimide is essential to obtain optimum adhesion and mechanical performance. The analytical techniques for the evaluation of the kinetics of cross-linking process are mentioned in section 5.2.

In this study, it was aimed to investigate curing kinetics of nadic end capped MDA-BTDA-ODA copolyimide resin by using dynamic mechanical analysis. The rheokinetics were examined by monitoring the time, temperature and frequency dependent behavior of viscoelastic properties such as viscosity, loss factor, storage and loss moduli during the curing process. The effect of imidization and crosslink formation processes rheological behavior the copolyimide prepolymer were examined. Time dependent isothermal viscoelastic behavior of the resin in close proximity to the gelation temperature was studied. The autocatalytic approach of Kamal and Sourour was applied to the viscoelastic degree of curing data in order to evaluate mechanical curing kinetics of the prepolymer. Glass transition teperature of cured resin was measured by DMA.

6.3. Experimental

6.3.1. Materials

3,3’,4,4’-benzophenonetetracarboxylic dianhydride (BTDA) (98%), 3,4’-oxydianiline (3,4’-ODA) (98%) and nadic anhydride (NA) (98%) were obtained from Ivy Fine Chemicals. 4,4’-methylene dianiline (MDA) (≥ 97.0%) was supplied from Fluka. N,N-dimethyl formamide (≥ 99.98%) was purchased from Aldrich. Methanol (≥99.98%) was received from Merck. All substances were used as received. Nadic end capped MDA-BTDA-ODA copolyimide prepolymer with equimolar MDA:ODA content was prepared according to the procedure of Acar et al.(Acar et al. 2018). The 50% (w/w) solution of the copolyimide prepolymer in methanol was used for both rheological and DMA measurements.

6.3.2. Rheological Measurements

The rheokinetics of crosslink formation process was examined for a 50% (w/w) methanol solution of MDA-BTDA-ODA copolyimide prepolymer by using a Metravib DMA 450+ dynamic mechanical analyzer with holders for liquids (see Figure 5.1). Both isothermal and non-isothermal rheological tests were performed under controlled thermal conditions. Two different types of rheological tests were carried out in this study:

1. A temperature ramp test with 2 °C/min rate at a multiple frequency mode and a single dynamic displacement. The test was run for the evaluation of the temperature effect on viscoelastic properties during the process and determination of the gelation point.
2. Isothermal rheological tests at different temperatures with multi-frequency mode and a constant displacement in order to examine viscoelastic and kinetic properties.

6.3.3. DMA Measurements

Dynamic mechanical analysis was performed by using a Metravib DMA 450+ dynamic mechanical analyzer. The cured thermoset resin was heated at 10 °C/min rate from 100 to 450 °C and at frequency of 10 Hz during the analysis

6.4. Results and Discussion

6.4.1. Effects of Imidization and Crosslink Formation Processes on Rheological Behavior

Effects of imidization and crosslink formation processes for the precursor of MDA-BTDA-ODA copolyimide on its rheological behavior were examined. The storage modulus (*G'*), the loss modulus (*G"*) and the viscosity were investigated in this context. *G'* shows the specimen elasticity. *G"* indicates the viscous dissipation. Complex viscosity, η^*, gives information about the resistance to flow. The temperature dependence of storage modulus, *G'*, during a temperature ramp from 28 to 440 °C at heating rate of 2 °C min^{-1} and different frequencies was represented in Figure 6.1. Firstly, the value of *G'* increases with increasing temperature up to 173 °C because of imidization reaction. After that, it starts to decrease up to the temperature of 278 °C as a result of melting. A gradual increase in the storage modulus was observed after 278 °C due to the formation of 3-dimensional thermoset network in the structure. The value of *G'* considerably increases with increasing temperature owing to the substantial increase in cross-links. In Figure 6.1. it is seen that *G'* is more or less frequency dependent in all the temperature range.

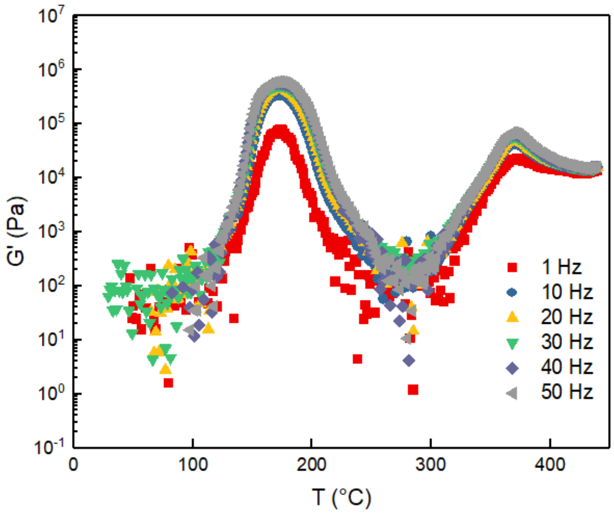

Figure 6.1. The temperature dependence of G' at a heating rate of 2 °C/min and different frequencies.

The complex shear viscosity behavior of the polymer during the process reveal a slightly different situation. A shown in Figure 6.2, η^* is much more frequency dependent (non-Newtonian behavior) especially at the temperatures of 172 and 369 °C. This behavior is related to the formation of solid-like structure. Particularly, the complex shear viscosity at around 369 °C is attributed to the construction of cross-linked structure.

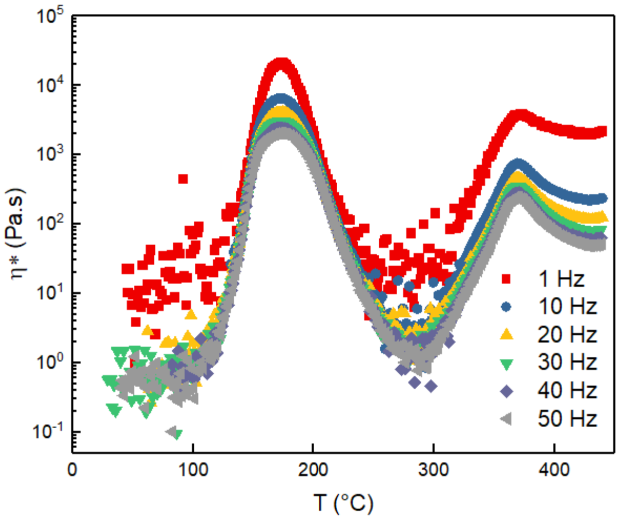

Figure 6.2. The temperature dependence of η* at heating rate of 2 °C/min and different frequencies.

The kinetics and curing behavior of MDA-BTDA-ODA thermoset copolyimide can be studied rheologically by evaluating the changes in its isothermal and non-isothermal visco-elastic properties, such as *G'*, *G"*, and η^* at different curing periods and frequencies. In fact, the determination of the gelation temperature, T_{gel}, is essential for the issue. T_{gel} is the temperature at which 3D infinite network structure of MDA-BTDA-ODA thermoset copolyimide is formed. The temperature of gelation can be determined by non-isothermal variation of *G'* and *G"* as shown in Figure 6.3. In terms of chemorheology, materials act as a liquid-like viscoelastic behavior where the value of *G"* is higher than *G'*. On the other hand, they behave as a solid-like manner where the values are vice versa. Here, the resin shows solid-like behavior at 173 °C. It starts to soften, and then melt around the temperature of 190 °C.

Above the gelation temperature, crosslinking process occurs and the rate of increase of *G'* becomes higher than the *G"*. Actually, it can be said that the value of T_{gel} is frequency dependent. T_{gel} at the frequencies of 10, 20, 40 and 50 Hz. is approximately 292, 298, 308, and 311 °C, respectively. As a matter of fact, in literature, the point at which *G'* and *G"* coincide is not generally considered to be the only criterion for the detection of gelation temperature because of its dependency on frequency (Madbouly and Ougizawa 2004; Zhao et al. 2003). In this study, the gelation point can vary up to 20 degrees relative to the frequency. Zhao et al. reports that the intersection temperature of *G'* and *G"* depends on shear stress and frequency (Zhao et al. 2003). On the other hand, Winter et al. mentioned that T_{gel} could be associated with the critical conversion temperature of network formation if there is uncertainty in the gelation temperature from the intersection of *G'* and *G"*. Therefore, the following conclusion can be reached. Branching of the polymer chain gets considerable level and crosslink formation is triggered at the gelation temperature (Madbouly, Xia, and Kessler 2012). At the temperatures higher than the gelation point, branching of polymer continues until the formation of 3D polymer structure (Madbouly, Xia, and Kessler 2012).

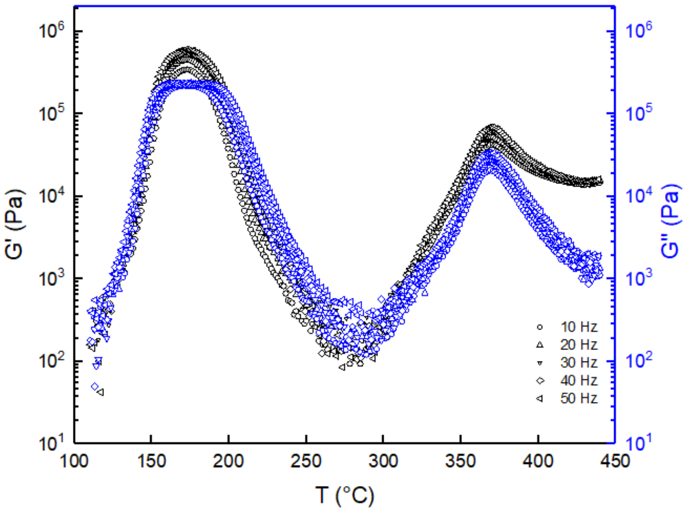

Figure 6.3. The temperature dependence of G' and G" at heating rate of 4 °C/min and different frequencies.

6.4.2. Isothermal Rheological Measurements During Crosslink Formation Processes

Time dependent viscoelastic behavior of the resin in close proximity to the gelation temperature is examined in this part. Figure 6.4 shows the effect of isothermal curing on the storage modulus at 10 Hz frequency and at the temperatures of 280, 300, 310 and 320 °C. As it is clearly seen in the figure that *G'* first dramatically increases due to crosslinking. The values reach to a plateau as time progresses. The rate of increase of *G'* strongly depends on the temperature. Whereas the leveling off period takes a long time at low temperatures, this time decreases as the temperature increases. In addition, the rate of rise of *G'* increases with rate of gelation and crosslink formation processes. Madbouly et al. reports that the value of *G'* at the plateau depends on curing temperature and equilibrium modulus (Madbouly, Xia, and Kessler 2012). As the temperature increases, the curing rate becomes faster. Therefore, the time necessary for leveling off is shortened as the temperature increases from 280 °C to 320 °C.

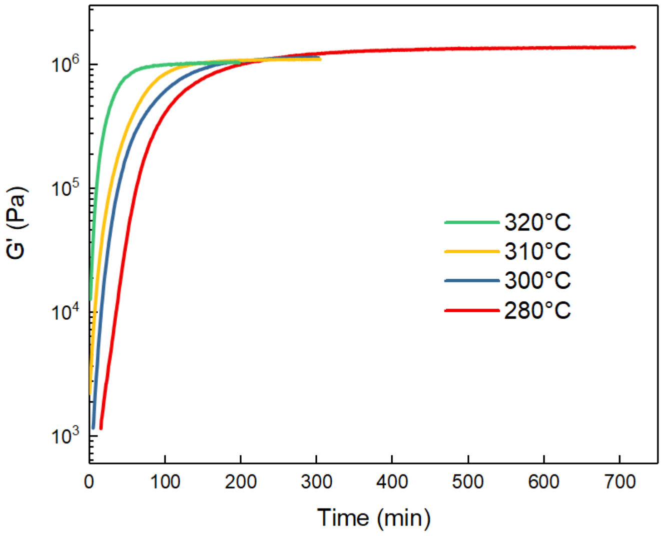

Figure 6.4. Time dependent behavior of storage modulus at 10 Hz frequency and constant temperatures of 280, 300, 310 and 320 °C.

In terms of isothermal time dependency of complex viscosity and loss modulus, a similar situation was found for the resin as indicated in Figure 6.5 and Figure 6.6. Under the same parameters of frequency and displacement at a constant temperature, it is observed that the level of increase in *G''* 'is lower than that of *G'*. This is because of the dominance of elastic behavior as a result of storage of the energy in the cross-links (Madbouly, Xia, and Kessler 2012).

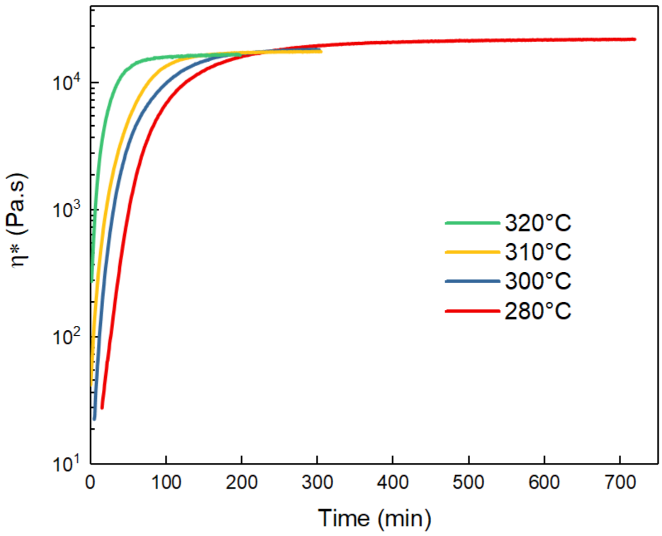

Figure 6.5. Time dependent behavior of complex viscosity at 10 Hz frequency and constant temperatures of 280, 300, 310 and 320 °C.

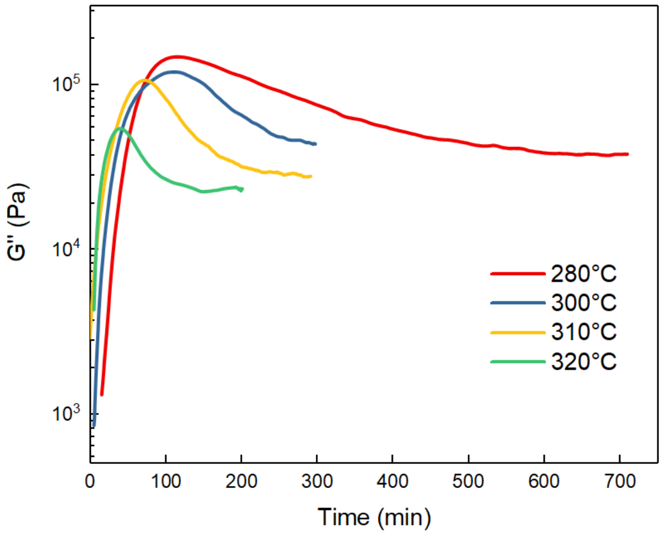

Figure 6.6. Time dependent behavior of loss modulus at 10 Hz frequency and constant temperatures of 280, 300 and 310 °C.

The curing process of the copolyimide prepolymer is also investigated as a function of different frequencies at a constant temperature. The effect of time and frequency on *G'* at the temperature of 280 °C is exhibited in Figure 6.7 As it is seen in the figure, the storage modulus of the resin follows two different stages during the curing process. While the values of *G'* increases rapidly up to 400 minutes, there is no significant increase due to the completion of the curing process after that time. Actually, the processes of crosslink and branch formation is time dependent at early stages of curing. At the end of 400 minutes, *G'* does not change and becomes independent of time due to the completion of the curing process. In addition to all of these mentioned above, it can be clearly seen from the figure that the change in *G'* is not dependent on the frequency in all the stages due to the formation of equilibrium modulus.

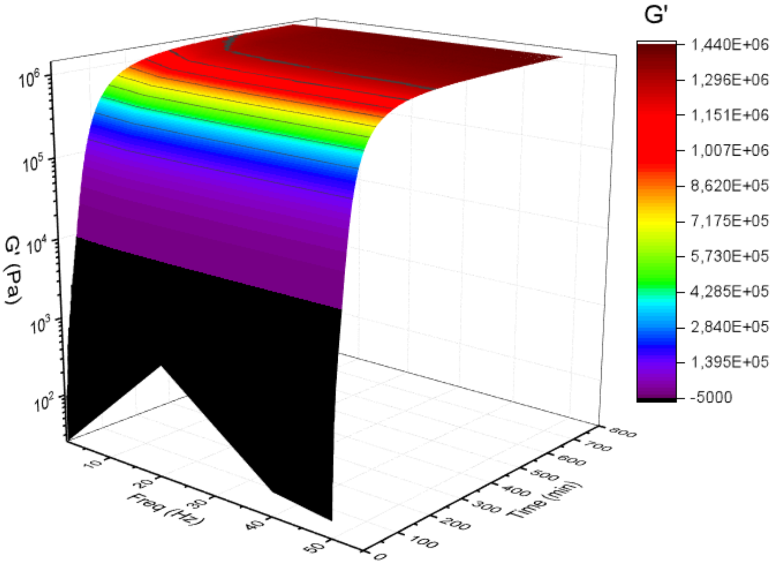

Figure 6.7. Time and frequency dependence of G′ during the curing process of MDA-BTDA-ODA copolyimide prepolymer at 280 °C.

Figure 6.8 shows time and frequency dependence of η^* at 280 °C. It can be seen that the complex viscosity is nearly independent of frequency at the initial stages of curing. η^* increases with the formation of three-dimensional network and then remains almost constant. At the later stages of crosslinking process, the resin shows a non-Newtonian behavior due to the frequency dependent variation of η^*.

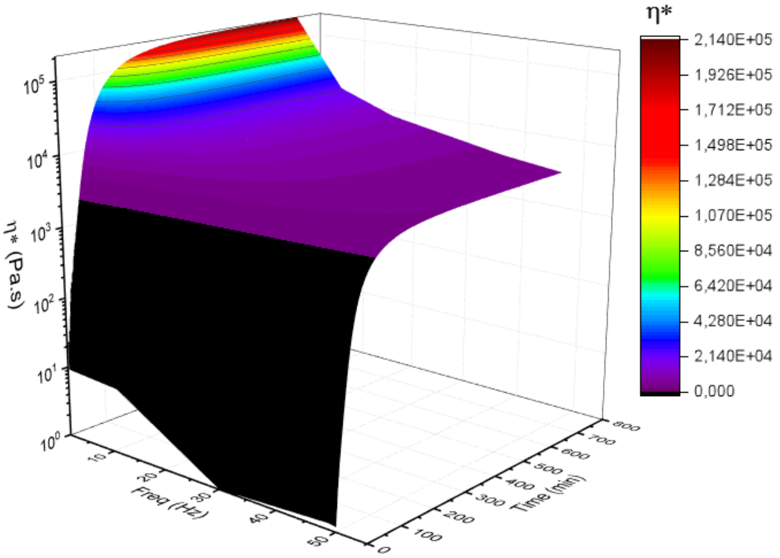

Figure 6.8. Time and frequency dependence of η* during the curing process of MDA-BTDA-ODA copolyimide prepolymer at 280 °C.

6.4.3. Determination of Gelation Time

As it was previously specified in section 5.4.3, there are several methods for the detection of gelation time, t_{gel}, of thermoset polymers. Here, Winter-Chambon method was used again for the determination of the gelation time of nadic ended MDA-BTDA-ODA copolyimide polymer (See eqn. 1 and 2 in section 5.4.3). t_{gel} was detected by finding intersection of *tan δ* curve as a function of time. This approach is also supported by Kramers-Kronig methodology which is explained previously in section 5.4.3. The isothermal effect of time and different frequencies on *tan δ* at 280 °C is indicated in Figure 6.9. It is obviously seen that as the resin begins to gel at the 33rd minute, *tan δ* becomes independent of the frequency. Thereafter, the formation of cross-link proceeds. Therefore, the loss factor decreases with the increase of difference between the rise rates of *G'* and *G"*. In other words, the magnitude of *G'* reaches a higher level than *G"* with the growth of three dimensional network in the resin structure (Madbouly, Xia, and Kessler 2012). The order of the curves that change depending on the frequencies is reversed after this point. The behavior of the resin found to be coherent with Winter- and Chambon criterion.

Therefore, it can be applied over many frequencies for the determination of critical gel formation.

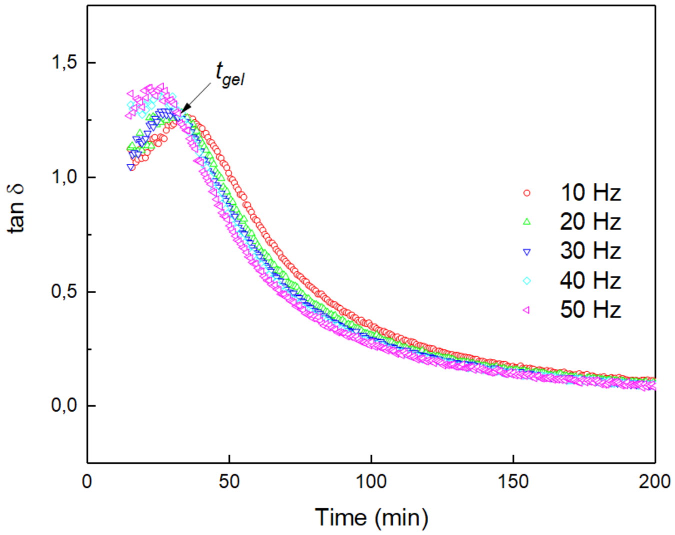

Figure 6.9. Loss factor, tan δ, as a function of time at 280 °C for the curing process of MDA-BTDA-ODA copolyimide at different frequencies. The gelation time, t_{gel}, is the intersection point of different tan δ curves.

Frequency dependence of storage modulus at different curing times of nadic end capped MDA-BTDA-ODA copolyimide at 280 °C is indicated in Figure 6.10. As the duration of curing process increases, the slope of *G'* versus frequency decreases while the value of *G'* increases on the other hand. Due to the elastic and cross-linked nature of the resin, *G'* becomes nearly independent of frequency and shows stabilized behavior towards the end of curing. Figure 6.11 indicates the frequency dependence of loss modulus at different curing times of the polymer at 280 °C. In comparison to the variation at the storage modulus, *G"* is found to be more frequency dependent. On the other hand, it increases at lower level. The situation can be related to decrease in the energy dissipation capability of the resin caused by the formation of branched and cross-linked structure. In trying to evaluate all the mentioned investigations, it can be said that the characterization of three-dimensional network formation of the copolyimide polymer can be successfully accomplished by the examination of its viscoelastic behavior during the curing process. Gelation time can be effectively detected by using power law depending on Winter-Chambon method.

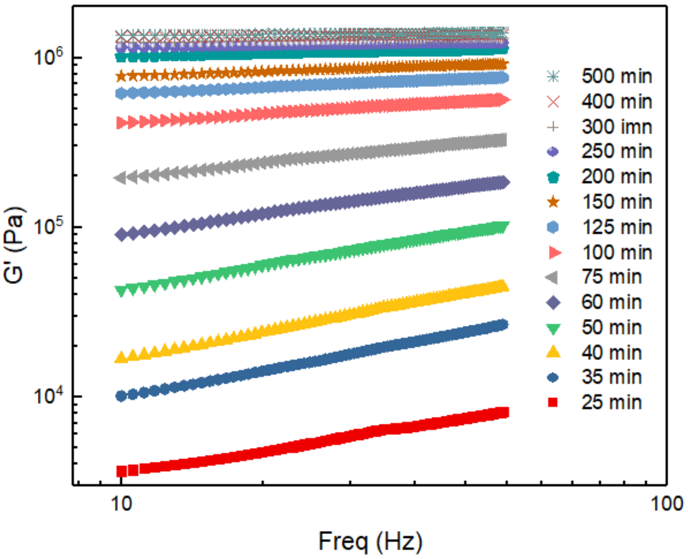

Figure 6.10. Frequency dependence of storage modulus at different curing times of MDA-BTDA-ODA copolyimide at 280 °C.

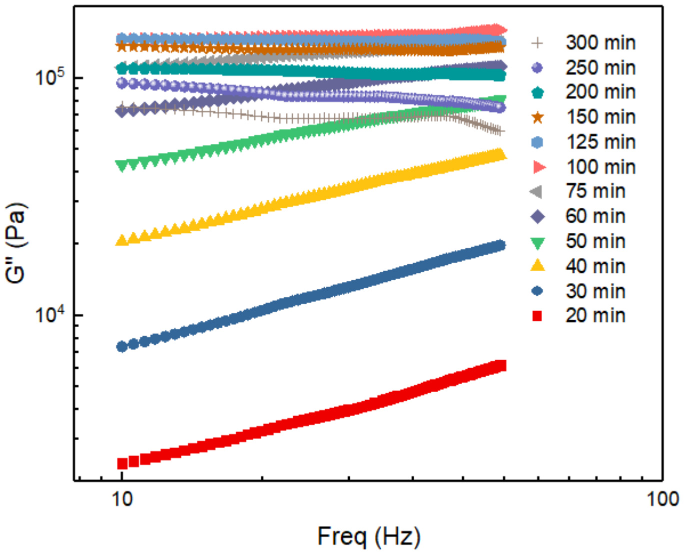

Figure 6.11. Frequency dependence of loss modulus at different curing times of MDA-BTDA-ODA copolyimide at 280 °C.

If the data in Figure 6.10 and Figure 6.11 are examined, it will be found that the behavior of *G'* and *G"* along the changing frequency agrees with the power law of Equation 5.1. The corresponding values of *n'* and *n"* mentioned in Equation 5.1 can be derived from the slopes of the lines in *G'* and *G"* vs. frequency graphs. Figure 6.12 shows that *n'* and *n"* vary as a function of time at 280 °C, isothermally. Both of the values of the exponents decrease with increasing time and become identical at t_{gel}. Gelation time, 33rd min, obtained from this technique overlaps with the result given by isothermal *tan δ* versus time graph (Figure 6.9).

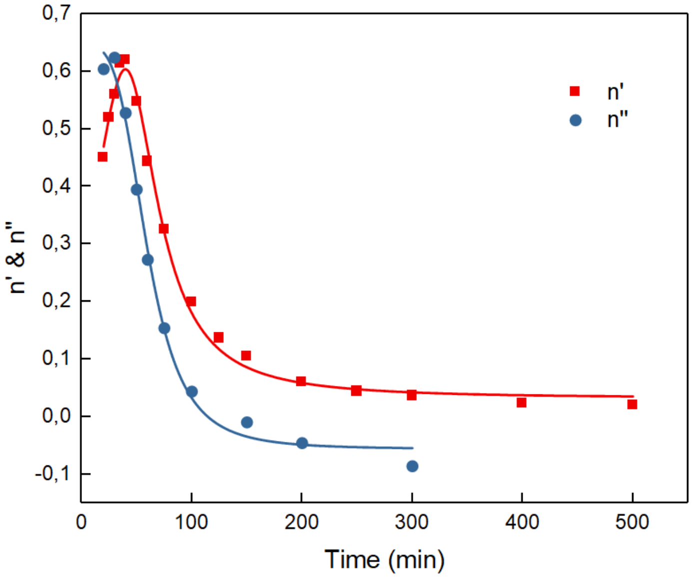

Figure 6.12. Isothermal variation of *n'* and *n"* as a function of time at 280 °C (derived from the slopes of *G'* and *G"* vs. frequency lines).

6.4.4. DMA Measurements

Dynamic mechanical analysis was performed at 10 °C/min heating rate and 10 Hz frequency for nadic end capped MDA-BTDA-ODA copolyimide which is isothermally cured at 280 °C for 12 hr. By using DMA result indicated in Figure 6.13, the glass transition temperature of the copolyimide is deduced from the maximum peak of *tan δ*. T_g is found as 367 °C. Storage modulus, *G'*, is constant up to 327 °C and then, it starts to decrease with the relaxation of polymer chains. After that, *G'* becomes constant due to limitation in the movements of the chains caused by crosslinks.

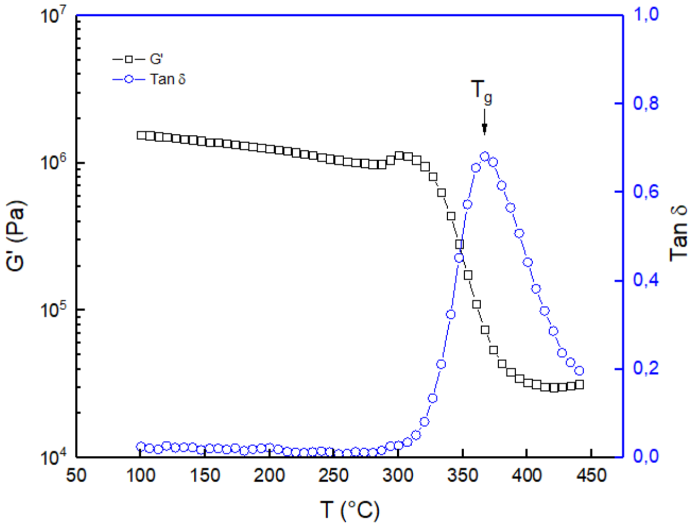

Figure 6.13. DMA results of MDA-BTDA-ODA copolyimide thermoset at 10 °C/min heating rate and 10 Hz frequency (*G'*: storage modulus; *tan δ*: loss factor)

6.4.5. Kinetic Analysis

As it was previously mentioned in section 6.4.5, there are two types of models, such as phenomenological models and rheological models, that define the kinetics of curing (M. Xie et al. 2009). In this study, kinetics of curing process was monitored by using dynamic mechanical analysis. In comparison to calorimetric and chemical methods, DMA gives more precise results at higher conversion degrees (Malkin, Gorbunova, and Kerber 2005). Therefore, the mechanism of network formation was examined in terms of rheokinetics by adapting DMA data to empirical cure kinetic models.

The cross-linking process occurring during the curing reaction was evaluated according to the behavior of *G'* during the process since the value of the storage modulus varies depending on the cross-link density (Yilgör, Yilgör, and Wilkes 2015). Therefore, the use of dynamic mechanical analysis is beneficial in terms of revealing viscoelastic properties of the resin during the network formation related to chemical bonds and physical entanglements. The rheological conversion β was calculated according to Equation 5.3. Time dependent rheological conversions are shown in Figure 6.14. The graphs are obtained from G' values measured by isothermal rheological analysis based on Equation 5.3. From the figure, it can be seen that the value of rheological conversion increases rapidly with the initiation of the curing process. Then it slows down and becomes stable after completion of the network formation process due to the increase in molecular mass and hindrance. The steep increase in the conversion as an "S" shape nature indicates that the curing reaction proceeds in autocatalytic manner (Malkin and Kulichikhin 1991; Santhosh Kumar, Reghunadhan Nair, and Ninan 2006). If the curing kinetics of the synthesized copolyimide and PMR-15 are compared, it can be seen that the rheological conversion rate during the curing process of nadic end capped MDA-BTDA-ODA copolymer is lower than that of PMR-15. This is due to the steric hindrance arising from the effects of flexible ODA ether groups as well as molecular irregularities.

Table 6.1. Rheokinetic parameters at different isothermal curing temperatures of MDA-BTDA-ODA copolyimide prepolymer.

Temperature (°C)	$k_1 \cdot 10^{-4}$ **(min^{-1})**	$k_2 \cdot 10^{-2}$ **(min^{-1})**	m	n	$m + n$	$\beta_{max} = m/(m+n)$	R^2
280	1.21	1.94	0.53	1.42	1.96	0.27	1.025
300	2.04	1.90	0.47	0.91	1.39	0.34	1.007
310	13.56	3.62	0,68	1.07	1.76	0.39	0.993
320	75.43	5.52	0.47	1.12	1.60	0.30	0.974

The curing kinetics of MDA-BTDA-ODA copolyimide prepolymer was evaluated in terms of rheology by using Kamal – Sourour model which is the most frequently used empirical model (Kamal and Sourour 1973). This autocatalytic model describes rheokinetics of the network formation by using Equation 5.4. The conversion dependent curing rate and fitted curves at the temperatures of 280, 300, 310 and 320 °C are indicated in Figure 6.15. As can be seen in figure, the rate of degree of cure increases with increasing temperature. The kinetic parameters k_1, k_2, m and n were determined by using nonlinear multiple regression analysis.

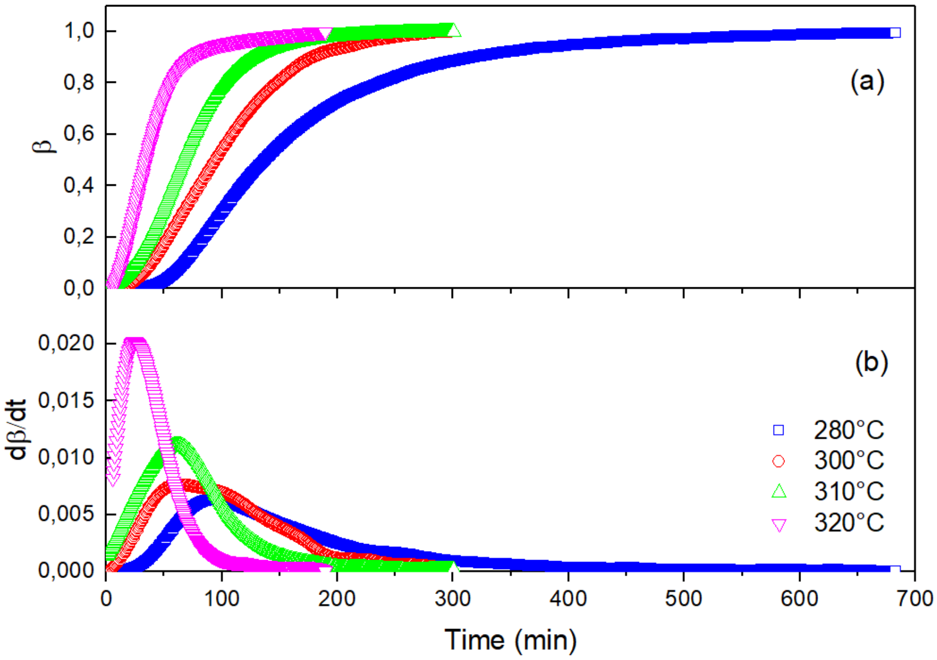

Figure 6.14. Time dependent (a) rheological conversion β and (b) conversion rate $d\beta/dt$ for the curing reaction of the copolyimide prepolymer at different temperatures of 280, 300, 310 and 320 °C.

The values obtained at different isothermal curing temperatures are listed in Table 6.1. A good agreement between experimental results and model was obtained for all the temperatures obtained with an $R^2 \geq 0.97$. An accelerating rate of isothermal reaction is observed in the figure. In a typical autocatalytic model, the reaction rate initiates with a non-zero value, and then reaches a peak value towards the halfway of the conversion (M. Xie et al. 2009). Also, the value rate constant k_2 is much higher than k_1. The same situation is observed in the figure. In terms of kinetics, this is indicative of the characteristic feature of the autocatalytic reaction mechanism. Values of the rate constants increase with increasing temperature. A good agreement between calculated and experimental conversion values, β_{max}, that correspond to maximum conversion rate is observed (Table 6.1). In terms of rheokinetics, the cure development of MDA-BTDA-ODA copolyimide prepolymer was explained by using Kamal – Sourour model and derived kinetic parameters.

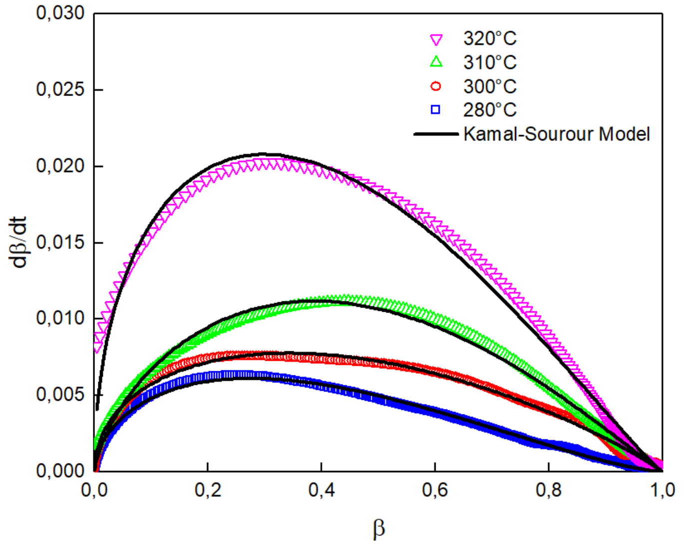

Figure 6.15. Conversion dependent curing rate of MDA-BTDA-ODA copolyimide prepolymer at the curing temperatures of 280, 300, 310 and 320 °C.

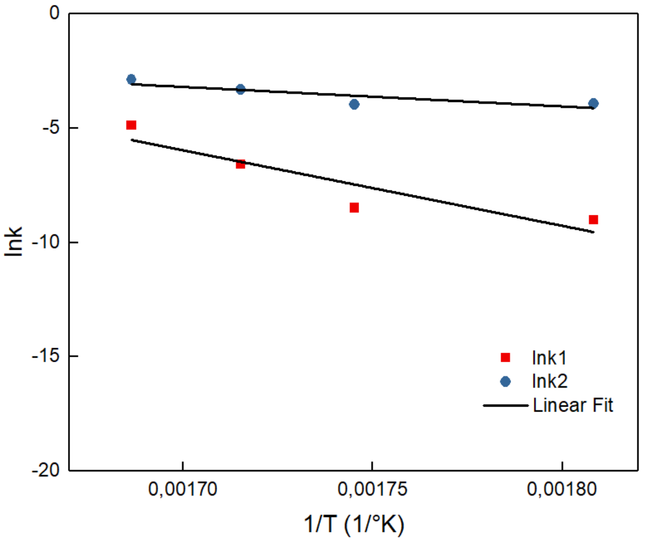

Figure 6.16. Arrhenius graphs of rate constants k_1 and k_2.

Apparent activation energy of cross-linking reaction was calculated from Arrhenius expression which was derived from Equation 5.4. The slopes of the linear lines shown in *lnk* versus *1/T* graph (Figure 6.16) give E_{a1} and E_{a2} activation energies. The activation energy for n^{th} order reaction path (E_{a1}) is higher than for the autocatalytic path (E_{a2}). The values of E_{a1} and E_{a2} are 274.4 and 70.8 kJ/mol, respectively.

6.5. Conclusion

Rheological effects of curing time, temperature and frequency on the curing behavior and viscoelastic properties of nadic end capped MDA-BTDA-ODA polyimide copolymer were evaluated in terms of dynamic mechanical analysis measurements. In addition to the increase in viscosity, a gradual increase in the values of storage and loss moduli was observed in the temperature sweep experiments. The gelation temperature was found by the determination of the temperature at which *G'* and *G"* are identical. Isothermal rheological investigations during crosslink formation were carried out by monitoring the variations in complex viscosity, $tan\ \delta$, storage and loss moduli at different temperatures (280, 300, 310 and 320 °C) and frequencies. Gelation time of the resin is determined from time dependent crossover point of $tan\ \delta$ at different frequencies. It was also found that the value of $tan\ \delta$ becomes independent from frequency at t_{gel}. Gelation time was also successfully determined by using power law depending on Winter-Chambon method which is applicable to wide range of frequencies. The value of t_{gel} which was obtained from the overlapping point of *n'* and *n"* exponents are identical to the value that was found from the intersection of $tan\ \delta$ as a function of time. As a result of the DMA measurements, T_g value of the cured resin was found to be 367 °C.

The kinetics of cross-link development of MDA-BTDA-ODA copolyimide prepolymer were modeled with a conventional autocatalytic model by using dynamic mechanical analysis data. Model fitting kinetics of Kamal-Sourour was chosen for description of rheological curing process. The kinetic parameters and behavior of conversion rate ensure that the cross-linking process occurs at autocatalytic level. Kinetic constants deduced from Kamal-Sourour model were used for calculation of activation energy.

CHAPTER 7

CONCLUDING REMARKS AND FUTURE WORK

In general speaking, the systems used in many parts of our daily lives are made up of many pieces assembled together. When these systems are being built, the joining technique to integrate all the parts is critical for the performance of the final product. Several assembling techniques such as mechanical fastening, welding, brazing and adhesive bonding are used during the integration of the parts into the systems. Adhesive bonding has the advantages of low cost and light weight compared to traditional joining methods. Among high-temperature adhesives, polyimides attract attentions due to their superior performance over 200 °C.

Within the scope of this thesis, MDA-BTDA-ODA copolyimide adhesives with nadic end caps were successfully developed. The adhesives were synthesized by a two-step method, including the preparation of polyamic ester prepolymer and thermal imidization. The chemical structures of the synthesized resins were verified by FTIR and ^{1}H NMR analysis. As a result of the thermal analysis, it is observed that the copolymers have a thermal stability as high as 500 °C and T_g at around 400 °C. The copolyimide resin with equimolar MDA:ODA ratio showed the highest adhesion performance with 16.3 MPa. Compared to both commercial PMR-15 and LARC RP-46 polyimides, copolyimide resins have been found to have significant processability by impairing the structural integrity and by introducing the flexible ether bridged ODA monomer into the backbone.

Curing time, temperature and frequency dependent rheological and viscoelastic properties of PMR-15 and MDA-BTDA-ODA copolyimides were evaluated by dynamic mechanical analysis. Viscosities, storage and loss moduli of the polymers increase with increasing temperature. The network formation temperature of PMR-15 and the copolyimide were found by the cross-section of temperature dependent G' and G'' curves. Gelation time of the polyimide resins were revealed by time dependent crossover point of $\tan \delta$ at different frequencies and power law depending on Winter-Chambon method. The values obtained from the both techniques were found to be identical. The T_g values of isothermally cured PMR-15 and nadic end capped MDA-BTDA-ODA resins were found to be 357 °C and 367 °C, respectively.

The curing kinetics of the developed copolyimide and PMR-15 were investigated by dynamic mechanic analysis. The autocatalytic kinetic model of Kamal – Sourour was used for the evaluation of the rheokinetics of curing process. The experimental data are well-fitted with the model. Kinetic parameters and the changes in mechanical conversion rates revealed that the curing reaction takes place in autocatalytic level. The activation energies were calculated by kinetic constants derived from the model.

Curing of polyimide resins at low temperatures close to room temperature is an important requirement. For further studies, this can be accomplished by using ring opening metathesis catalysts. High curing temperatures sometimes causes interfacial thermal stress for different kinds of substrates, such as ceramic-metal. Therefore, cracking can occur between a ceramic and an adhesive layer. In the future, the situation can be eliminated by developing flexible polyimides. In addition, the solubility resistance and thermal aging of the polymide resin can be examined. Increasing the thermal resistance and adhesion strength of polyimide adhesives by using additives such as carbon nanotube, nanosilica, fused silica, boron carbide and aluminum nitride is another important issue to be considered. The study on fatigue and long-term thermal behavior of the copolyimide will be also beneficial for the engineering and the design of joints composed of polyimide adhesives. The copolyimide resin can also be used as a matrix in composite structures. The studies mentioned above can be adapted to carbon or glass fiber reinforced composite structures which includes the copolyimide resin as a matrix.

REFERENCES

Abadie, M. J. 2012. *High Performance Polymers-Polyimides Based-from Chemistry to Applications*. *Croatia*. 1st ed. InTech.

Abouhamzeh, M., J. Sinke., K. M. B. Jansen., and R. Benedictus. 2015. “Kinetic and Thermo-Viscoelastic Characterisation of the Epoxy Adhesive in GLARE.” *Composite Structures* 124. Elsevier:19–28.

Abuhaimed, T., M. A. Nawareg., and R. Baier. 2014. “Pressable Glass Ceramic as a Repair Material for Fractures in Metal-Ceramic Restorations.” *Journal of Adhesion* 90 (8):717–31.

Acar, O., S. Varis., T. Isık., S. Tirkes., and M. M. Demir. 2018. “Synthesis and Characterization of Novel High Temperature Structural Adhesives Based on Nadic End Capped MDA-BTDA-ODA Copolyimide.” *Materials Research Express* 5. IOP Publishing:1–11.

Adams, R. D., and W. C. Wake. 1984. *Structural Adhesive Joints in Engineering*. *Structural Adhesive Joints in Engineering*. Dordrecht: Springer.

Akram, M. 2015. “Surface Modification of Titanium and Polyimide Sheet for Adhesive Bonding.” TU Deft.

Allen, K. W. 1993. “Some Reflections on Contemporary Views of Theories of Adhesion.” *International Journal of Adhesion and Adhesives* 13 (2):67–72.

Alston, W. B. 1992. “Structure-to-Property Relationships in Addition Cured Polymers. IV. Correlations Between Thermo-Oxidative Weight Losses of Norbornenyl Cured Polyimide Resins and Their Composites.” *Polymer Preprints(USA)* 33 (1):428–30.

Alvino, W. M., and L. E. Edelman. 1975. “Polyimides from Diisocyanates, Dianhydrides, and Tetracarboxylic Acids.” *Journal of Applied Polymer Science* 19 (11):2961–80.

Alvino, W. M., and L. E. Edelman. 1978. “Polyimides from Diisocyanates, Dianhydrides, and Their Dialkyl Esters.” *Journal of Applied Polymer Science* 22 (7). Wiley Subscription Services, Inc., A Wiley Company:1983–90.

ASTM, D. 2005. “907-05. Standard Terminology of Adhesives.” In *Annu. Book ASTM Stand.*

Avadhani, C. V., P. P. Wadgaonkar., and S. P. Vernekar. 1990. “Synthesis and Characterization of Oxyethylene Containing Diisocyanates and Polyimides Therefrom.” *Journal of Polymer Science Part A: Polymer Chemistry* 28 (7):1681–91.

Ayesha, K. 2011. “Synthesis And Characterization Of New Polyamides, Poly (Amide Imide) s, Polyimides And Polyurethanes Bearing Thiourea Moieties.” Quaid-i-Azam University, Islamabad.

Banea, M. D., and L. F. M. da Silva. 2010. “Static and Fatigue Behaviour of Room Temperature Vulcanising Silicone Adhesives for High Temperature Aerospace Applications. Statisches Verhalten Und Dauerfestigkeitsanalyse von Vulkanisierten Silikonklebstoffen Für Luftfahrtanwendungen Bei Hohen Temperat.” *Materialwissenschaft Und Werkstofftechnik* 41 (5). WILEY-VCH Verlag:325–35.

Behniafar, H., and M. Ghorbani. 2008. “New Heat Stable and Processable Poly (Amide–ether–imide) s Derived from 5-(4-Trimellitimidophenoxy)-1-Trimellitimido Naphthalene and Various Diamines.” *Polymer Degradation and Stability* 93 (3). Elsevier:608–17.

Bessonov, M. I., M. M. Koton., V. V. Kudryavtsev., and L. A. Laius. 1987. *No Title*. 1st ed. New York, NY, United States: Springer US.

Bhowmik, S., H. W. Bonin., V. T. Bui., and R. D. Weir. 2006. “Durability of Adhesive Bonding of Titanium in Radiation and Aerospace Environments.” *International Journal of Adhesion and Adhesives* 26 (6):400–405.

Bikerman, J. J. 1967. “Causes of Poor Adhesion: Weak Boundary Layers.” *Industrial & Engineering Chemistry* 59 (9). ACS Publications:40–44.

Boehme, B., K. M. B. Jansen., S. Rzepka., and K. Wolter. 2009. “Thermo Mechanical Characterization of Packaging Polymers.” In *European Microelectronics and Packaging Conference (EMPC).*

Bogert, M. T., and R. R. Renshaw. 1908. “4-Amino-o-Phthalic Acid and Some of Its Derivatives.” *Journal of the American Chemical Society* 30 (7):1135–44.

Bolger, J., and A. Michaels. 1968. “Molecular Structure and Electrostatic Interaction of Polymer Solid Interface.” In *Interface Conversion for Polymer Coatings*, edited by P Weiss and GD Cheever. New York, NY, United States: Elsevier.

Brill, R. P., and G. R. Palmese. 2000. “An Investigation of Vinyl-Ester-Styrene Bulk Copolymerization Cure Kinetics Using Fourier Transform Infrared Spectroscopy.” *J. Appl. Polym. Sci.* 76 (10):1572–82.

Bryant, R. G. 2000. “Polyimides.” In *Ullmann’s Encyclopedia of Industrial Chemistry*. Wiley-VCH Verlag GmbH & Co. KGaA.

Carleton, P. S., W. J. Farrissey., and J. S. Rose. 1972. “The Formation of Polyimides from Anhydrides and Isocyanates.” *Journal of Applied Polymer Science* 16 (11):2983–89.

Castelli, M. G., J. K. Sutter., and D. Benson. 1998. “Thermomechanical Fatigue Durability of T650-35/PMR-15 Sheet Molding Compound.” In *Symposium on Time Dependent and Non-Linear Effects in Polymers and Composites*.

Chambon, F., and H. H. Winter. 1987. “Linear Viscoelasticity at the Gel Point of a Crosslinking PDMS with Imbalanced Stoichiometry.” *Journal of Rheology* 31 (8). SOR:683–97.

Chao, M., K. Kou., G. Wu., J. Zhang., N. Li., and D. Zhang. 2012. “Synthesis and Properties of Semicrystalline Copolyimides Based on 4,4′-Diaminodiphenylether and 1,3-Bis(4-Aminophenoxy) Benzene.” *Journal of Macromolecular Science, Part B* 51 (10). Taylor & Francis:2003–14.

Chen, C., W. Qin., and X. Huang. 2008. “Synthesis and Characterization of Novel Polyimides Derived from 1, 4-Bis (4-aminophenoxymethylene) Cyclohexane (BAMC) and Two Aromatic Dianhydrides.” *Journal of Macromolecular Science, Part B: Physics* 47 (4):783–93.

Cheng, S. Z. D., F. E. Arnold., A. Zhang., S. L. C. Hsu., and F. W. Harris. 1991. “Organosoluble, Segmented Rigid-Rod Polyimide Film. 1. Structure Formation.” *Macromolecules* 24 (21):5856–62.

Chun, B. 1994. “Preparation and Characterization of Organic-Soluble Optically Transparent Polyimides from Alicyclic Dianhydride, Bicyclo [2.2. 2]-Oct-7-Ene-2, 3, 5, 6-Tetracarboxylic Dianhydride.” *Polymer* 35 (19):4203–8.

Cole, G. S., and A. M. Sherman. 1995. “Light Weight Materials for Automotive Applications.” *Materials Characterization* 35 (1):3–9.

Creton, C. 2017. “Pressure-Sensitive Adhesives: An Introductory Course.” *MRS Bulletin* 28 (06):434–39.

DeLollis, N. J. 1970. *Adhesives for Metals: Theory and Technology*. Industrial Press.

Delvigs, P., L. Hsu., and T. T. Serafini. 1970. “The Synthesis of a Novel Polyimide Precursor.” *Journal of Polymer Science Part C: Polymer Letters* 8 (1). Wiley Online Library:29–35.

Derjagin, B. V., and N. A. Krotova. 1948. “Elektricheskaya Teoriya Adgezii (Prilipaniya) Plenok K Tverdym Poverkhnostyam.” *Doklady Akademii Nauk SSSR* 61 (5). Mezhdunarodnaya Kniga 39 Dimitrova Ul., 113095 Moscow, Russia:849–52.

Derjaguin, B. V., and V. P. Smilga. 1967. “Electronic Theory of Adhesion.” *Journal of Applied Physics* 38 (12):4609–16.

Derjaguin, B. V., and Y. P. Toporov. 1983. “Role of The Molecular and The Electrostatic Forces in The Adhesion of Polymers.” *Physico-Chemical Aspects of Polymer Surface* 2:605–12.

Ding, M. 2007. “Isomeric Polyimides.” *Progress in Polymer Science* 32 (6):623–68.

Eashoo, M., D. Shen., Z. Wu., C. J. Lee., F. W. Harris., and S. Z. D. Cheng. 1993. “High-Performance Aromatic Polyimide Fibres: 2. Thermal Mechanical and Dynamic Properties.” *Polymer* 34 (15):3209–15.

Ebnesajjad, S. 2014. *Surface Treatment of Materials for Adhesive Bonding*. *William Andrew*. 2nd ed. Oxford: Elsevier Inc.

Ebnesajjad, S., and A. H. Landrock. 2014. *Adhesives Technology Handbook*. William Andrew.

Economy, J., and A. G. Andreopoulos. 1993. “Factors Which Influence the High Temperature Adhesive Characteristics of Liquid Crystalline Copolyesters.” *The Journal of Adhesion* 40 (2–4):115–25.

Economy, J., T. Gogeva., and V. Habbu. 1992. “Liquid Crystalline Copolyesters as High Temperature Adhesives for Aluminum.” *The Journal of Adhesion* 37 (4):215–24.

Ferry, J. D. 1980. *Viscoelastic Properties of Polymers. Viscoelastic Properties of Polymers*. New York, NY, United States: John Wiley & Sons.

Fowkes, F. M. 1964. "Attractive Forces at Interfaces." *Industrial & Engineering Chemistry* 56 (12):40–52.

Fowkes, F. M. 1981. "Acid-Base Interactions in Polymer Adhesion." *Tribology Series* 7 (C):119–37.

Fowkes, F. M., and M. A. Mostafa. 1977. "Acid-Base Interactions in Polymer Adsorption." *Am Chem Soc Div Org Coat Plast Chem Prepr* 37 (1):142–45.

Fowkes, F. M., and M. A. Mostafa. 1978. "Acid-Base Interactions in Polymer Adsorption." *Industrial and Engineering Chemistry Product Research and Development* 17 (1):3–7.

Frey, T., K. H. Große-Brinkhaus., and U. Röckrath. 1996. "Cure Monitoring of Thermoset Coatings." *Progress in Organic Coatings*.

Frost, L. W., and I. Kesse. 1964. "Spontaneous Degradation of Aromatic Poly(Pyromellitamic Acids)." *J. Appl. Polym. Sci.* 8 (3):1039–51.

Furukawa, N., Y. Yamada., and Y. Kimura. 1997. "Lap Shear Bond Strength of Thermoplastic Polyimides and Copolyimides." *High Performance Polymers* 9 (1):17–31.

Gao, C., X. Wu., G. Lv., M. Ding., and L. Gao. 2004. "Syntheses and Properties of Soluble Biphenyl-Based Polyimides from Asymmetric Bis(Chlorophthalimide)S." *Macromolecules* 37 (8):2754–61.

Gao, J. P., and Z. Y. Wang. 1995. "Synthesis and Properties of Polyimides from 4, 4′-binaphthyl-1, 1′, 8, 8′-tetracarboxylic Dianhydride." *Journal of Polymer Science Part A: Polymer Chemistry* 33 (10):1627–35.

Gao, W. J. 1994. "Modern Testing Technology for Polymer Materials." Beijing University Press of Aeronautics and Astronautics, Beijing.

George, G. A. 2009. *Chemorheology of Polymers: From Fundamental Principles to Reactive Processing. Cambridge University Press*. 1st ed. New York, NY, United States: Cambridge University Press.

Ghatge, N. D., and D. K. Dandge. 1976. “Polyimides from Diisocyanates and Dianhydrides.” *Die Angewandte Makromolekulare Chemie* 56 (1):163–71.

Ghosh, M. K., and K. L. Mittal. 1996. *Polyimides: Fundamentals and Applications. Marcel Dekker Inc: New York*. New York, NY, United States.

Goldschmidt, A., and H.-J. Streitberger. 2003. *BASF Handbook on Basics of Coating Technology*. William Andrew.

Goldstein, H. E., D. B. Leiser., and V. W. Katvala. 1978. “Reaction Cured Glass and Glass Coatings.” Google Patents.

Haddadi, S. A., M. Mahdavian-Ahadi., and F. Abbasi. 2014. “Effect of Nanosilica and Boron Carbide on Adhesion Strength of High Temperature Adhesive Based on Phenolic Resin for Graphite Bonding.” *Industrial and Engineering Chemistry Research* 53 (29):11747–54.

Halley, P. J., and M. E. Mackay. 1996. “Chemorheology of Thermosets - An Overview.” *Polymer Engineering and Science* 36 (5):593–609.

Han, S. H., J. S. Do., M. A. Kader., J. H. Lee., M. H. Lee., and C. Nah. 2004. “Preparation and Characterization of a Polyimide Nanofoam through Grafting of Labile Poly(Propylene Glycol) Oligomer.” *Polymers for Advanced Technologies* 15 (7):370–76.

Han, Y., X. Z. Fang., and X. X. Zuo. 2010. “The Influence of Molecular Weight on Properties of Melt-Processable Copolyimides Derived from Thioetherdiphthalic Anhydride Isomers.” *Journal of Materials Science* 45 (7):1921–29.

Harper, C. A. 2002. “Handbook of Plastics , Elastomers , and Composites.” *Technology*, xii, 884 p.

Harris, F. W., M. W. Beltz., and P. M. Hergenrother. 1987. “New Readily Processable Polyimide.” *SAMPE Journal* 23 (1):6–9.

Hasegawa, M., and K. Horie. 2001. “Photophysics, Photochemistry, and Optical Properties of Polyimides.” *Progress in Polymer Science (Oxford)*.

Hendricks, C., and J. Hale. 1985. “High-Temperature Adhesive Development and Evaluation.” In *Welding, Bonding, and Fastening 1984.*, edited by D Buckley John and A Stein Bland, 351–70. Washington, DC, USA Hampton, VA, USA: NASA.

Hergenrother, P. M. 2003. “The Use, Design, Synthesis, and Properties of High Performance/High Temperature Polymers: An Overview.” *High Performance Polymers* 15 (1):3–45.

Hergenrother, P. M., J. W. Connell., and J. G. Smith. 2000. “Phenylethynyl Containing Imide Oligomers.” *Polymer* 41 (13):5073–81.

Hergenrother, P. M., and J. G. Smith. 1994. “Chemistry and Properties of Imide Oligomers End-Capped with Phenylethynylphthalic Anhydrides.” *Polymer* 35 (22):4857–64.

Ho, P. S. 1989. “Chemistry and Adhesion of Metal-Polymer Interfaces.” *Applied Surface Science* 41–42:559–66.

Hopewell, J., G. A. George., and D. J. T. Hill. 2000. “Analysis of the Kinetics and Mechanism of the Cure of a Bismaleimide–diamine Thermoset.” *Polymer* 41 (23):8231–39.

Hornung, M., and M. Hajj. 2009. “Structural Bonding for Lightweight Construction.” *Materials Science Forum.*

Hou, T. H., S. P. Wilkinson., N. J. Johnston., R. H. Pater., and T. L. Schneiderk. 1996. “Processing and Properties of IM7/LARC ^{TM} -RP46 Polyimide Composites.” *High Performance Polymers* 8 (4):491–505.

Hrdlovič, P. 2004. “Column: Photochemical Reactions and Photophysical Processes.” *Polymer News* 29 (8). Taylor & Francis:247–52.

Hu, A. J., J. Y. Hao., T. He., and S. Y. Yang. 1999. “Synthesis and Characterization of High-Temperature Fluorine-Containing PMR Polyimides.” *Macromolecules* 32 (24):8046–51.

Huo, H. T., S. Mo., H. J. Sun., S. Y. Yang., and L. Fan. 2011. “Synthesis of Phthalic End-Capped Copolyimides and Their Adhesive Properties.” *High Performance Polymers* 23 (5):374–83.

Hurd, C. D., and A. G. Prapas. 1959. “Preparation of Acyclic Imides.” *Journal of Organic Chemistry* 24 (3):388–92.

Hwang, S. H., and G. S. Lee. 2000. “Curing and Decomposition Kinetics for Diglycidylether of Bisphenol-A/Di(4-Aminobenzanilide)Ether System.” *European Polymer Journal* 36 (10):2305–8.

Immarigeon, J. P., R. T. Holt., A. K. Koul., L. Zhao., W. Wallace., and J. C. Beddoes. 1995. “Lightweight Materials for Aircraft Applications.” *Materials Characterization* 35 (1):41–67.

International, A. 2010. *Standard Test Method for Apparent Shear Strength of Single-Lap-Joint Adhesively Bonded Metal Specimens by Tension Loading (Metal-to-Metal)*. ASTM international.

Iqbal, H. M. S., S. Bhowmik., and R. Benedictus. 2014. “Process Optimization of Solvent Based Polybenzimidazole Adhesive for Aerospace Applications.” *International Journal of Adhesion and Adhesives* 48:188–93.

Iqbal, M., A. Knijnenberg., H. Poulis., and T. J. Dingemans. 2010. “All-Aromatic Liquid Crystalline Thermosets as High Temperatures Adhesives.” *International Journal of Adhesion and Adhesives* 30 (8):682–88.

Ivanković, M., N. Džodan., I. Brnardić., and H. J. Mencer. 2002. “DSC Study on Simultaneous Interpenetrating Polymer Network Formation of Epoxy Resin and Unsaturated Polyester.” *Journal of Applied Polymer Science* 83 (12):2689–98.

Jiang, H., J. Wang., Z. Duan., and F. Li. 2007. “Study on the Microstructure Evolution of Phenol-Formaldehyde Resin Modified by Ceramic Additive.” *Frontiers of Materials Science in China* 1 (1):35–39.

Jin, L., Q. Zhang., Y. Xu., Q. Xia., and D. Chen. 2009. “Homogenous One-Pot Synthesis of Polyimides in Polyphosphoric Acid.” *European Polymer Journal* 45 (10):2805–11.

Johnston, J. C., M. A. B. Meador., and W. B. Alston. 1987. “A Mechanistic Study of Polyimide Formation from Diester-diacids.” *Journal of Polymer Science Part A: Polymer Chemistry* 25 (8):2175–83.

Kadiyala, A. K., M. Sharma., and J. Bijwe. 2016. “Exploration of Thermoplastic Polyimide as High Temperature Adhesive and Understanding the Interfacial Chemistry Using XPS, ToF-SIMS and Raman Spectroscopy.” *Materials and Design* 109. Elsevier Ltd:622–33.

Kamal, M. R., and S. Sourour. 1973. “Kinetics and Thermal Characterization of Thermoset Cure.” *Polymer Engineering & Science* 13 (1):59–64.

Khayer Dastjerdi, A., E. Tan., and F. Barthelat. 2013. “Direct Measurement of the Cohesive Law of Adhesives Using a Rigid Double Cantilever Beam Technique.” *Experimental Mechanics* 53 (9):1763–72.

Kim, J. H., and J. A. Moore. 1993. “A Low-Temperature Route to Polyimides.” *Macromolecules* 26 (14). American Chemical Society:3510–13.

King, F. A., and J. J. King. 1985. *Engineering Thermoplastics*. New York, NY, United States: Marcel Dekker Inc.

Kinloch, A. J. 1980. “The Science of Adhesion.” *Journal of Materials Science* 15 (9). Springer:2141–66.

Kreuz, J. A., A. L. Endrey., F. P. Gay., and C. E. Sroog. 1966. “Studies of Thermal Cyclizations of Polyamic Acids and Tertiary Amine Salts.” *Journal of Polymer Science. Part A-1, Polymer Chemistry* 4 (10):2607–16.

Krishnan, P. S. G., C. He., and C. T. S. Shang. 2004. “Synthesis, Characterization, and Curing Kinetics of Novel Ladder-like Polysilsesquioxanes Containing Side-Chain Maleimide Groups.” *Journal of Polymer Science, Part A: Polymer Chemistry* 42 (16):4036–46.

Kumar, A., V. Sudarkodi., P. V. Parandekar., N. K. Sinha., O. Prakash., N. N. Nair., and S. Basu. 2018. “Adhesion between a Rutile Surface and a Polyimide: A Coarse Grained Molecular Dynamics Study.” *Modelling and Simulation in Materials Science and Engineering* 26 (3):1–26.

Kuramoto, N., K. Hayashi., and K. Nagai. 1994. “Thermoreversible Reaction of Diels-Alder Polymer Composed of Difurufuryladipate with Bismaleimidodiphenylmethane.” *Journal of Polymer Science Part A: Polymer Chemistry* 32 (13):2501–4.

Laurienzo, P., M. Malinconico., N. Perenze., and A. L. Segre. 1994. “Synthesis and Characterization of New Siloxane Modified Addition Polyimides.” *Macromolecular Chemistry and Physics* 195 (9):3057–65.

Lee, M.-H., T. H. Woo., M. Lee., C. Lee., and S. B. Rhee. 1999. “Studies on Imidization Behaviors of Differently Processed Samples of Poly (Imide-Alt-Amic Ester) Prepared from MDPM and 6FDA.” *Macromolecules* 32 (7):2378–81.

Lefebvre, J., V. Mamleev., M. Le Bras., and S. Bourbigot. 2005. “Kinetic Analysis of Pyrolysis of Cross-Linked Polymers.” In *Polymer Degradation and Stability*, 88:85–91.

Leroy, E., J. Dupuy., and A. Maazouz. 2001. “A Method of Estimating Kinetic Parameters of Thermoset Cures: Application to a Dicyanate Ester Resin.” *Macromolecular Chemistry and Physics* 202 (4):465–74.

Li, D., Y. Yang., C. Yang., and D. Lai. 2015. “Synthesis and Characterization of a Novel High-Temperature Structural Adhesive Based on MDA-BAPP-BTDA Co-Polyimide.” *Journal of Macromolecular Science, Part A: Pure and Applied Chemistry* 52 (7):540–47.

Liaw, D. J. 2004. “Synthesis and Characterization of New Highly Soluble Organic Polyimides.” In *Macromolecular Nanostructured Materials*, edited by A. Ueyama N. Harada, 80–100. Osaka.

Liaw, D. J., K. L. Wang., Y. C. Huang., K. R. Lee., J. Y. Lai., and C. S. Ha. 2012. “Advanced Polyimide Materials: Syntheses, Physical Properties and Applications.” *Progress in Polymer Science* 37 (7):907–74.

Lu, X., G. Cao., Z. Niu., and Q. Pan. 2014. “Viscoelastic and Adhesive Properties of Single-Component Thermo-Resistant Acrylic Pressure Sensitive Adhesives.” *Journal of Applied Polymer Science* 131 (7):1–10.

Lu, Y. C., D. C. Jones., G. P. Tandon., S. Putthanarat., and G. A. Schoeppner. 2010. “High Temperature Nanoindentation of PMR-15 Polyimide.” *Experimental Mechanics* 50 (4):491–99.

Madbouly, S. A., and T. Ougizawa. 2004. “Thermal Cross-Linking of Poly(Vinyl Methyl Ether). II. Rheological Behavior at the Gel Point.” *Journal of Macromolecular Science, Part B* 43 (3). Taylor & Francis:655–70.

Madbouly, S. A., Y. Xia., and M. R. Kessler. 2012. “Rheokinetics of Ring-Opening Metathesis Polymerization of Bio-Based Castor Oil Thermoset.” *Macromolecules* 45 (19). American Chemical Society:7729–39.

Malkin, A. Y., I. Y. Gorbunova., and M. L. Kerber. 2005. “Comparison of Four Methods for Monitoring the Kinetics of Curing of a Phenolic Resin.” *Polymer Engineering and Science* 45 (1):95–102.

Malkin, A. Y., and S. G. Kulichikhin. 1991. “Rheokinetics of Curing.” In *Polymer Compositions Stabilizers/Curing. Advances in Polymer Science*, 101:217–57. Berlin, Heidelberg: Springer, Berlin, Heidelberg.

Malkin, A. Y., and S. G. Kulichikhin. 2008. *Rheokinetics: Rheological Transformations in Synthesis and Reactions of Oligomers and Polymers*. John Wiley & Sons.

Malkin, A. Y., S. G. Kulichikhin., M. L. Kerber., I. Y. Gorbunova., and E. A. Murashova. 1997. “Rheokinetics of Curing of Epoxy Resins near the Glass Transition.” *Polymer Engineering and Science* 37 (8):1322–30.

Marques, E. A. S., L. F. M. Da Silva., M. D. Banea., and R. J. C. Carbas. 2015. "Adhesive Joints for Low- and High-Temperature Use: An Overview." *Journal of Adhesion* 91 (7):556–85.

Matsumoto, A., Y. Miwa., S. Inoue., T. Enomoto., and H. Aota. 2010. "Discussion of 'Greatly Delayed Gelation from Theory in Free-Radical Cross-Linking Multivinyl Polymerization Accompanied by Microgel Formation' Based on Multiallyl Polymerization." *Macromolecules* 43 (16):6834–42.

Matsuzaki, R., M. Shibata., and A. Todoroki. 2008. "Reinforcing an Aluminum/GFRP Co-Cured Single Lap Joint Using Inter-Adherend Fiber." *Composites Part A: Applied Science and Manufacturing* 39 (5):786–95.

Maya, E. M., A. E. Lozano., J. G. De La Campa., and J. De Abajo. 2004. "Soluble Polyamides and Polyimides Functionalized with Benzo-15-Crown-5- Pendant Groups." *Macromolecular Rapid Communications* 25 (4):592–97.

Meador, M. A. B., J. C. Johnston., and P. J. Cavano. 1997. "Elucidation of the Cross-Link Structure of Nadic-End-Capped Polyimides Using NMR of 13C-Labeled Polymers." *Macromolecules* 30 (3):515–19.

Milhourat-Hammadi, A., H. Chayrigues., C. Merienne., and A. Gaudemer. 1994. "NMR Study of PMR-15 Prepolymerization Steps." *Journal of Polymer Science Part A: Polymer Chemistry* 32 (2):203–17.

Mititelu, A., T. Hamaide., C. Novat., J. Dupuy., C. N. Cascaval., B. C. Simionescu., and P. Navard. 2000. "Curing Kinetics of Liquid-Crystalline Epoxy Resins with Inverse Reactivity Ratios." *Macromolecular Chemistry and Physics* 201 (12):1209–13.

Mittal, K. . L. 2012a. *Surface Contamination: Genesis, Detection, and Control*. Springer Science & Business Media.

Mittal, K. L. 2001. *Polyimides and Other High Temperature Polymers: Synthesis, Characterization and Applications. Volume 1*. Polyimides and Other High Temperature Polymers: Synthesis, C. Taylor & Francis.

Mittal, K. L. 2013. *Polyimides: Synthesis, Characterization, and Applications*. Vol. 1. Springer Science & Business Media.

Mittal, K. L. . 2012b. *Adhesive Joints: Formation, Characteristics, and Testing*. Springer Science & Business Media.

Montserrat, S., and J. G. Martín. 2002. “The Isothermal Curing of a Diepoxide-Cycloaliphatic Diamine Resin by Temperature Modulated Differential Scanning Calorimetry.” *Journal of Applied Polymer Science* 85 (6). Wiley-Blackwell:1263–76.

Moy, T. M., C. D. DePorter., and J. E. McGrath. 1993. “Synthesis of Soluble Polyimides and Functionalized Imide Oligomers via Solution Imidization of Aromatic Diester-Diacids and Aromatic Diamines.” *Polymer* 34 (4):819–24.

Mulle, M., F. Collombet., P. Olivier., and Y. H. Grunevald. 2009. “Assessment of Cure Residual Strains through the Thickness of Carbon-Epoxy Laminates Using FBGs, Part I: Elementary Specimen.” *Composites Part A: Applied Science and Manufacturing* 40 (10):1534–44.

Naito, K., M. Onta., and Y. Kogo. 2012. “The Effect of Adhesive Thickness on Tensile and Shear Strength of Polyimide Adhesive.” *International Journal of Adhesion and Adhesives* 36:77–85.

Pater, R., and C. D. Morgan. 1988. “Interpenetrating Polymer Network Approach to Tougher and More Microcracking Resistant High Temperature Polymers. I - LaRC-RP40.” *SAMPE Journal* 24:25–32.

Pater, R. P. 1991. “No Title.” *“The 316°C and 371°C Composite Properties of an Improved PMR Polyimide”, Proceedings of the 36th International SAMPE Symposium*, 78.

Perry, R. J., S. E. Tunney., and B. D. Wilson. 1996. “Polyimide Formation through the Palladium-Mediated Carbonylation and Coupling of Bis (o-Iodo Amides) and Diamines.” *Macromolecules* 29 (3). ACS Publications:1014–20.

Petrie, E. M. 2004. “Unexpected Adhesives, SpecialChem.” 2004. www.specialchem4adhesives.com.

Pilyugin, G. T., and B. M. . Gutsulyak. 1963. “Advances in The Preparation, Investigation, and Use of Quinolinium Compounds.” *Russian Chemical Reviews* 32 (4):167.

Progar, D. J., and T. L. ST. Clair. 1994. “Adhesive Bonding Study of Amorphous LARC-TPI.” *Journal of Adhesion Science and Technology* 8 (1):67–83.

Ramos, M. M. D., A. M. Stoneham., and A. P. Sutton. 1993. “Aluminium/Polyimide Adhesion.” *Acta Metallurgica Et Materialia* 41:2105–11.

Ratta, V., E. J. Stancik., A. Ayambem., H. Pavatareddy., J. E. McGrath., and G. L. Wilkes. 1999. “A Melt-Processable Semicrystalline Polyimide Structural Adhesive Based on 1,3-Bis(4-Aminophenoxy) Benzene and 3,3’,4,4’-Biphenyltetracarboxylic Dianhydride.” *Polymer* 40 (7):1889–1902.

Ritter, G. W. 2008. “Bonding Lines-Phenolics-Oldies but Goodies.” *Assembly* 51 (11):10.

Roberts, A. D. 1977a. “Nature of Adhesion Forces in Rubber Friction.” *Adhesion* 1:207.

Roberts, A. D. 1977b. “Surface Charge Contribuition in Rubber Adhesion and Friction.” *J Phys D* 1801 (13). IOP Publishing:10:1801.

Rozhanskii, I., K. Okuyama., and K. Goto. 2000. “Synthesis and Properties of Polyimides Derived from Isomeric Biphenyltetracarboxylic Dianhydrides.” *Polymer* 41 (19):7057–65.

Ruggles-Wrenn, M. B., and M. Noomen. 2018. “Fatigue of Unitized Polymer/Ceramic Matrix Composites with 2D and 3D Fiber Architecture at Elevated Temperature.” *Polymer Testing* 72:244–56.

Rupnowski, P., M. Gentz., and M. Kumosa. 2006. “Mechanical Response of a Unidirectional Graphite Fiber/Polyimide Composite as a Function of Temperature.” *Composites Science and Technology* 66 (7–8):1045–55.

S.P., P. 1992. *Encyclopedia of Chemistry*. 2nd ed. New York, NY, United States: McGraw-Hill Inc.

Sadeghinia, M., K. M. B. Jansen., and L. J. Ernst. 2012a. “Characterization and Modeling the Thermo-Mechanical Cure-Dependent Properties of Epoxy Molding Compound.” *International Journal of Adhesion and Adhesives* 32 (1):82–88.

Sadeghinia, M., K. M. B. Jansen., and L. J. Ernst. 2012b. “Characterization of the Viscoelastic Properties of an Epoxy Molding Compound during Cure.” *Microelectronics Reliability* 52 (8):1711–18.

Saeed, M. B., and M. S. Zhan. 2007a. “Adhesive Strength of Nano-Size Particles Filled Thermoplastic Polyimides. Part-I: Multi-Walled Carbon Nano-Tubes (MWNT)-Polyimide Composite Films.” *International Journal of Adhesion and Adhesives* 27 (4):306–18.

Saeed, M. B., and M. S. Zhan. 2007b. “Adhesive Strength of Partially Imidized Thermoplastic Polyimide Films in Bonded Joints.” *International Journal of Adhesion and Adhesives* 27 (1):9–19.

Santhosh Kumar, K. S., C. P. Reghunadhan Nair., and K. N. Ninan. 2006. “Rheokinetic Investigations on the Thermal Polymerization of Benzoxazine Monomer.” *Thermochimica Acta* 441 (2):150–55.

Scariah, K. J., K. M. Usha., K. Narayanaswamy., K. Shanmugam., and K. S. Sastri. 2003. “Evaluation of Isomeric Composition of Resol-Type Phenol Formaldehyde Matrix Resins for Silica-Phenolic Composites and Its Effect on Cure Characteristics of the Resin.” *Journal of Applied Polymer Science* 90 (9):2517–24.

Schmitz, L., M. Rehahn., and M. Ballauff. 1993. “Soluble, Rigid-Rod Polyimides Having Phenyl Substituted Pyromellitic Diimide Units via Pd-Catalysed Polycondensation.” *Polymer* 34 (3):646–49.

Schneberger, G. L. 1983. *Adhesives in Manufacturing*. 1st ed. New York, NY, United States: Marcel Dekker.

Scola, D. A. 1993. “Synthesis and Thermooxidative Stability of Poly[1,4-Phenylene-4,4′-(2,2,2-Trifluoro-1-Phenylethylidene)Bisphthalimide] and Other Fluorinated Polyimides.” *Journal of Polymer Science Part A: Polymer Chemistry* 31 (8). John Wiley & Sons, Inc.:1997–2008.

Scola, D. A. 2001. “Polyimide Resins.” In *ASM Handbook*, edited by A S M International Inc., Composites:105–19.

Scola, D. A., and M. Wai. 1994. “The Thermo-Oxidative Stability of Fluorinated Polyimides and Polyimide/Graphite Composites at 371°C.” *Journal of Applied Polymer Science* 52 (3). Wiley Subscription Services, Inc., A Wiley Company:421–29.

Serafini, T. T., P. Delvigs., and G. R. Lightsey. 1972. “Thermally Stable Polyimides from Solutions of Monomeric Reactants.” *Journal of Applied Polymer Science* 16 (4). Wiley Subscription Services, Inc., A Wiley Company:905–15.

Sharpe, L. H. 1966. “The Materials, Processes and Design Methods for Assembly with Adhesives.” *Machine Design* 38 (19):179–200.

Sharpe, L. H., and H. Schonhorn. 1964. “Surface Energetics, Adhesion, and Adhesive Joints.” In *Contact Angle, Wettability, and Adhesion*, 43:12–189. Advances in Chemistry. American Chemical Society.

Shinde, B. M., N. D. Ghatge., and N. J. Patil. 1985. “Studies in the Synthesis of Diisocyanates and Polyimides Therefrom.” *Journal of Applied Polymer Science* 30 (8):3505–14.

Silva, L. F. M. Da., A. Öchsner., and R. D. Adams. 2011. *Handbook of Adhesion Technology*. *Handbook of Adhesion Technology*. Berlin: Springer-Verlag Berlin Heidelberg.

Simone, C. D., Y. Xiao., X. D. Sun., and D. A. Scola. 2005. “Some Aspects of the Cure of RP-46, a Nadic End-Capped Polyimide, and Phenyl Nadimide and Bis-Nadic-3,4’-ODA Model Compounds.” *High Performance Polymers* 17 (1):51–72.

Smith, J. G., J. W. Connell., and P. . M. Hergenrother. 2000. “The Effect of Phenylethynyl Terminated Imide Oligomer Molecular Weight on the Properties of Composites.” *Journal of Composite Materials* 34 (7). SAGE Publications Ltd STM:614–28.

Song, R., A. H. Muliana., and A. Palazotto. 2016. “An Empirical Approach to Evaluate Creep Responses in Polymers and Polymeric Composites and Determination of Design Stresses.” *Composite Structures* 148:207–23.

Soucek, M. D., and R. H. Pater. 1993. “The Effects of Curing Temperature on Deformation and Fracture Toughness in Thin Films of LaRC^{TM} RP46 Polyimide.” *Journal of Plastic Film & Sheeting* 9 (1):67–79.

Sroog, C. E. 1976. “Polyimides.” *Journal of Polymer Science: Macromolecular Reviews* 11 (1):161–208.

Sroog, C. E., A. L. Endrey., S. V. Abramo., C. E. Berr., W. M. Edwards., and K. L. Olivier. 1965. “Aromatic Polypyromellitimides from Aromatic Polyamic Acids.” *Journal Of Polymer Science Part A General Papers* 3 (4):1373–90.

Staemmler, V. 1979. “The Donor-Acceptor Approach to Molecular Interactions. Von V. Gutmann. Plenum Press, New York 1978. XVI, 279 S., Geb. £ 33.00.” *Angewandte Chemie* 91 (7):595.

Stenzenberger, H. 1986. “Bismaleimide Resins.” *Structural Adhesives: Developments in Resins and Primers(A 87-47826 21-37). London and New York, Elsevier Applied Science Publishers, 1986,* 77–126.

Subramani, S., A. Sultan Nasar., T. Philip Gnanarajan., N. Padmanabha Iyer., and G. Radhakrishnan. 2000. “Structure–property Relationship of Blocked Diisocyanates:

Synthesis of Polyimides Using Imidazole-Blocked Isocyanates." *Polymer International* 49 (6). John Wiley & Sons, Ltd.:546–50.

Tamai, S., A. Yamaguchi., and M. Ohta. 1996. "Melt Processible Polyimides and Their Chemical Structures." *Polymer* 37 (16):3683–92.

Tang, Y., C. K. W. Jim., Y. Liu., L. Ye., A. Qin., J. W. Y. Lam., C. Zhao., and B. Z. Tang. 2010. "Synthesis and Curing of Hyperbranched Poly(Triazole)s with Click Polymerization for Improved Adhesion Strength." *ACS Applied Materials and Interfaces* 2 (2):566–74.

Ton-That, M. T., K. C. Cole., C. K. Jen., and D. R. França. 2000. "Polyester Cure Monitoring by Means of Different Techniques." *Polymer Composites* 21 (4):605.

Tracton, A. A. 2005. *Coatings Technology Handbook*. CRC press.

Troughton, M. J. 2008. *Handbook of Plastics Joining: A Practical Guide. Handbook of Plastics Joining: A Practical Guide.*

Turk, M. J., A. S. Ansari., W. B. Alston., G. S. Gahn., A. A. Frimer., and D. A. Scheiman. 1999. "Evaluation of the Thermal Oxidative Stability of Polyimides via TGA Techniques." *Journal of Polymer Science Part A Polymer Chemistry* 37 (21):3943–56.

Urbaczewski, E., J.-P. Pascault., H. Sautereau., C. C. Riccardi., S. S. Moschiar., and R. J. J. Williams. 2018. "Influence of the Addition of an Aliphatic Epoxide as Reactive Diluent on the Cure Kinetics of Epoxy/Amine Formulations." *Die Makromolekulare Chemie* 191 (4). Wiley-Blackwell:943–53.

van't Hof, C., K. M. B. Jansen., G. Wisse., L. J. Ernst., D. G. Yang., G. Q. Zhang., and H. J. L. Bressers. 2007. "Novel Shear Tools for Viscoelastic Characterization of Packaging Polymers." *Microelectronics Reliability* 47 (2–3):240–47.

Vasenin R.M. 1960. "No Title." *Vysokomol. Soedin.* 2:851.

Venables, J. D. 1984. "Adhesion and Durability of Metal-Polymer Bonds." *Journal of Materials Science* 19 (8):2431–53.

Vilas, J. L., J. M. Laza., M. T. Garay., M. Rodríguez., and L. M. León. 2001. "Unsaturated Polyester Resins Cure: Kinetic, Rheologic, and Mechanical-Dynamical Analysis. I. Cure Kinetics by DSC and TSR." *Journal of Applied Polymer Science* 79 (3):447–57.

Volkersen, O. 1938. “Die Nietkraftverteilung in Zugbeanspruchten Nietverbindungen Mit Konstanten Laschenquerschnitten.” *Luftfahrtfor Schung* 15:41–47.

Volksen, W., R. D. Miller., and G. Dubois. 2009. “Low Dielectric Constant Materials.” *Chemical Reviews* 110 (1):56–110.

Voyutskii, S. S., and V. L. Vakula. 1963. “The Role of Diffusion Phenomena in Polymer to Polymer Adhesion.” *Journal of Applied Polymer Science* 7 (2):475–91.

Wallach, J., and J. Manassen. 1969. “Anionic Polymerization of Cyanoacetylene (Propiolnitrile).” *Journal of Polymer Science Part A-1: Polymer Chemistry* 7 (7). John Wiley & Sons, Inc.:1983–96.

Wang, J., H. Jiang., and N. Jiang. 2009a. “Study on the Pyrolysis of Phenol-Formaldehyde (PF) Resin and Modified PF Resin.” *Thermochimica Acta* 496 (1–2):136–42.

Wang, J., N. Jiang., and H. Jiang. 2009b. “Effect of the Evolution of Phenol-Formaldehyde Resin on the High-Temperature Bonding.” *International Journal of Adhesion and Adhesives* 29 (7):718–23.

Wang, X., J. Wang., and H. Wang. 2013. “Performance and Structural Evolution of High-Temperature Organic Adhesive for Joining Al2O3 Ceramics.” *International Journal of Adhesion and Adhesives* 45 (Supplement C):1–6.

Wang, X. Z., J. Wang., and H. Wang. 2012. “Preparation and Performance of a Heat-Resistant Organic Adhesive Obtained via a Liquid SiC Precursor.” *International Journal of Adhesion and Adhesives* 35:17–20.

Wilson, D. 1988. “PMR- 15 Processing, Properties and Problems - a Review.” *British Polymer Journal* 20 (5):405–16.

Wilson, D., H. D. Stenzenberger., and P. M. Hergenrother. 1990. *Polyimides*. Springer.

Winter, H. H., P. Morganelli., and F. Chambon. 1988. “Stoichiometry Effects on Rheology of Model Polyurethanes at the Gel Point.” *Macromolecules* 21 (2). ACS Publications:532–35.

Wright, M. E., D. A. Schorzman., and L. E. Pence. 2000. “Thermally Curing Aryl-Ethynyl End-Capped Imide Oligomers: Study of New Aromatic End Caps.” *Macromolecules* 33 (23):8611–17.

Wu, J., G. Huang., X. Wang., X. He., and B. Xu. 2012. “Changes in the Viscoelastic Mechanisms of Polyisobutylene by Plasticization.” *Macromolecules* 45 (19):8051–57.

Xiao, T. J., S. Q. Gao., A. J. Hu., X. C. Wang., and S. Y. Yang. 2001. “Thermosetting Polyimides with Improved Impact Toughness and Excellent Thermal and Thermo-Oxidative Stability.” *High Performance Polymers* 13 (4):287–99.

Xie, M., Z. Zhang., Y. Gu., M. Li., and Y. Su. 2009. “A New Method to Characterize the Cure State of Epoxy Prepreg by Dynamic Mechanical Analysis.” *Thermochimica Acta* 487 (1–2):8–17.

Xie, W., W. P. Pan., and K. C. Chuang. 2001. “Thermal Characterization of Pmr Polyimides.” *Thermochimica Acta* 367 (368):143–53.

Xu, B., and G. B. McKenna. 2011. “Evaluation of the Dyre Shoving Model Using Dynamic Data near the Glass Temperature.” *Journal of Chemical Physics* 134 (12):1–7.

Yanpeng, E., L. Wan., F. Huang., and L. Du. 2013. “New Heat-Resistant Polytriazole Adhesives: Investigation of Adhesion of Polytriazole Resins to Metals.” *Journal of Adhesion Science and Technology* 27 (16):1767–77.

Yi, L., W. Huang., and D. Yan. 2016. “Polyimides with Side Groups: Synthesis and Effects of Side Groups on Their Properties.” *Journal of Polymer Science Part A: Polymer Chemistry* 55 (4):533–559.

Yilgör, I., E. Yilgör., and G. L. Wilkes. 2015. “Critical Parameters in Designing Segmented Polyurethanes and Their Effect on Morphology and Properties: A Comprehensive Review.” *Polymer* 58 (10):A1–36.

Yu-wei, P., L. Long-bo., C. Yi., Z. Peng., W. Xu., P. Chao-rong., and L. Xiang-yang. 2012. “Influence of Steric Hindrance Between Hydrogen Atoms of Linkage Groups and Adjacent Phenyls on Properties of Polyimide.” *Chemical Research in Chinese Universities* 28 (5):926–30.

Zhao, Y., Y. Cao., Y. Yang., and C. Wu. 2003. “Rheological Study of the Sol−Gel Transition of Hybrid Gels.” *Macromolecules* 36 (3). American Chemical Society:855–59.

APPENDIX A

^{1}H NMR SPECTRA OF PREPOLYMER PRODUCTS

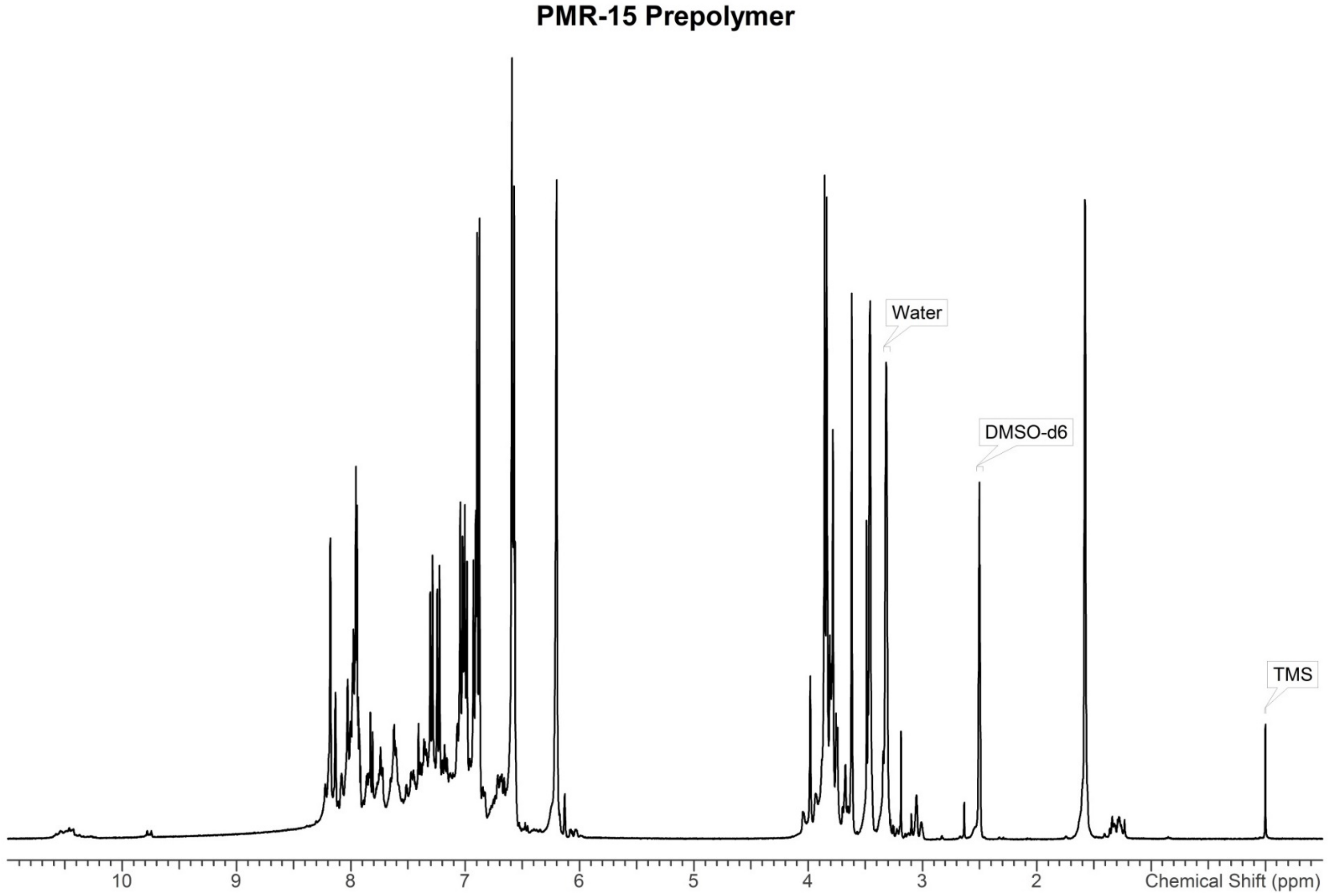

Figure S 1. ^{1}H NMR spectrum of PMR-15 prepolymer in DMSO-d_6.

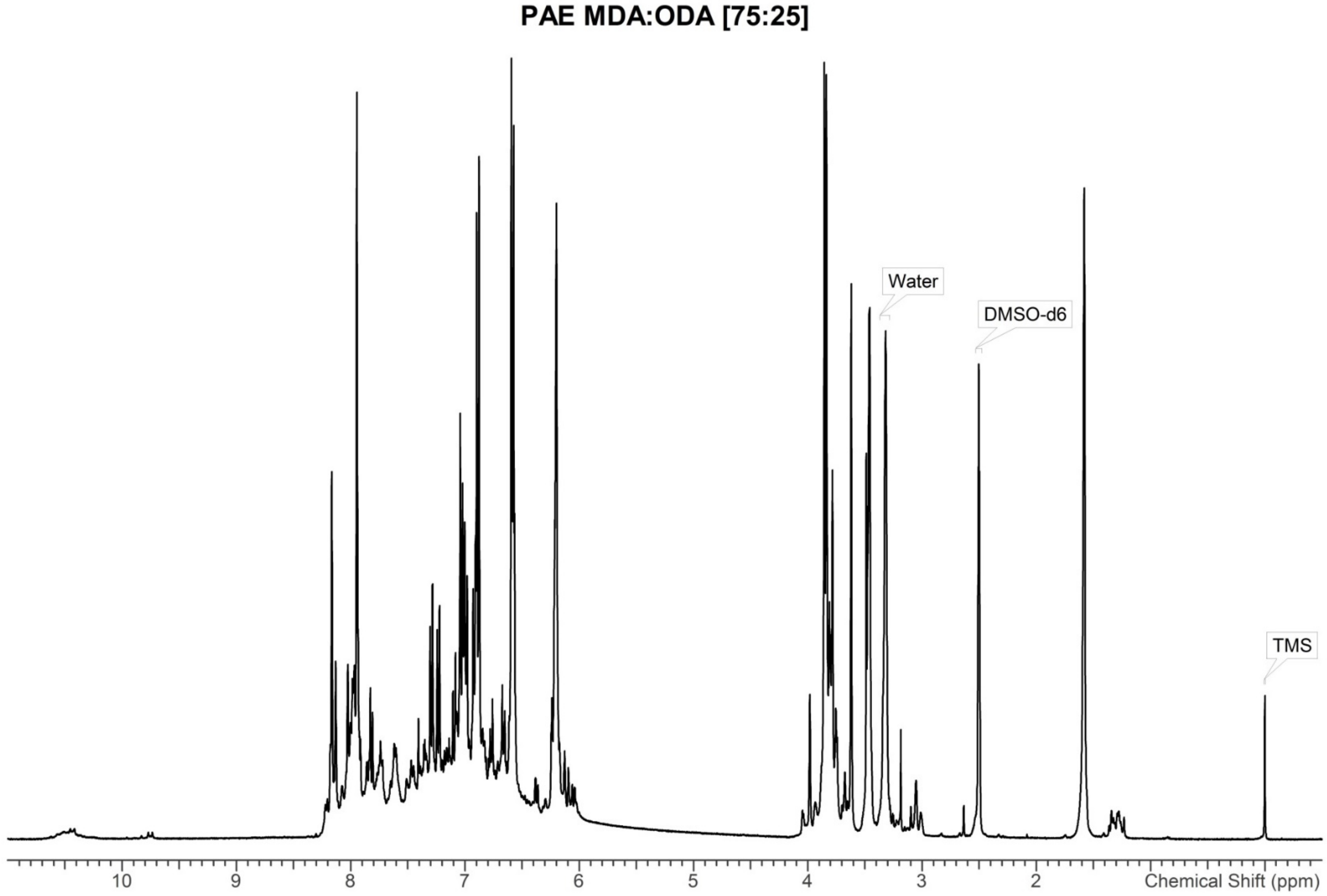

Figure S 2. ^{1}H NMR spectrum of PAE MDA:ODA [75:25].in DMSO-*d*$_6$.

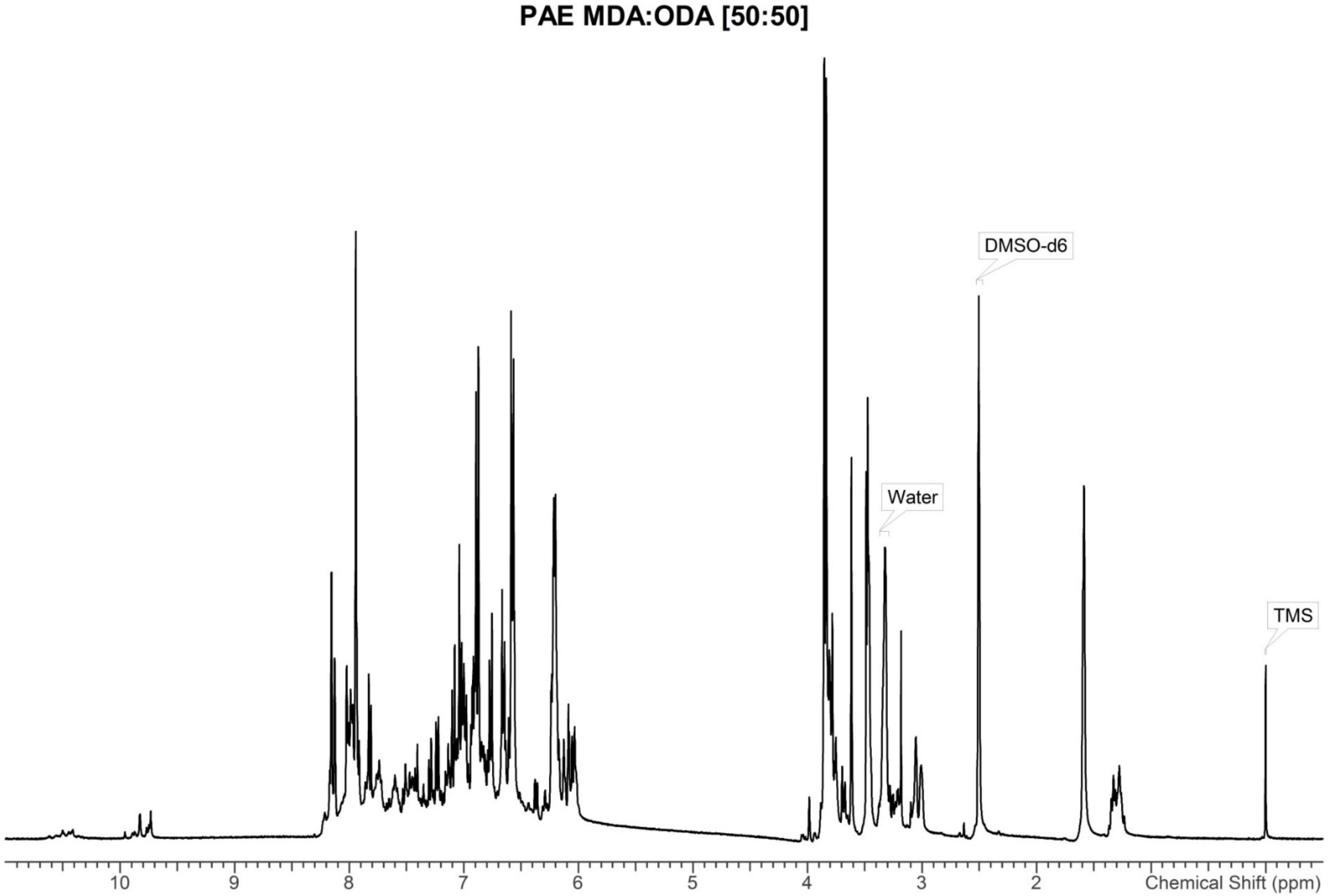

Figure S 3. ^{1}H NMR spectrum of PAE MDA:ODA [50:50] in DMSO-d_6.

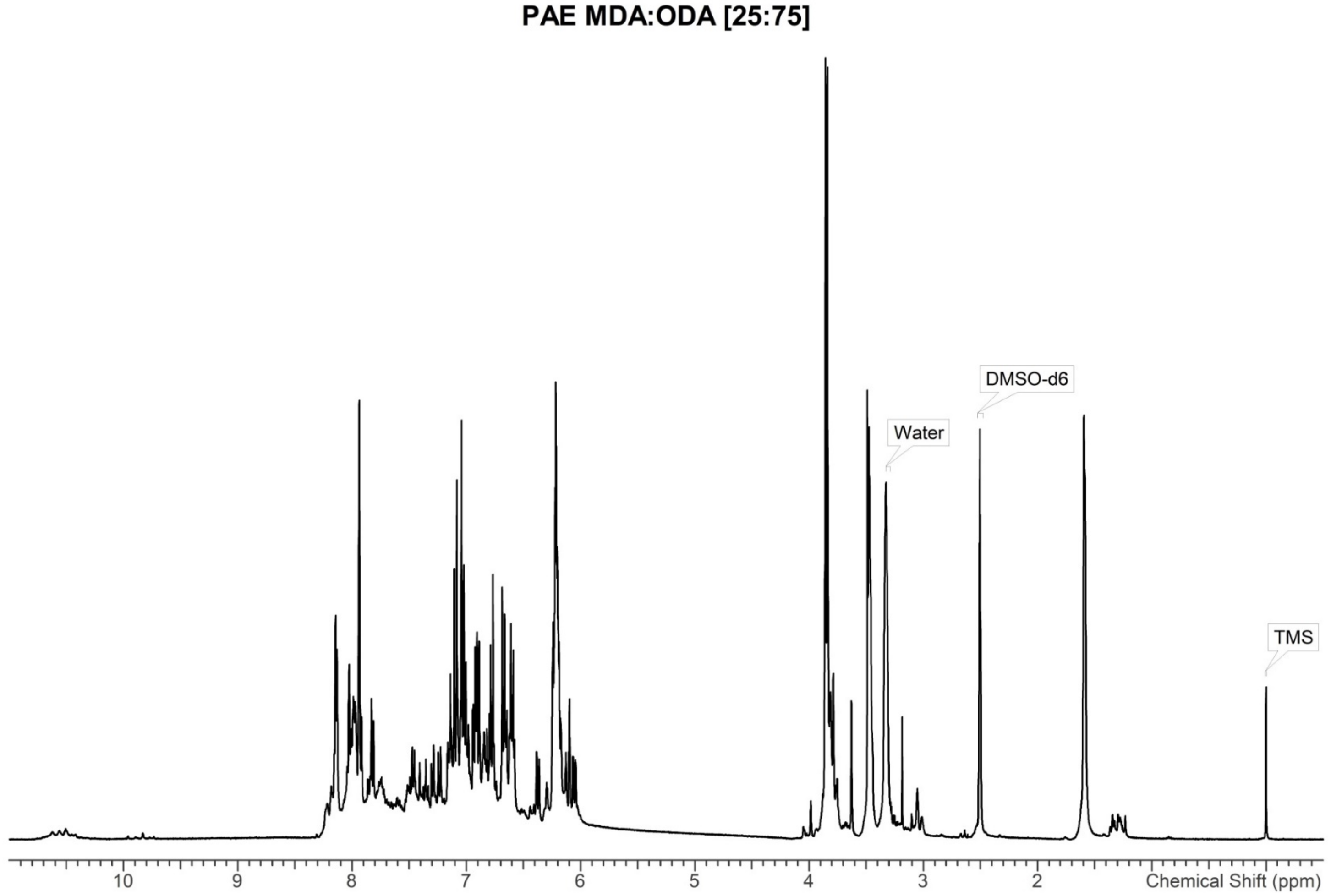

Figure S 4. ^{1}H NMR spectrum of PAE MDA:ODA [25:75] in DMSO-d_6.

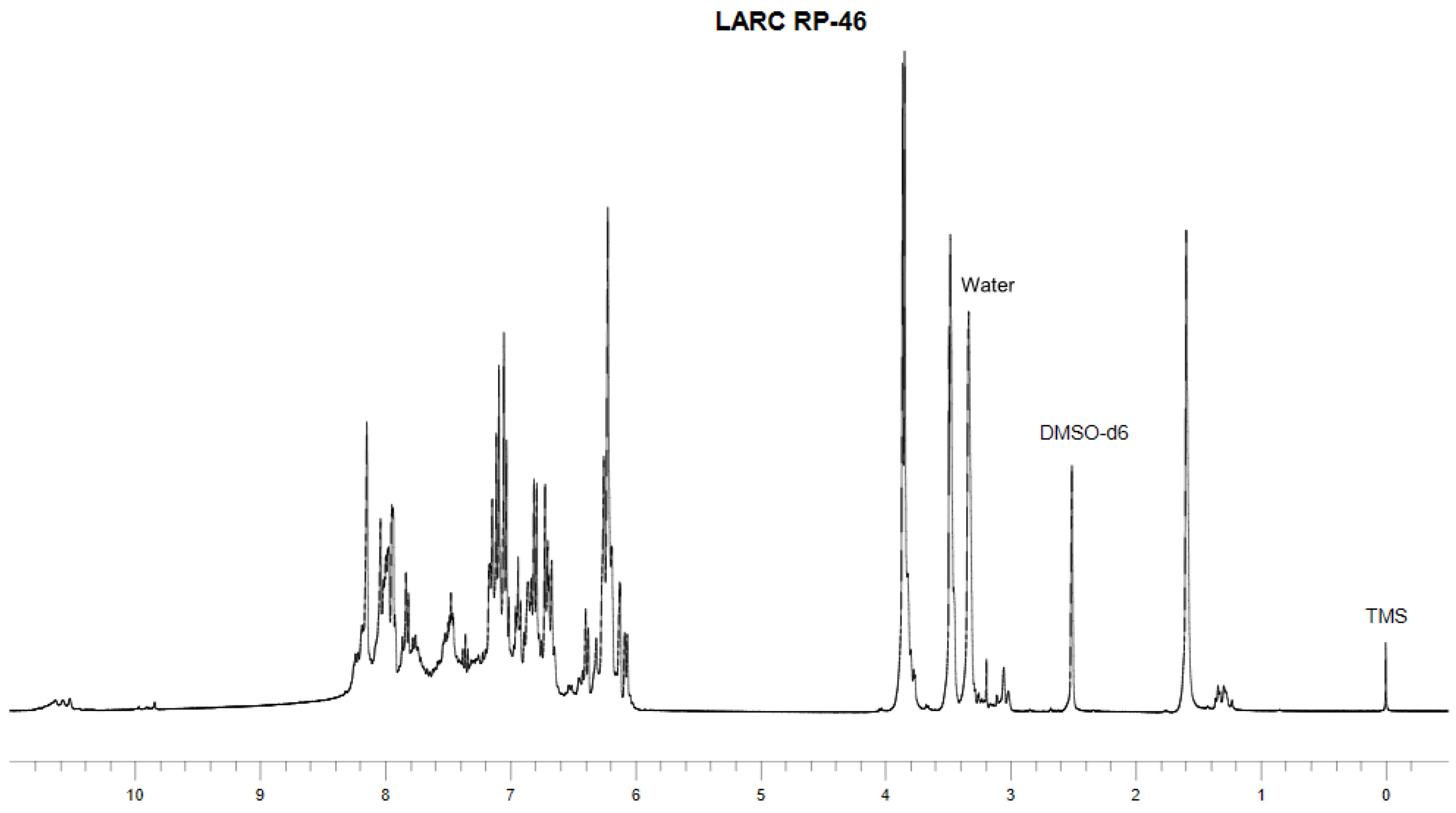

Figure S 5. ^{1}H NMR spectrum of LARC RP-46 prepolymer in DMSO-d_6.

VITA

PERSONAL INFORMATION

Surname, Name	: ACAR OKTAY
Nationality	: Turkish (TC)
Date and Place of Birth	: 12.02.1983, Ortaköy/AKSARAY
Marital Status	: Married
Phone	: +90 (555) 709 33 03
E-mail	: oktayacarx@gmail.com

EDUCATION

Degree	Institution	Year of Graduation
MSc	Gebze Institute of Technology	2009
BSc	Boğaziçi University	2007

WORK EXPERIENCE

08.2014 – Present	TUBITAK –SAGE, Turkey, Senior Researcher
03.2012 – 07.2014	Petkim Petrochemical Holding Inc., Turkey, Product Development Chemist
03.2008 – 06.2009	Gebze Institute of Technology, Turkey, Project Assistant
02.2011 – 09.2011	Istanbul Technical University, Turkey, Project Assistant
07.2006 – 09.2006	Henkel-Ecolab GmbH & Co OHG, Germany, Intern
07.2005 – 09.2005	Koç University, Turkey, Intern

PUBLICATIONS

Acar, O., Varis, S., Isik, T., Tirkes, S., Demir, M. M. 2018. “Synthesis and Characterization of Novel High Temperature Structural Adhesives Based on Nadic End Capped MDA-BTDA-ODA Copolyimide.” Materials Research Express 5:105305.

Sen, U., Usta, H., Acar, O., Citir, M., Canlier, A., Bozkurt, A., Ata, A. 2015. “Enhancement of Anhydrous Proton Conductivity of Poly(vinylphosphonic acid) – Poly(2,5-benzimidazole) Membranes via in Situ Polymerization.” Macromolecular Chemistry and Physics 216:106-112.

Sen, U., Acar, O., Celik, S. U., Bozkurt, A., Ata, A., Tokumasu, T., Miyamoto, A. 2013. “Proton-Conducting Blend Membranes of Nafion/Poly(Vinylphosphonic Acid) For Proton Exchange Membrane Fuel Cells.” Journal of Polymer Research 20:1-7.

Acar, O., Sen, U., Bozkurt, A., Ata, A. 2011. “Poly(2,5-benzimidazole) (ABPBI)-Poly(2-acrylamido-2-methyl-1-propane sulfonic acid) (PAMPS) based Proton Conducting Polymer Electrolytes for Fuel Cells.” Journal of Applied Polymer Science 2:1193-1198.

Acar, O., Sen, U., Bozkurt, A., Ata A. 2010. “Blend Membranes from Poly(2,5-Benzimidazole) And Poly(Styrene Sulfonic Acid) As Proton-Conducting Polymer Electrolytes for Fuel Cells.” Journal of Materials Science 45:993-998.

Acar, O., Sen, U., Bozkurt, A., Ata A. 2009. “Proton Conducting Membranes Based on Poly(2,5-benzimidazole) (ABPBI)–Poly(vinylphosphonic acid) Blends for Fuel Cells.” International Journal of Hydrogen Energy 34:2724- 2730.